



Alexandria University
Faculty of Engineering,
Electrical Power and Machines Department

Fast DC Off-Board Charger for Electric Vehicles

Supervised by
Prof. Dr. Ragi Hamdy
Prof. Dr. Ayman Samy Abdel-Khalik

Hassan Tarek Ali
Mahmoud Yousry Moustafa
Muhammad Ibrahim Gaber
Mennat Allah Hassan
Nouran Ahmed El-Sayed
Yousef Mohamed Zaghlol

Ahmed Saeed Abdullatif
Mohamed Raafat Abdelgaber
Alaa Ashraf Mohamed
Ahmed Mostafa Kamel
Mennat Allah Khaled
Moamen Mohamed Eltayeb

Academic Year 2023/2024

Abstract

This graduation project presents the design and development of a fast off-board charger for electric vehicles, involving two primary stages: AC to DC rectification and DC to DC conversion. The integration of these stages is critical to ensure efficient, reliable, and high-performance charging.

The first stage, AC to DC rectification, employs a three-phase high-power inverter with a two-level Sinusoidal Pulse Width Modulation (SPWM) technique. This stage converts incoming three-phase AC power into a stable DC output. The use of SPWM enhances power conversion efficiency and reduces harmonic distortions, essential for maintaining the quality of the DC power supplied to the next stage.

The second stage, DC to DC conversion, is implemented using a Dual Active Bridge (DAB) converter. The DAB converter is chosen for its high efficiency and bidirectional power transfer capabilities, crucial for fast charging applications. This stage steps down the high voltage DC from the rectification stage to the appropriate voltage levels required by the electric vehicle's battery.

Integration between these two stages is achieved through a well-coordinated control algorithm ensuring seamless power flow and stability. The control algorithm monitors and regulates output voltage and current, ensuring that the power delivered to the battery is within safe and optimal parameters. This integration is further supported by the hardware design, which includes four key PCB boards: the main inverter board, the interfacing board for connecting the inverter with the sensors, the current sensor board, and the voltage sensor board.

The interfacing board plays a vital role in integrating the two stages by providing necessary feedback and control signals. It ensures accurate communication between the inverter and the DAB converter, enabling real-time adjustments to maintain efficiency and safety. The current and voltage sensor boards provide critical data for the control algorithm, allowing it to dynamically adjust the system's operation based on the charging conditions.

This project not only demonstrates the technical feasibility of a high-power fast off-board charger but also addresses practical integration challenges, offering valuable insights into the design and implementation of efficient electric vehicle charging systems.

Acknowledgments

First and foremost, we would like to express our gratitude to our Mentor, Prof. Dr. Ayman Samy Abdel-Khalik, who was a continual source of inspiration. He pushed us to think imaginatively and urged us to do this homework without hesitation. His vast knowledge, extensive experience, and professional competence in Automotive field enabled us to successfully accomplish this project. This endeavor would not have been possible without his help and supervision. We could not have asked for a finer mentor in our studies. This initiative would not have been a success without the contributions of each and every individual.

We would also like to thank eJad for their generous support and funding of this project by supplying the equipment that was essential and vital, without which we would not have been able to perform efficiently on this project.

Last but not least, we would like to express our gratitude to our families, colleagues, and friends for their invaluable assistance, and we are deeply grateful to everyone who has contributed to the successful completion of this project.

Contents

Abstract	3
Acknowledgments	5
I AC/DC Conversion	19
1 Introduction to AC/DC Conversion	21
1.1 What is Rectification?	21
1.2 Topologies for AC/DC Conversion Stage	22
1.2.1 Three-Phase Two-Level Six-Switch Boost-Type Rectifier	22
2 Implementation of Closed-Loop AC/DC Converter	25
2.1 Proportional Integral (PI)	26
2.1.1 P-Controller	26
2.1.2 I-Controller	26
2.1.3 Tuning of PI Controller	27
2.1.4 The Main Control Circuit	27
2.2 Phase-Locked Loop (PLL)	29
2.3 Clarke and Park Transformations	30
2.3.1 Clarke Transform	30
2.3.2 Park Transform	31
3 AC/DC Converter Simulation	33
3.1 Low-Rating System (1KW)	34
4 AC/DC Converter Design	37
4.1 Filter Design	37

4.1.1	Filters for Grid-Connected Inverters	38
	Design Example: Low-Rating System (1KW)	40
	Simulation	41
4.2	DC-Link Capacitor Calculations	42
4.2.1	System Design (1KW)	42
4.3	Component Selection	43
4.3.1	The Inverter Module	43
4.3.2	The Current Sensor	43
4.3.3	The Voltage Sensor	44
	Interfacing with Micro-Controller - Op-Amp Technique	45
4.3.4	The Micro-Controller	47
4.4	Hardware Design	47
4.4.1	The Inverter Module	48
4.4.2	DC-Link	49
4.4.3	Current Sensors	50
4.4.4	Voltage Sensors	51
4.4.5	Micro-Controller Interfacing	52
5	Hardware Calibration	55
5.1	Testing of Voltage Sensor (LV 25-P)	55
5.1.1	Objective	55
5.1.2	Equipment	55
5.1.3	Procedure	55
5.1.4	Documentation	56
5.1.5	Notes	56
5.2	Testing of Current Sensor (LTS 25-P)	57
5.2.1	Objective	57
5.2.2	Equipment	57
5.2.3	Connection	57
5.2.4	Procedure	58
5.3	Open Loop Test Procedure	58
5.3.1	Objective	58
5.3.2	Equipment	58

CONTENTS 9

5.3.3	Procedure	58
5.3.4	Documentation	59
5.3.5	Notes	59
5.4	Phase Locked Loop Test	59
5.4.1	Objective	59
5.4.2	Equipment	59
5.4.3	Procedure	60
5.4.4	Documentation	60
5.4.5	Notes	60
5.5	Current-Controlled Inverter	60
5.5.1	Objective	60
5.5.2	Equipment	61
5.5.3	Procedure	61
Part 1: Star-Connected Inductive Load Connection	61
Part 2: Grid Connection	62
5.5.4	Documentation	62
5.5.5	Notes	62
5.5.6	Results	63
5.6	VOC Controlled Rectifier	64
5.6.1	Objective	64
5.6.2	Equipment	64
5.6.3	Procedure	65
Part 1: Current Control Rectifier connected to DC Supply	65
Part 2: Voltage Control rectifier with Charging the battery	65
5.6.4	Documentation	65
5.6.5	Notes	65
II	DC/DC Conversion	67
6	Introduction to DC-DC Converters	69
6.1	Principle of Operation	70
6.2	Types of DC-DC Converters	71
6.3	Applications	73

7 Dual Active Bridge	75
7.1 Introduction	75
7.2 Structure	75
7.3 Simplified Circuit Model	76
7.4 Principle of Operation	77
7.5 Control Techniques	78
7.5.1 Phase Shift Control PSC	78
7.5.2 Single Phase Shift Control SPS	79
7.6 Some Considerations and Design Parameters	80
7.6.1 Zero Voltage Switching (ZVS)	80
7.6.2 Switching Frequency	81
7.6.3 Filter Circuit Design	81
7.6.4 HF Transformer Turns Ratio	82
7.6.5 Leakage Inductance Design	82
7.7 Simulation	82
7.7.1 MATLAB Model	83
7.7.2 PWM Generator	83
7.7.3 PI Controller	84
7.7.4 The Results of Current Control	85
7.7.5 The Results of Voltage Control	86
7.7.6 Converter Efficiency	86
7.8 Hardware Implementation	86
7.8.1 Power Circuit	87
7.8.2 Gate Drive Circuit	87
7.8.3 Current Sensor	88
7.8.4 MCU	89
8 LLC Converters	91
8.1 Introduction	91
8.2 Resonant Tank	92
8.3 Behavior of the Voltage-Gain Function	93
8.4 Design Steps and Considerations	97
8.5 Design Using MATLAB Script	99

CONTENTS	11
-----------------	-----------

8.6 LLC Resonant Converter Closed Loop Control	100
8.7 Matlab Model	101
8.8 Conclusion	106
9 High Frequency (HF) Transformer Design	107
9.1 Introduction to HF Transformer	107
9.1.1 Operating Frequency	107
9.1.2 Core Materials	107
9.1.3 Winding Configurations	107
9.1.4 Wire and Insulation	108
9.1.5 Losses and Efficiency	108
9.1.6 Magnetic Design	108
9.1.7 Electromagnetic Interference (EMI)	108
9.1.8 Temperature Rise and Cooling	108
9.2 HF Transformer Design	108
9.2.1 General Procedures	108
9.2.2 Procedures in Detail	109
Starting with the Primary Side:	109
9.2.3 Results for both high and low ratings:	120
III Charger Integration	121
10 Introduction to Electric Vehicle Chargers	123
10.1 Wired Charging	123
10.1.1 AC Charging	124
10.1.2 DC Charging	124
10.2 Wireless Charging	124
10.3 EV Charging Stages	125
10.3.1 AC-DC Rectifier	125
10.3.2 DC-DC Converter	125
11 Comparison Between On-Board and Off-Board Chargers	127
11.1 On-Board Chargers	127
11.2 Off-Board Chargers	128

11.3 Summarized Comparison	128
11.4 Why Use Off-Board Chargers?	129
12 MATLAB Simulation	131
12.1 Integrating the AFE Rectifier with DAB Converter	131
12.2 Integrating the AFE Rectifier with LLC Converter	133
Bibliography	134

List of Figures

1.1	Three-phase two-level six-switch boost-type rectifier	22
2.1	The implemented model of 10KW system using VOC	25
2.2	The effect of P-gain on a system	26
2.3	PI-control process	26
2.4	Control circuit of AFE (Active Front-end Rectifier) with 800V output voltage	27
2.5	PI control loop of AFE	28
2.6	PLL control using VOC method	29
2.7	$\alpha - \beta$ signals to d-q signals	29
2.8	ABC frame	30
2.9	Clarke transform	30
2.10	Park transform	31
3.1	The implementation of PLL for 1KW system	33
3.2	The outer loop PI-control block of 1KW system	34
3.3	The inner loop PI-control block of 1KW system	34
3.4	The quadrature PI-control block of 1KW system	35
3.5	The three-phase input voltage and current of 1KW system	35
3.6	The input voltage and current of phase-R of 1KW system	36
3.7	The DC-link output of 1KW system	36
4.1	Three-phase inverter with passive filter	38
4.2	The output voltage on the DC-link	41
4.3	The current and the phase voltage of phase R	41
4.4	V_{out} versus I_p plot	43
4.5	The schematic of the supply for the voltage sensor	44
4.6	The internal connection of the voltage sensor	44

4.7	Op-amp circuit	45
4.8	The circuit diagram of the op-amp	46
4.9	The schematic of the op-amp circuit	46
4.10	DSP LaunchpadF28069M	47
4.11	The schematic of the inverter module board	48
4.12	Inverter module hardware board design	48
4.13	The schematic of the DC-link board	49
4.14	DC-link hardware board design	49
4.15	The schematic of the current sensors board	50
4.16	Current sensors hardware board design	51
4.17	The schematic of the voltage sensors board	51
4.18	Voltage sensors PCB	52
4.19	The schematic of the DSP interfacing board	52
4.20	DSP interfacing hardware board design	53
5.1	The schematic of the current sensor	57
5.2	Current-controlled inverter - Simulink model	61
5.3	Current behavior during normal operation with inductive load	63
5.4	Current behavior when DC supply voltage changes	63
5.5	Current behavior when reference current is changed	64
6.1	DC-DC Conversion from one voltage level to another	69
6.2	DC-DC Converters for Multiple Voltage Requirements	70
6.3	Feedback and Control of a Closed-loop Isolated DC/DC Converter	71
6.4	ON and OFF States of Buck Converter	71
6.5	ON and OFF States of Boost Converter	72
6.6	ON and OFF States of Buck-Boost Converter	72
6.7	Applications of DC-DC Converters	73
7.1	Diagram of a DAB DC-DC Converter	76
7.2	DAB Simplified Circuit Model	77
7.3	Gate Signals, Transformer Primary and Secondary Voltages, and Inductor Current . .	80
7.4	Dual Active Bridge DC-DC Converter Simulation Model	83
7.5	PWM Generator for Single Shift Control For DAB	83

7.6	Shifted PWM Signal Between First and Second Bridge	84
7.7	PI Controller for DAB converter	84
7.8	Output Current and Voltage Using CC for DAB	85
7.9	Relation between The Primary Voltage, Secondary voltage and The Inductor Current	85
7.10	Output Current and Voltage Using CV for DAB	86
7.11	DAB Power Circuit Design and 3D Model	87
7.12	Gate Drive Circuit Design and 3D Model	88
7.13	Current Sensor Module ACS712	88
7.14	F28069M LaunchPad™	89
8.1	LLC Resonant Converter circuit	91
8.2	resonant tank	92
8.3	parallel resonant tank response	93
8.4	series resonant tank response	93
8.5	Plots of voltage-gain function (M_g) with different values of L_n	94
8.6	voltage gain	98
8.7	The created $M g_{ap}$ curves	98
8.8	Cascaded Closed Loop Control for LLC Resonant Converter	100
8.9	MATLAB Simulink Model For LLC Resonant Converter	101
8.10	LLC Resonant Converter Power Circuit	102
8.11	Cascaded Control for LLC Resonant Converter	102
8.12	Variable Frequency Pulse Generator	102
8.13	Results in case of Reference voltage equal 350V	103
8.14	Results in case of Reference voltage equal 400V	104
8.15	Results in case of Reference voltage equal 500V	105
9.1	Typical Power Handling Chart	109
9.2	Typical Power Handling Chart	113
9.3	Typical Power Handling Chart	114
9.4	Typical Power Handling Chart	114
9.5	Typical Power Handling Chart	115
9.6	Typical Power Handling Chart	115
9.7	Flux Density Vs Frequency (P-Material)	116
9.8	Core OR47228EC	118

10.1 Overall charging system for BEVs using wired/wireless	123
10.2 AC Vs DC Charging	124
10.3 Electric vehicle (EV) charging system including off-board and on-board charger	125
11.1 On-board charger versus off-board charger.	127
12.1 The integration model	131
12.2 The phase input voltage and current	132
12.3 The DC output voltage from the rectifier side (DC-link voltage)	132
12.4 The DC output voltage from the DAB side (battery voltage)	132
12.5 The output current flowing through the load (battery)	132
12.6 The overall system	133
12.7 The power factor in AC to Dc phase	133
12.8 The output DC voltage of the rectifier part	134
12.9 The output voltage and current in DC to DC	134

List of Tables

4.1	Recommended connections for different sensitivities	43
9.1	AWG Table	117
9.2	Core Dimension	118
9.3	Comparison Between the Results for High and Low Rating	120
11.1	Comparison between On-Board and Off-Board Chargers	128

Part I

AC/DC Conversion

Chapter 1

Introduction to AC/DC Conversion

The electrical power supplied by wall outlets varies globally, offering 50Hz or 60Hz AC with voltages around 120VAC or 230VAC. Devices like phones and laptops, which run on low-voltage DC, require adapters. Despite the prevalence of DC-powered electronics, AC is preferred for mains power distribution due to historical and technical reasons.

AC became prominent because early AC generators were simpler and more reliable, transformers allowed easy voltage changes, and multiple pole alternators enabled lower rotation speeds in powerful generators. Thomas Edison initially supported DC systems but faced challenges with unreliable high-voltage DC motors, leading him to adopt AC distribution [1].

AC minimizes power losses in transmission lines by allowing voltage to be doubled and current halved, which made long-distance transmission practical. Modern technology allows efficient conversion between AC and DC, increasing interest in DC distribution for long-distance transmission without needing generator synchronization. An example is the 2000MW high-voltage DC link between England and France for power exchange based on demand [1].

AC/DC converters are essential for electric vehicles (EVs) to convert AC from outlets to DC for charging batteries. Fast charging, requiring high power (over 50 kW), relies on larger AC/DC converters typically located in charging stations rather than vehicles due to size constraints [2].

1.1 What is Rectification?

Rectification refers to the process of transforming an alternating current (AC) waveform into a direct current (DC) waveform, producing a signal with a single polarity. It is essential to note that a DC voltage or current does not necessarily have to be constant; it simply means the signal's polarity remains unchanged. In some cases, a varying amplitude DC signal is referred to as pulsating DC.

The concept of rectification is fundamental in modern electronic circuits as many electronic devices require a stable, unvarying DC voltage to power their internal circuitry. Given that residential and commercial power distribution is typically in the form of AC, some form of AC to DC conversion is necessary.

Rectifiers, which perform the conversion of AC to DC, are classified into two categories based on the type of conversion: half-wave rectifiers and full-wave rectifiers. The former involves converting half cycles of AC into DC, while the latter processes full cycles of AC into DC. Understanding the

differences between half-wave and full-wave rectifiers, as well as a brief exploration of each type, facilitates a clearer grasp of their distinct functionalities.

1.2 Topologies for AC/DC Conversion Stage

The AC-DC converter of an off-board charger is a front-end rectifier before the DC-DC conversion stage of the complete EV fast charging station. Various topologies are available that convert AC power from the utility grid to DC power. Such topologies are expected to manage high power fed directly to the battery as part of an EV fast charging solution.

- Three-Phase Passive Rectifier
- Three-Phase Vienna Rectifier
- Three-Phase Two-Level Six-Switch Boost-Type Rectifier
- Three-Phase Three-Level Neutral Point Clamped Converter
- Three-Phase Three-Level T-Type Converter

but we will focus on a three-phase two-level six-switch boost-type rectifier for its simplicity.

1.2.1 Three-Phase Two-Level Six-Switch Boost-Type Rectifier

The configuration for the three-phase two-level boost-type rectifier is depicted in 1.1. It forms six active switches (MOSFETs or IGBTs), AC side boost inductors, and a DC side filter capacitor. Known for its simplicity, robustness, and familiarity, the two-level six-switch rectifier topology needs larger-volume input inductors and is constrained by a maximum switching frequency compared to three-level converters.

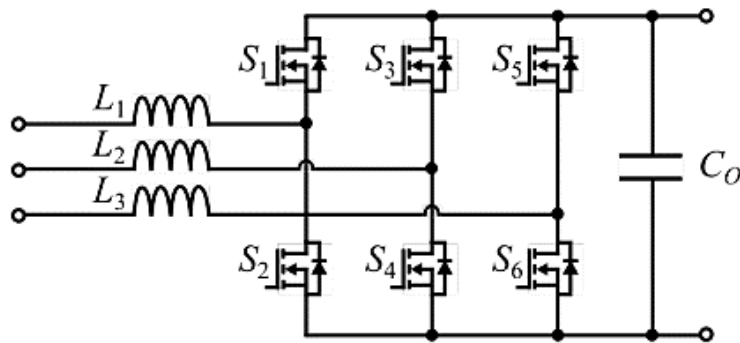


Figure 1.1: Three-phase two-level six-switch boost-type rectifier

The rectifier, being of a boosting nature, imposes a lower limit on the DC link voltage. For instance, if the rectifier is connected to a three-phase grid with a 400 V RMS line-to-line voltage, the smallest DC link voltage would be 653.19 V, equal to twice the phase voltage amplitude. Ideally, keeping a DC link voltage 15–20% higher is recommended to mitigate distortion in current waveforms.

In a two-level topology line-to-neutral rectifier, the voltage is either zero or matches the DC link voltage. Consequently, this gives rise to a three-level line-to-line voltage.

Chapter 2

Implementation of Closed-Loop AC/DC Converter

We will now address challenges through the design and implementation of a closed-loop AC/DC rectifier system. The closed-loop architecture, with its feedback mechanism, promises not only enhanced control over the rectification process but also the mitigation of issues associated with traditional rectifiers. The journey towards an optimized closed-loop system involves a meticulous exploration of key components, each playing a pivotal role in achieving the desired efficiency and stability.

The aims of this research encompass a detailed examination of critical aspects, including filter selection, DC-link configuration, phase-locked loop (PLL), Clarke and Park transformations, and Proportional-Integral (PI) control.

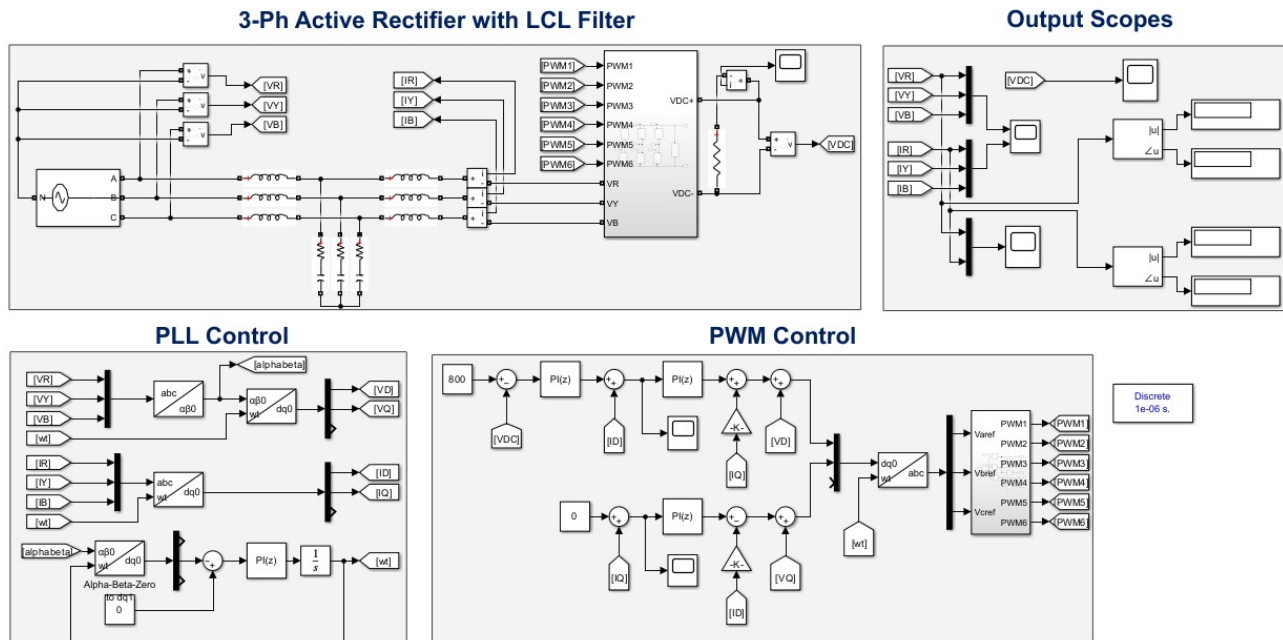


Figure 2.1: The implemented model of 10KW system using VOC

2.1 Proportional Integral (PI)

A proportional-integral (PI) controller is a feedback mechanism used in industrial systems and applications requiring continuous modulation. It combines proportional and integral adjustments to automatically compensate for system changes.

PI control is popular for its robust performance and simplicity. It uses two coefficients, proportional and integral, which are adjusted for optimal response. It reduces error between the process variable and the set point through closed-loop operations and tuning of its parameters.

2.1.1 P-Controller

Proportional or P- controller gives an output that is proportional to error $e(t)$. It compares the desired or set point with the actual value or feedback process value.

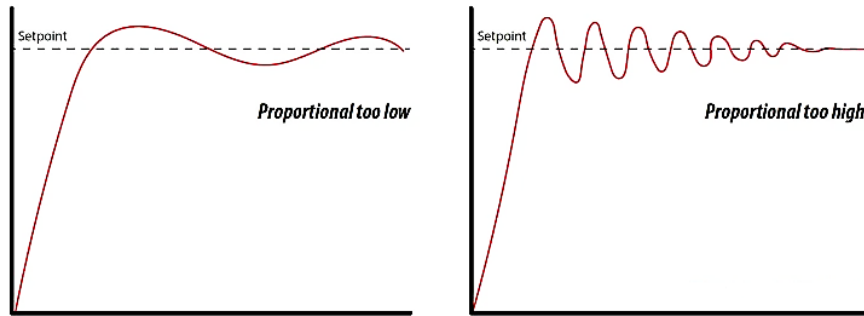


Figure 2.2: The effect of P-gain on a system

A proportional (P) controller multiplies the error by a proportional constant (K_P) to determine the output. If the error is zero, the output is zero. The P controller requires biasing or manual reset because it maintains a steady-state error. Increasing K_P speeds up the response. P-Controller Equation:

$$u(t) = K_p e(t) \quad (2.1)$$

2.1.2 I-Controller

Due to the limitation of p-controller where there always exists an offset between the process variable and set-point, I-controller is needed, which supplies necessary action to cut the steady-state error.

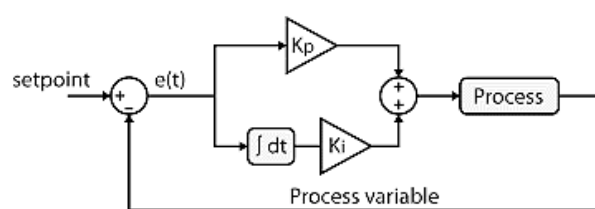


Figure 2.3: PI-control process

A PI controller integrates the error over time until it reaches zero, maintaining the value at which the error becomes zero. It decreases output with negative error, affecting response speed and system stability. Reducing the integral gain (K_i) increases response speed. PI-Controller Equation:

$$u(t) = K_p e(t) + K_i \int_0^t e(\tau) d\tau \quad (2.2)$$

2.1.3 Tuning of PI Controller

In our project, we tuned the PI controller using the Trial and Error method for simplicity and efficiency. We started with K_i set to zero and increased K_p until the system exhibited consistent oscillations. Then, we adjusted K_i to reduce these oscillations, enabling effective control.

2.1.4 The Main Control Circuit

The following figure shows the main control circuit which is used to control the voltage with the outer loop and the current with the inner loop and finally generates the corresponding PWM signals that are used to run and control the inverter.

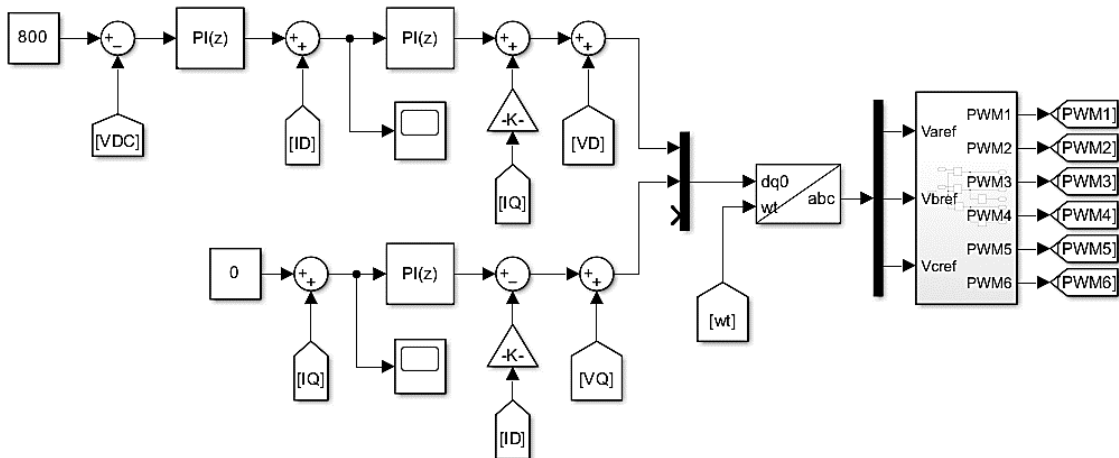


Figure 2.4: Control circuit of AFE (Active Front-end Rectifier) with 800V output voltage

There are a lot of methods to control but we used a Voltage Oriented Control for its simplicity [3]. In voltage-oriented control (VOC), the line input current is oriented with respect to the line voltage vector. The line voltage vector can be obtained by measurement by using sensors or estimation. In synchronous rotating reference frame, the d-axis is aligned with the line voltage vector. The d-axis component of the line current “id” is proportional to the active power and its q-axis component is proportional to reactive power. To achieve unity power factor the reactive component of current reference i_q^* is set to zero. While the active component of current reference i_d^* is obtained from the PI controller, which gives the output by comparing the dc link voltage at the output with the reference voltage set as per the load requirements.

Coupling occurs due to voltage drop across inductors due to orthogonal current component coming in phase with the voltage components. Decoupling is essential to have proper control.

$$V_{sd} = V_{ld} - L \frac{di_d}{dt} + \omega L i_q \quad (2.3)$$

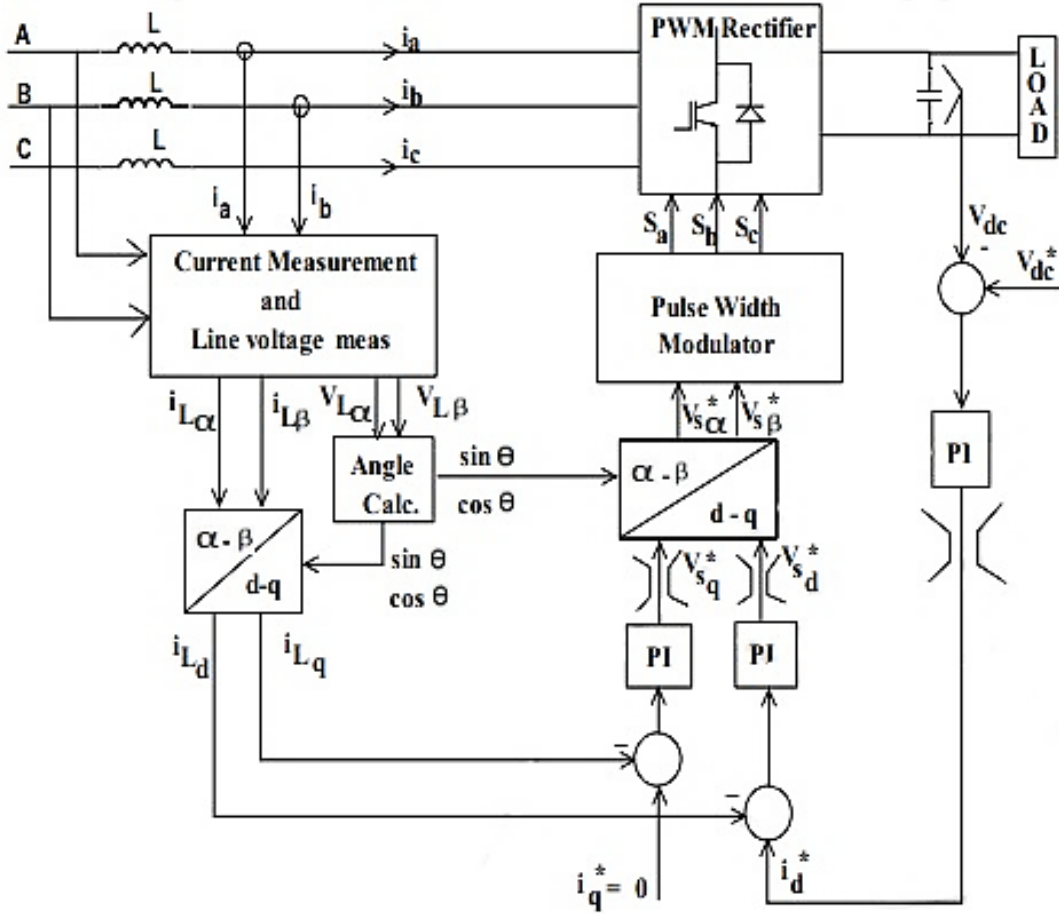


Figure 2.5: PI control loop of AFE

$$V_{sq} = V_{lq} - L \frac{di_q}{dt} - \omega L i_d \quad (2.4)$$

The voltage V_{lq} is zero by aligning the line voltage vector along the d-axis and q-axis current is regulated to zero. The current controller is decoupled as

$$V_{sd} = \omega L i_{lq} + V_{ld} + \Delta V_d \quad (2.5)$$

$$V_{sq} = -\omega L i_{ld} + \Delta V_q \quad (2.6)$$

where

$$\Delta V_d = K_p (i_d^* - i_d) + K_i \int (i_d^* - i_d) dt \quad (2.7)$$

$$\Delta V_q = K_p (i_q^* - i_q) + K_i \int (i_q^* - i_q) dt \quad (2.8)$$

In VOC it is possible to calculate the voltage across the input inductor by differentiating the current flowing through it. It is then possible to estimate the line voltage by adding voltage drop across the inductor with rectifier input voltage.

2.2 Phase-Locked Loop (PLL)

The reason why we need PLL is: suppose we want to send an active current to the grid the current should be in phase with the voltage that means that for grid connected inverters we need synchronization, so a reference signal is generated which is in phase with the actual voltage with an amplitude of 1, -1 using phase-locked loop (PLL).

The signal is used as a reference for the implementation of current controller in the grid connected inverters.

Here we start by transforming ABC signals into $\alpha - \beta$ signals then into dq voltages as shown in the figure below, this method is also called voltage oriented control (VOC), where the line input current is oriented with respect to the line voltage vector [4].

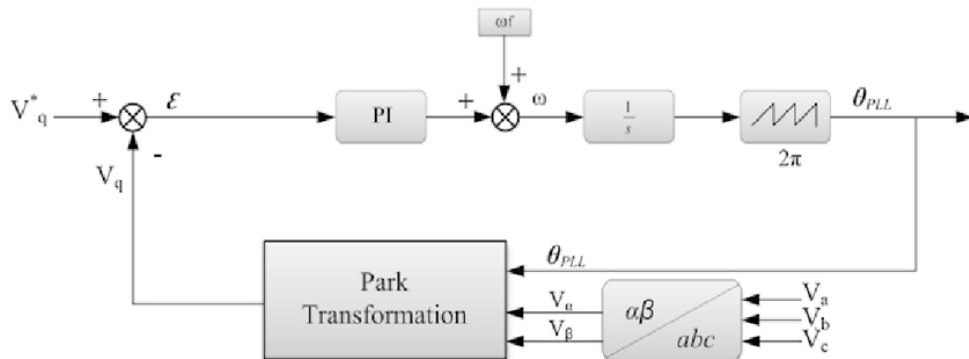


Figure 2.6: PLL control using VOC method

We can observe from the phasor diagram that D-axis is not aligned with the grid voltage so, by using the control mechanism shown in the figure we can make $V_q = 0$ using a PI controller and then the o/p is given to an integrator to find ω_t .

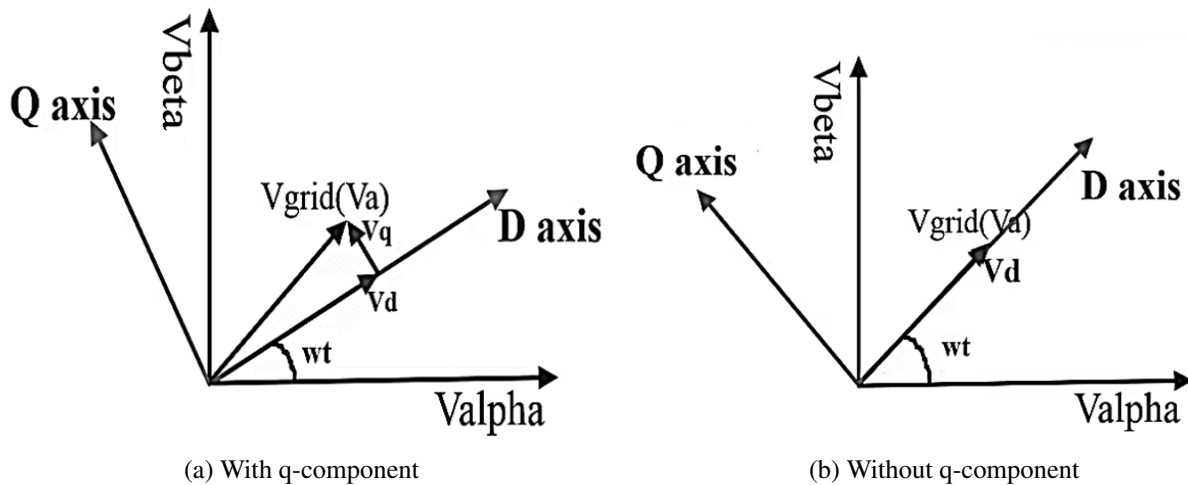


Figure 2.7: $\alpha - \beta$ signals to d-q signals

After making the V_q equal to zero the D-axis got aligned with the grid voltage and the angle between alpha-component and the D-axis has also changed to a new value which will be used in generating the reference signal.

2.3 Clarke and Park Transformations

Clarke and Park transforms are commonly used in field-oriented control of three-phase AC machines. The Clarke transform converts the time domain components of a three-phase system (in ABC frame) to two components in an orthogonal stationary frame ($\alpha - \beta$). The Park transform converts the two components in the $\alpha - \beta$ frame to an orthogonal rotating reference frame (d-q). Implementing these two transforms in a consecutive manner simplifies computations by converting AC current and voltage waveform into DC signals.

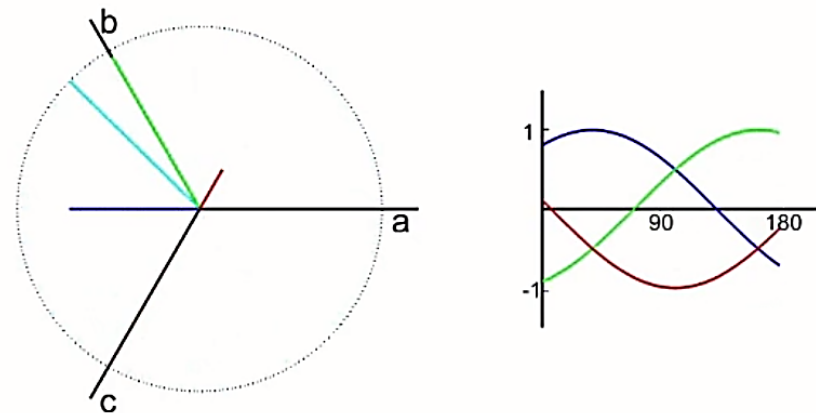


Figure 2.8: ABC frame

2.3.1 Clarke Transform

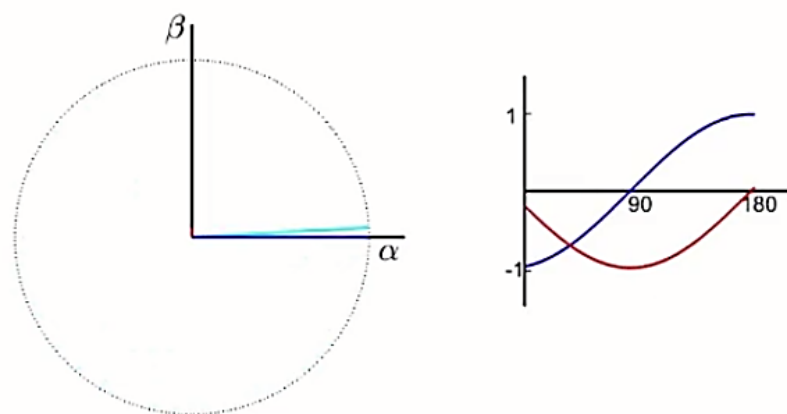


Figure 2.9: Clarke transform

The Clarke Transform converts the time-domain components of a three-phase system in an ABC reference frame to components in a stationary $\alpha\beta\gamma$ reference frame. For a balanced system, the zero part is equal to zero. The block implements the Clarke transform as

$$\begin{bmatrix} \alpha \\ \beta \\ 0 \end{bmatrix} = \frac{2}{3} \begin{bmatrix} 1 & \frac{-1}{2} & \frac{-1}{2} \\ 0 & \frac{\sqrt{3}}{2} & \frac{-\sqrt{3}}{2} \\ \perp & \perp & \perp \\ 2 & 2 & 2 \end{bmatrix} \begin{bmatrix} a \\ b \\ c \end{bmatrix} \quad (2.9)$$

where

- a, b, and c are the components of the three-phase system in the ABC reference frame.
- α and β are the components of the two-axis system in the stationary reference frame.
- 0 is the zero component of the two-axis system in the stationary reference frame.

2.3.2 Park Transform

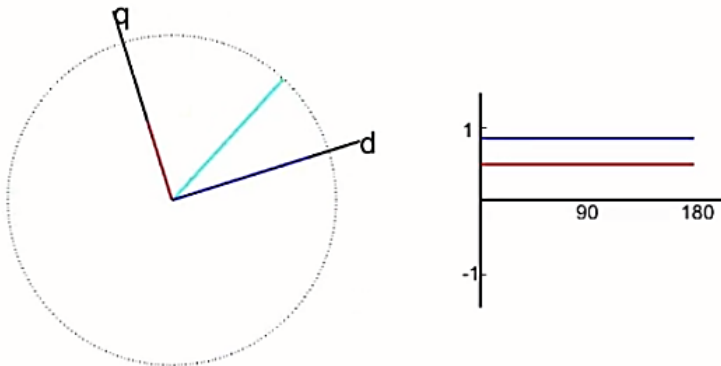


Figure 2.10: Park transform

The Park Angle Transform block converts the alpha, beta, and zero components of Clarke Transformer in a stationary reference frame to direct, quadrature, and zero components in a rotating reference frame. For balanced three-phase systems, the zero components are equal to zero.

The Clarke to Park Angle Transform block implements the transform for an a-phase to q-axis alignment as

$$\begin{bmatrix} d \\ q \\ 0 \end{bmatrix} = \begin{bmatrix} \sin(\theta) & -\cos(\theta) & 0 \\ \cos(\theta) & \sin(\theta) & 0 \\ 0 & 0 & 1 \end{bmatrix} \begin{bmatrix} \alpha \\ \beta \\ 0 \end{bmatrix} \quad (2.10)$$

where

- α and β are the components of the two-axis system in the stationary reference frame.
- 0 is the zero component of the two-axis system in the stationary reference frame.
- d and q are the direct-axis and quadrature-axis components of the two-axis system in the rotating reference frame.

Chapter 3

AC/DC Converter Simulation

It is very crucial to simulate the circuit before diving in hardware design to make sure that the circuit would work fine when it's fabricated. Therefore, for this chapter we will provide the steps to simulate an AC/DC converter of low ratings and its results.

Refer to figure 2.1 that shows the model circuit diagram that was built on MATLAB Simulink for 1KW system which is almost the same implementation for the high-rating system in aspect of circuit diagram. Note that for the low-rating system the reference voltage of the DC-link is set to be 200V.

The design of the filter design and the DC-link capacitor calculations will be discussed in details in a later chapter.

The implementation of the PLL of the 1KW system is shown in the following figure with the value of its PI-controller to produce zero-shift.

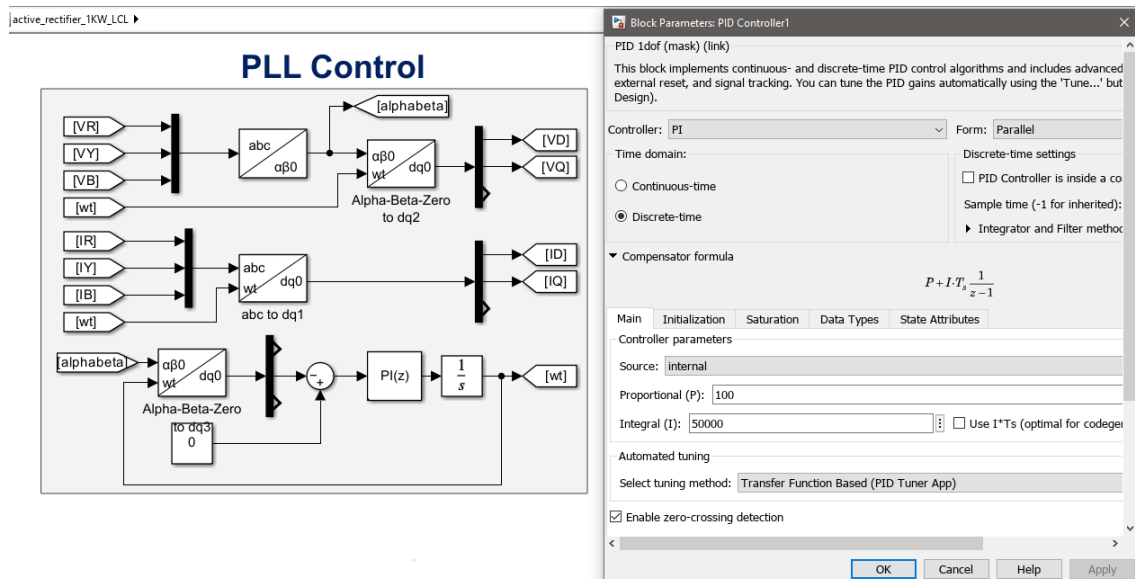


Figure 3.1: The implementation of PLL for 1KW system

3.1 Low-Rating System (1KW)

The implementation of a three-phase low-rating rectifier was done to produce 200V at the DC-link as an output while the input line-to-line voltage was 100V at 50Hz frequency. The parameters of the system is as follows:

$$C_f = 15.915\mu F$$

$$L_i = 4mH$$

$$L_g = 95.492\mu H$$

$$R_f = 0.8027\Omega$$

$$C_{dc} = 1000\mu F$$

After the DC-link, a load was set in parallel to limit the current to produce exactly 1KW power at the output. The value of the this resistance was set to be 40Ω .

The PWM control block is implemented using three PI-controllers as discussed previously (refer to figures 3.2 ~ 3.4).

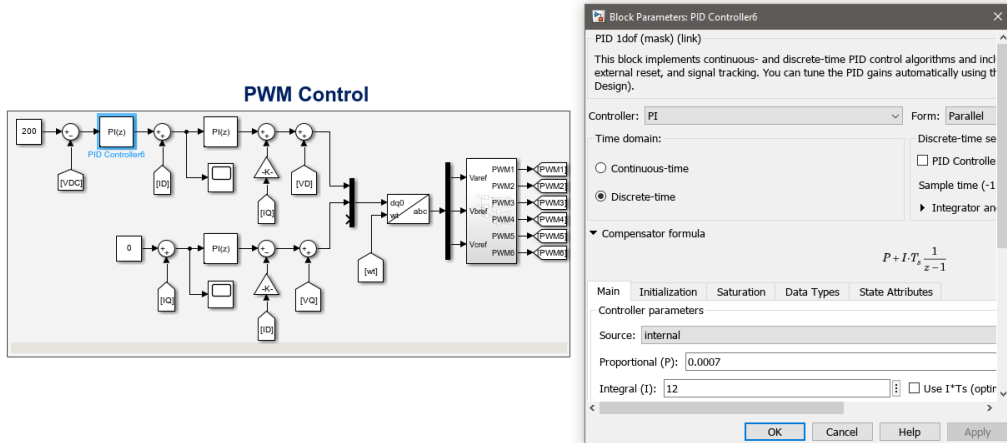


Figure 3.2: The outer loop PI-control block of 1KW system

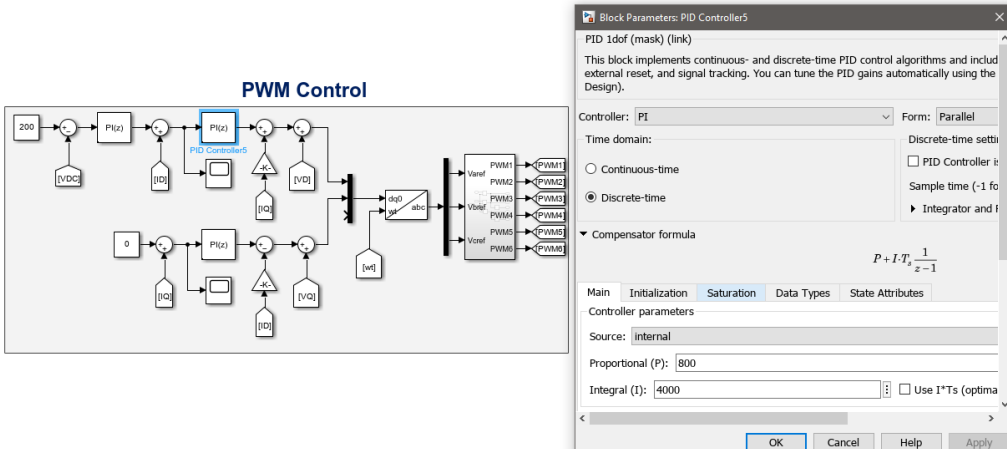


Figure 3.3: The inner loop PI-control block of 1KW system

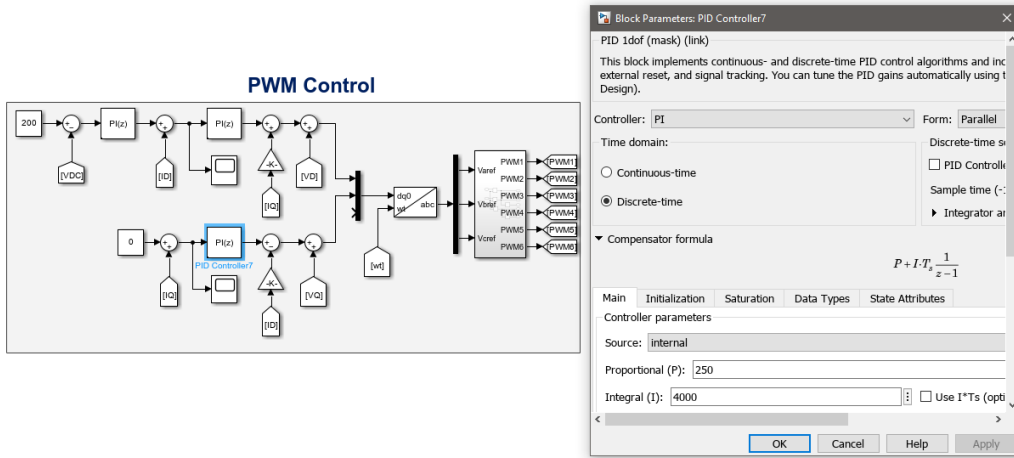


Figure 3.4: The quadrature PI-control block of 1KW system

The following results were obtained to show the input voltages and currents, the synchronism between the current and the voltage to show the power factor correction and the DC-link output voltage.

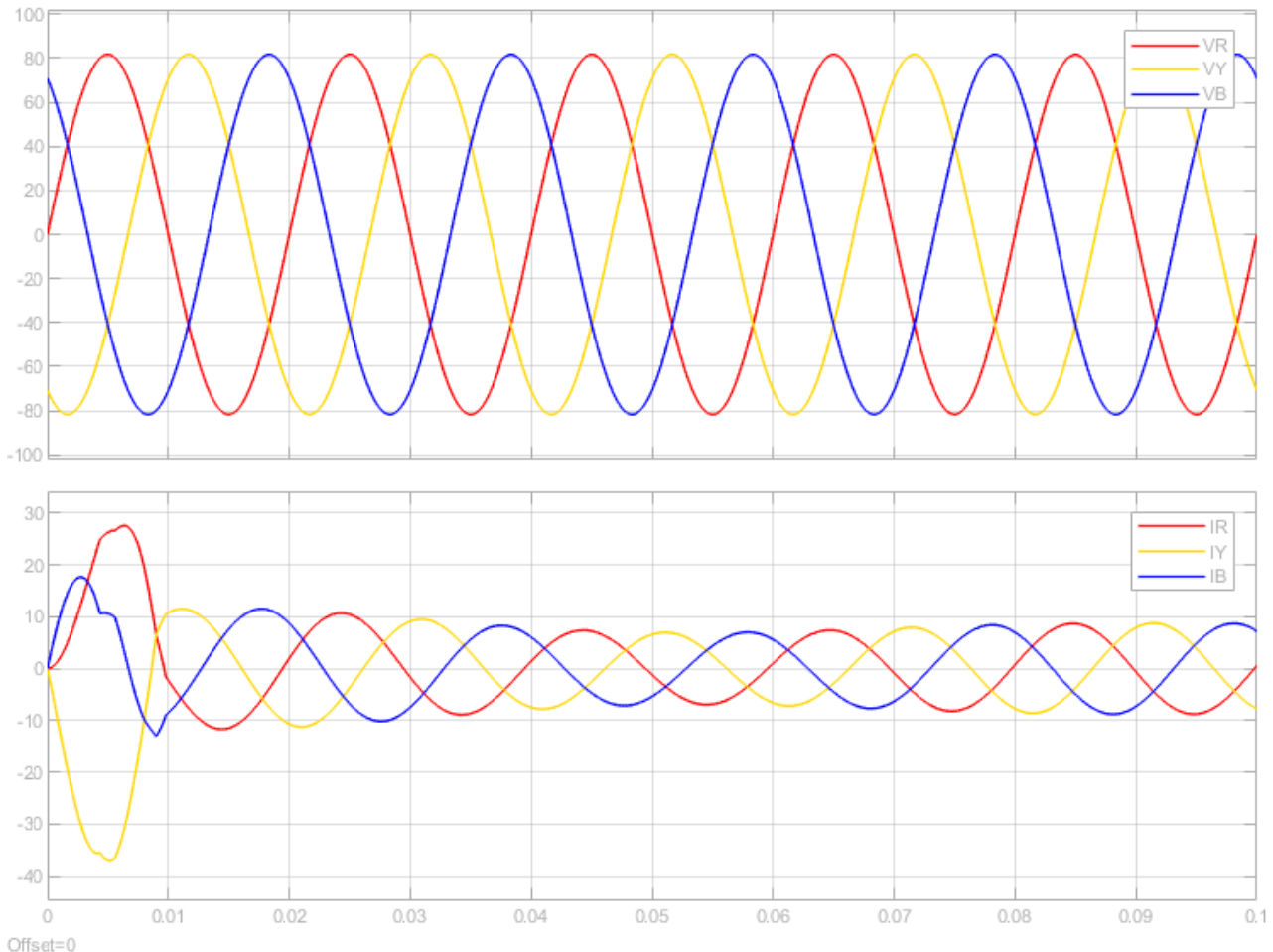


Figure 3.5: The three-phase input voltage and current of 1KW system

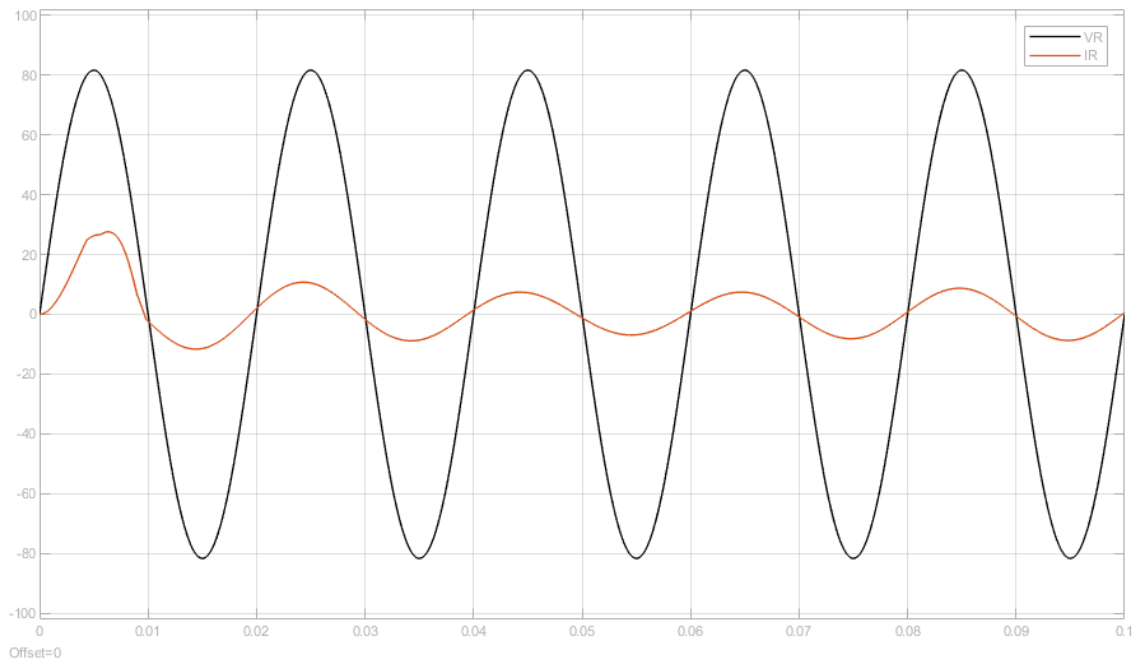


Figure 3.6: The input voltage and current of phase-R of 1KW system

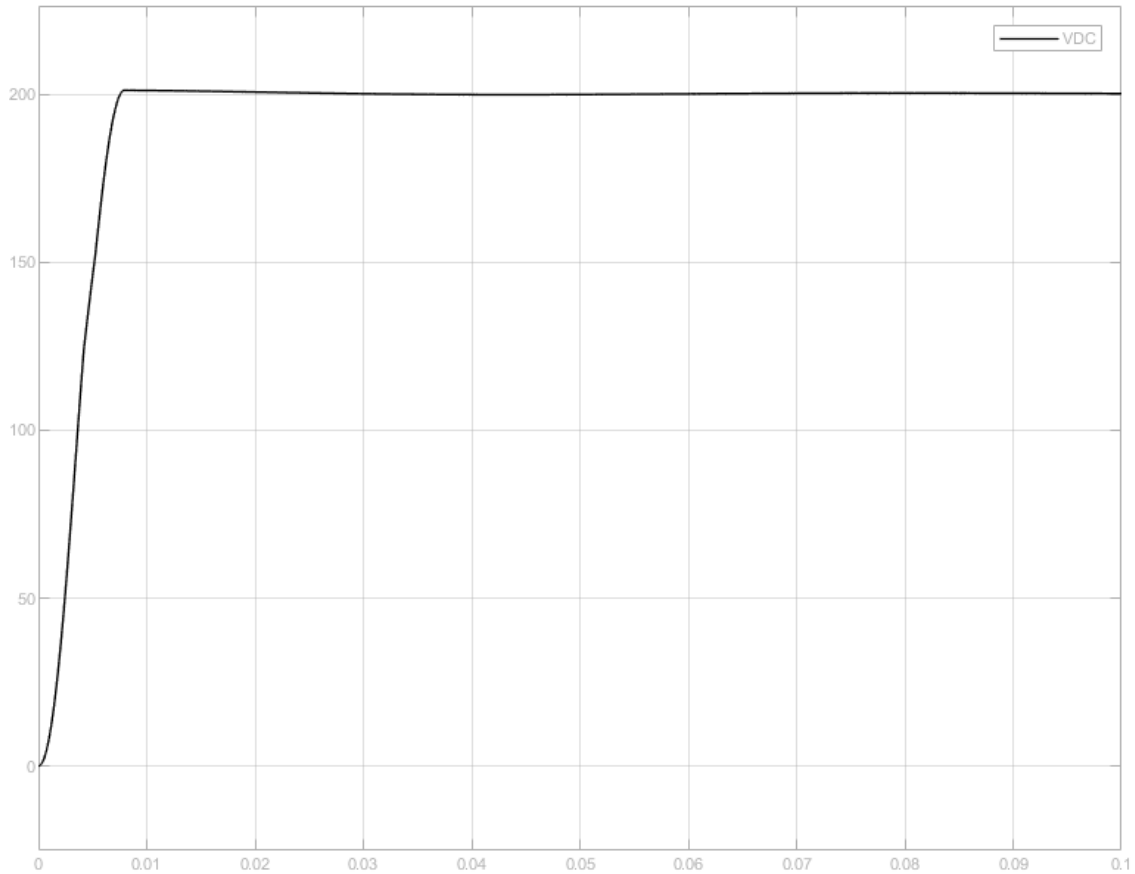


Figure 3.7: The DC-link output of 1KW system

Chapter 4

AC/DC Converter Design

This chapter delves into the realm of AC/DC converter design, shedding light on key aspects such as Filter Design, DC-link capacitor Selection, and Hardware Design. These components play a crucial role in the functionality of the converter, akin to building blocks that contribute to its optimal performance.

Firstly, we explore Filter Design, where we discuss various methods to improve the converter's performance using different types of filters. The aim is to provide a clear understanding of these methods, enabling practitioners to choose the most suitable one for their specific applications.

Moving on, DC-Link Capacitor Selection takes center stage, emphasizing the importance of selecting the right component for effective converter operation. This section guides through the considerations involved in making informed choices.

The chapter then addresses Hardware Design, focusing on the configuration of electronic components to ensure seamless functionality. We will discuss the software program used to design the PCB boards and each board schematic will be presented for elaboration.

The discussion on the significance of precise calculations in determining system parameters forms a critical part of this chapter. These calculations are essential, especially in the design of fast off-board chargers for electric vehicles. By carefully considering factors like filter tuning and DC-link optimization, engineers can make informed decisions, aligning the converter with the demanding requirements of electric vehicle technology.

In essence, this chapter serves as a guide for practitioners, providing insights into the nuanced world of AC/DC converter design, where methodical considerations and informed choices pave the way for an efficient and reliable product.”

4.1 Filter Design

As we are concerned about our health, we use water filters to purify the water. The same happens with electricity; there are impurities in it called harmonics, which are not wanted in our electrical systems. Harmonics affect electrical equipment, increasing its heat, reducing its lifetime and efficiency, and introducing noise to any system connected to the grid. These are just a few of the negativities of harmonics.

So, we use filters, which are devices that filter the frequency of electronic signals by manipulating the waves' amplitude and phase shift. As we know, the sine wave has its amplitude and phase shift, so anything outside the boundaries of its amplitude and phase shift is not desired and needs to be eliminated. This leads us to Fourier series, a mathematical theory that analyzes the signal into the fundamental wave and its harmonics[5].

4.1.1 Filters for Grid-Connected Inverters

The main consideration in choosing between LC and LCL filters is whether the system is connected to the grid or not. Suppose we have an inverter connected to the grid, as in Figure 4.1. We cannot use an LC filter here.

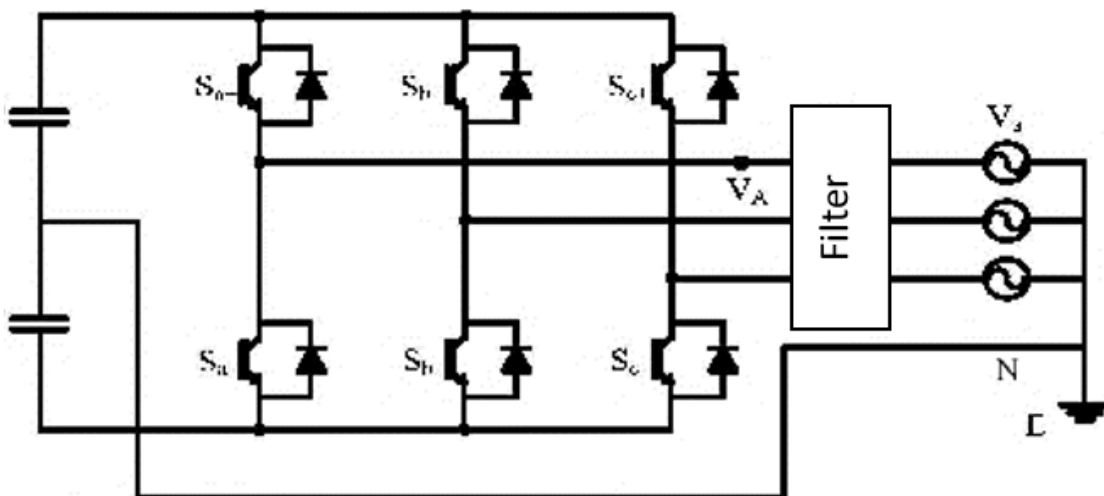


Figure 4.1: Three-phase inverter with passive filter

If we use an LC filter, the capacitors would be considered capacitive loads to the grid, so the power factor (PF) would be leading. This means that the voltage across the capacitors would come before the grid's voltage, and the output current from the inverter would not pass through to the grid but would flow to the capacitors.

In high-frequency harmonics, the grid impedance is less than the capacitive reactance, so in an LC filter, the current will flow to the grid with harmonics. However, in the case of an LCL filter, the grid-connected inductor will block the current, and it will flow to the capacitors. Therefore, we use LCL filters in grid-connected inverters because of the tiny impedance of the grid, which causes a problem in high frequencies.

Here are some specific scenarios where an LCL filter would be a better choice than an LC filter:

- Grid-connected inverters: LCL filters are commonly used in grid-connected inverters to attenuate harmonics and follow grid harmonics standards. The lower resonant frequency of LCL filters makes them less susceptible to resonances caused by the grid impedance.
- High-power applications: In high-power applications, the switching frequency of the power converter is often higher to reduce the size and weight of the inductors and capacitors. This

higher switching frequency can lead to more harmonics, so an LCL filter is often necessary to supply adequate attenuation.

- Applications with a sensitive load: If the load is sensitive to harmonics, such as a motor or a computer system, an LCL filter can help to protect the load from damage.

The design of LCL filters must consider several critical constraints, including current ripple, filter size, and switching ripple attenuation. As noted in [6], the reactive power variation introduced by the capacitor can cause resonance, potentially destabilizing the system. To address this issue, a damping mechanism, such as a resistor in series with the capacitor, is recommended.

This method meticulously outlines the LCL filter design process, emphasizing the importance of proper damping to prevent resonance. The algorithm for selecting LCL filter parameters utilizes the converter's power rating, grid frequency, and switching frequency as inputs.

The following parameters are needed for the design: E_n – Line to line RMS voltage (rectifier input), V_{ph} – phase voltage (rectifier input), P_n – rated active power, V_{DC} – DC bus voltage, f_g – grid frequency, f_{sw} – switching frequency and f_{res} – resonance frequency.

The base impedance and base capacitance are defined by equations 4.1 and 4.2. Thus, the filter values will be referred in % of the base values:

$$Z_b = \frac{E_n^2}{P_n} \quad (4.1)$$

$$C_b = \frac{1}{\omega_n Z_b} \quad (4.2)$$

For the design of the filter capacitance, it is considered that the maximum power factor variation seen by the grid is 5%, as it is multiplied by the value of base impedance of the system: $C_f = 0.05 C_b$, where L_i is inverter side inductor. A 10% ripple of the rated current for the design parameters is given by:

$$\Delta I_{Lmax} = 0.1 I_{max} \quad (4.3)$$

where

$$I_{max} = \frac{P_n \sqrt{2}}{3V_{ph}} \quad (4.4)$$

$$L_i = \frac{V_{DC}}{6f_{sw}\Delta I_{Lmax}} \quad (4.5)$$

The main objective of the LCL filter design is in fact to reduce the expected 10% current ripple limit to 20% of its own value, resulting in a ripple value of 2% of the output current. To calculate the ripple reduction, the LCL filter equivalent circuit is first analyzed considering the inverter as a current source for each harmonic frequency.

The following equations give the relation between the harmonic current generated by the inverter and the once injected in the grid:

$$L_g = \frac{\sqrt{\frac{1}{K_a^2} + 1}}{C_f \omega_{sw}^2} \quad (4.6)$$

where, K_a is the desired attenuation.

A resistor in series (R_f) with the capacitor attenuates part of the ripple on the switching frequency to avoid the resonance. The value of this resistor should be one third of the impedance of the filter capacitor at the resonant frequency and the resistor in series with the filter capacitance is given by 4.9.

$$\omega_{res} = \sqrt{\frac{L_i + L_g}{L_i L_g C_f}} \quad (4.7)$$

$$10f_g < f_{res} < 0.5f_{sw} \quad (4.8)$$

It is necessary to check resonant frequency to satisfy 4.8. If it does not, the parameters should be re-chosen.

$$R_f = \frac{1}{3\omega_{res}C_f} \quad (4.9)$$

Design Example: Low-Rating System (1KW)

A step-by-step procedure to obtain parameters of the filter with considering the following given data, needed for the filter design: $E_n = 100V$ - line to line RMS voltage, $V_{ph} = 57.73V$ - phase RMS voltage, $P_n = 1000W$ - rated active power, $V_{DC} = 200V$ - DC bus voltage, $f_g = 50Hz$ -grid frequency, $f_{sw} = 10KHz$ - switching frequency, $K_a = 20\%$ - attenuation factor is done. Therefore, the base impedance and the base capacitance are:

$$Z_b = \frac{100^2}{1000} = 10\Omega$$

$$C_b = \frac{1}{2\pi * 50 * 10} = 3.18 * 10^{-4}F$$

The filter capacitance can be calculated by:

$$C_f = 0.05 * 3.18 * 10^{-4} = 15.915\mu F$$

To calculate the inverter-side inductor:

$$I_{max} = \frac{1000\sqrt{2}}{3 * 57.73} = 8.16A$$

$$\Delta I_{Lmax} = 0.1 * 8.16 = 0.816A$$

$$L_i = \frac{200}{6 * 10000 * 0.816} = 4mH$$

For the grid-side inductor:

$$L_g = \frac{\sqrt{\frac{1}{0.2^2} + 1}}{15.915 * 10^{-6} (2\pi * 10000)^2} = 95.492\mu H$$

Now, we shall check if the system is within the stable region to avoid resonance:

$$\omega_{res} = \sqrt{\frac{4 * 10^{-3} + 95 * 10^{-6}}{4 * 10^{-3} * 95 * 10^{-6} * 15.915 * 10^{-6}}} = 25952.26rad$$

$$f_{res} = \frac{25952.26}{2\pi} = 4130.4Hz$$

$$10 * 50 < f_{res} < 0.5 * 10000$$

Therefore, the resonant frequency satisfies the equation, and the damping resistance can be calculated as follows:

$$R_f = \frac{1}{3 * 2\pi * 4130.4 * 16 * 10^{-6}} = 0.8027\Omega$$

Simulation

A simulation of this method was done on MATLAB-Simulink to check the performance of the system with the filter using the design example that was mentioned previously in that method. Here is the output voltage V_{DC} :

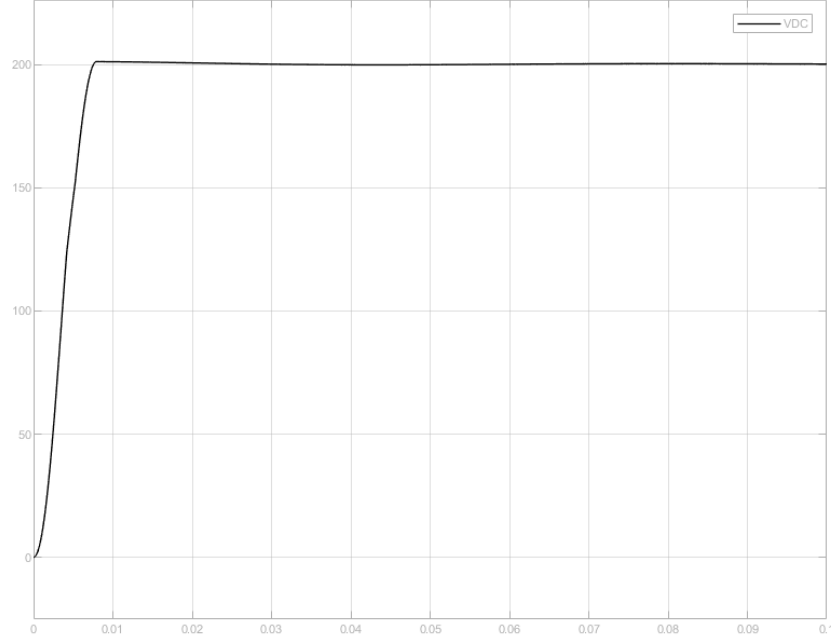


Figure 4.2: The output voltage on the DC-link

Also, we had to check the phase shift between voltage and current of one of the phases as shown in Figure 4.3:

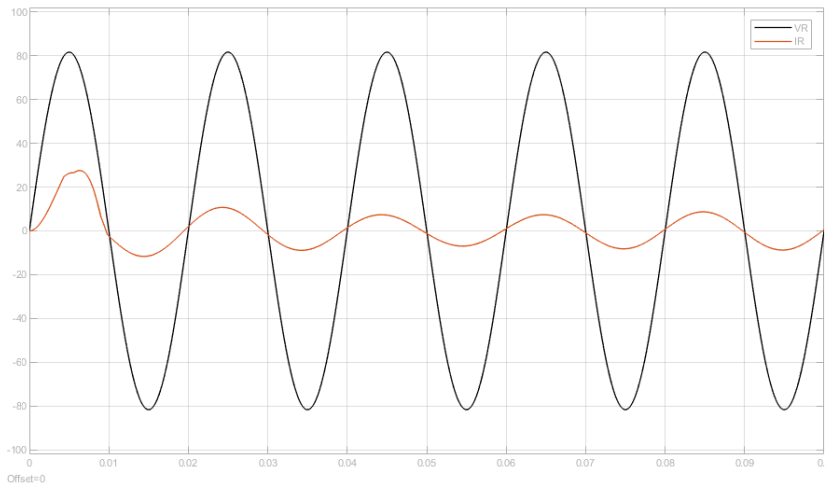


Figure 4.3: The current and the phase voltage of phase R

Note that this is not the actual waveform of the current but a multiple of it. It was multiplied by fifty just so we can observe the two wave-forms at the same time.

The PI controllers were calibrated in a way to have a leading power factor of 0.9998 with settling time of less than a half cycle with settling error of 0.5%. Also, this method's design was checked by equation 4.8, to make sure that the design would avoid resonance problems.

4.2 DC-Link Capacitor Calculations

The DC link capacitor in a three-phase grid-connected inverter serves several critical functions:

- *Smoothing pulsating DC voltage:* Acts as a reservoir to smooth out pulsations, providing stable DC voltage to the inverter.
- *Energy storage:* Provides or absorbs energy during transient conditions to maintain the desired DC voltage level.
- *Filtering harmonics:* Filters harmonic currents generated by the inverter's switching operations, ensuring a cleaner DC supply.
- *Limiting fault currents:* Limits surge currents during faults, protecting the inverter and connected equipment.

Selecting the appropriate DC link capacitor size is critical and depends on several factors:

1. Power rating of the inverter.
2. DC voltage level.
3. Permissible ripple current.
4. Desired ripple voltage.
5. Transient response requirements.
6. Environmental factors (temperature, humidity, vibration).

Using capacitor's stored energy law:

$$C_{dc} = \frac{2 * P_{dc}}{V_{dc}^2 * f} \quad (4.10)$$

where

- f is the grid frequency
- V_{dc} is the DC voltage.
- P_{dc} is the maximum DC power.

4.2.1 System Design (1KW)

A step-by-step procedure to obtain parameters of the filter with considering the following given data, needed for the filter design: $P_n = 1\text{KW}$ - rated active power, $V_{DC} = 200\text{V}$ - DC bus voltage, $f_g = 50\text{Hz}$ - grid frequency. Therefore, the DC-link capacitance is equal to:

$$C_{dc} = \frac{2 * 1000}{200^2 * 50} = 1mF$$

4.3 Component Selection

4.3.1 The Inverter Module

We chose an inverter module for the AC/DC rectification stage prototype in our project. We aim to build a charger that can scale from 7kW to 22kW by cascading. To validate our topology, we started with a lower-rated prototype of 1kW, providing 200V DC and 5A at the output. We selected the 3-phase inverter IC IKCM30F60GDXKMA1, rated at 600V and 35A. We biased the bootstrap with 15V using a DC/DC transformer for isolation and built a protection circuit against over-current and overheating. The module includes an ITRIP pin for automatic shutdown in case of faults, sending a signal to the micro-controller for alerts.

4.3.2 The Current Sensor

The core of our topology is the closed loop feedback, so the measurement must be as accurate as we could to be accurate. We have chosen the CAS transducer, the latest version of the LTS series. The nominal current is 25A to help us with future products. The transducer has a multi-functional primary circuit that changes the nominal current lower to get more accuracy.

Number of primary turns	Primary nominal current rms I_{pn} [A]	Nominal* output voltage V_{out} [V]	Primary resistance R_p [$m\Omega$] (typ.) at $+25^\circ C$	Recommended connections
1	± 25	2.5 ± 0.625	0.24	
2	± 12	2.5 ± 0.600	1.08	
3	± 8	2.5 ± 0.600	2.16	

Table 4.1: Recommended connections for different sensitivities

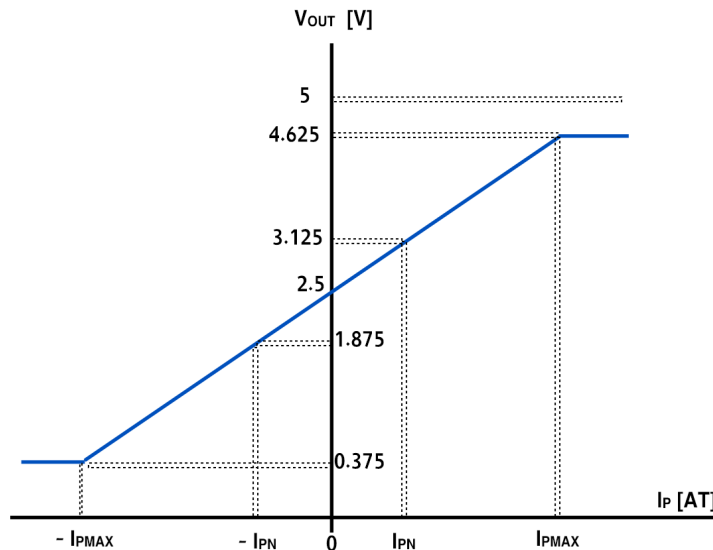


Figure 4.4: V_{out} versus I_p plot

In our Prototype, we used the second technique nominal current 12A. The biggest advantage is that the output signal does not need to re-scale or bias and is ready to send to the micro-controller.

4.3.3 The Voltage Sensor

We have chosen LV 25-P voltage transducer to get the voltage feedback

This transducer needs an external circuit to re-scale and biasing the output signal before the controller, so we used an op-amp circuit after simulating it and get the desired output.

The transducer and the op-amp needed a positive and negative source power, so we used this topology to get the negative source. The following figure shows the internal connection of the sensor:

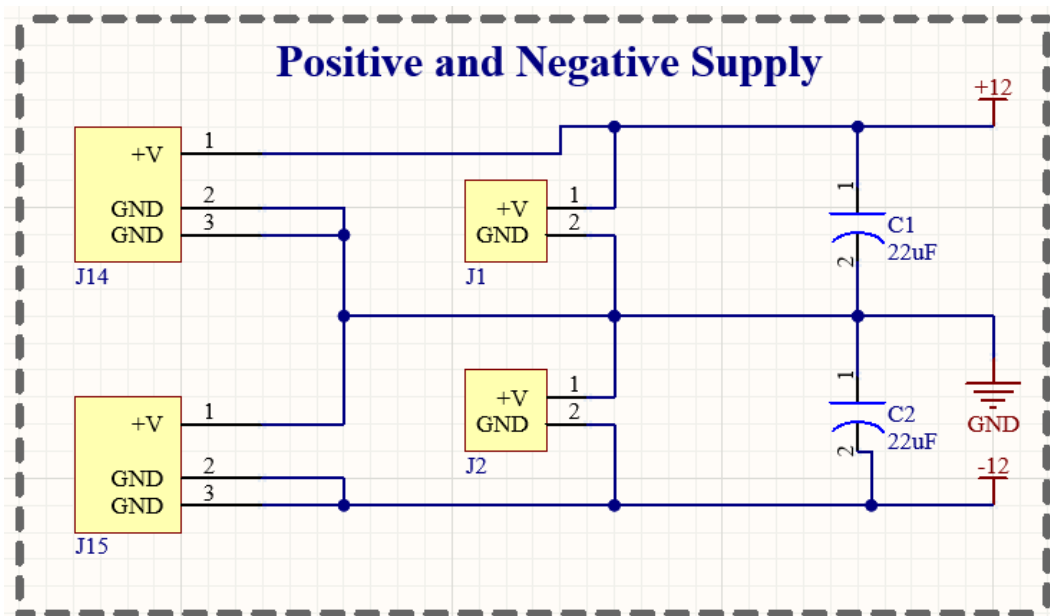


Figure 4.5: The schematic of the supply for the voltage sensor

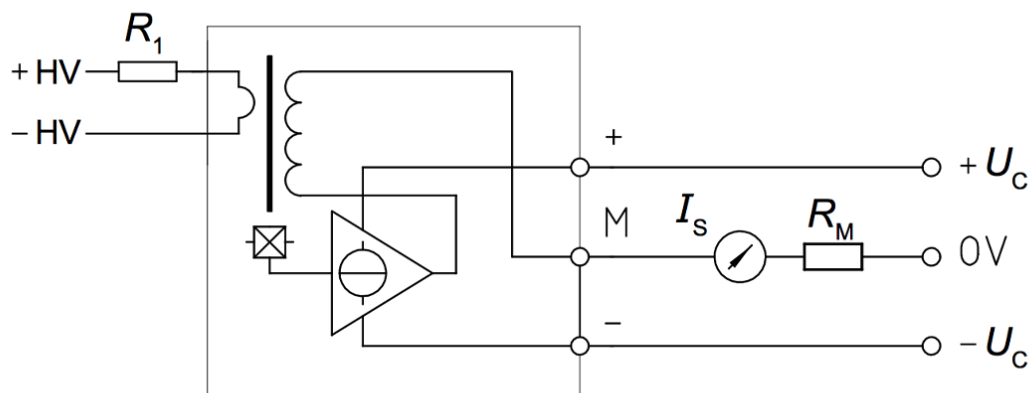


Figure 4.6: The internal connection of the voltage sensor

Primary Side (High Voltage):

- P1 and P2: terminals Connected to the voltage to be measured.
- R1 (External Resistor): Sets the primary voltage range corresponding to primary current of 10 mA.

Secondary Side (Low Voltage):

- +Vc: Connect this terminal to a positive power supply (5 to 15 V DC).
- -Vc: Connect this terminal to the negative power supply.
- OUT: signal to the micro-controller
- Rm (Scaling Resistor): Sets the output voltage range and sensitivity.

The resistors values can be calculated using the following equations:

$$R_m = \frac{V_{out}}{I_{out}} = 132\Omega \quad (4.11)$$

where

- V_{out} is the desired output voltage. (designed for 3.3V)
- I_{out} is the secondary circuit current.

$$R_1 = \frac{V_{in}}{I_p} = 50K\Omega \quad (4.12)$$

where V_{in} is equal to 500V and I_p is 10mA.

Interfacing with Micro-Controller - Op-Amp Technique

In case of AC voltage measurements, DSP can not receive negative voltage So we need to shift the signal out of the transducer to the positive and re-scale it to get the desired output. Op-amp adder circuit will perform this operation to convert $(-3.3V, 3.3V)$ to $(0V, 3.3V)$. *Procedures to Design the Op-Amp circuit:*

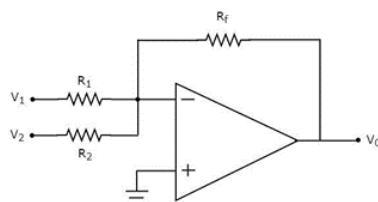


Figure 4.7: Op-amp circuit

where the first terminal represents the scale of input signal and the second terminal is the shift for scaled signal.

For input signal from sensor ,the AC voltage is first scaled to half, then shifted above x axis by this scaled value to obtain its peak positive value (V_{in}) and 0V.

$$-V_{out} = \left(\frac{R_f}{R_1} * V_{in} \right) + \left(\frac{R_f}{R_2} * V_2 \right) \quad (4.13)$$

for AC $V_{in} = 3.3V$

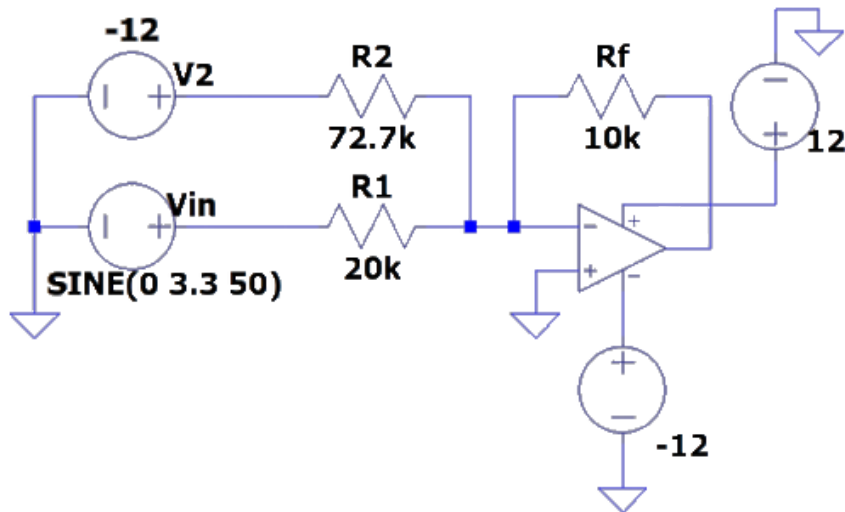


Figure 4.8: The circuit diagram of the op-amp

1. Scale the input signal to $\frac{1}{2}V_{in}$
 $\frac{R_f}{R_1} * V_{in} = 3.3/2$, assume $R_f = 10k\Omega$, so $R_1 = 20k\Omega$
2. Shift by $\frac{1}{2}V_{in}$
 $\frac{R_f}{R_2} * (V_2) = 3.3/2$, assume $V_2 = -12v$, so $R_2 = 72.7k\Omega$

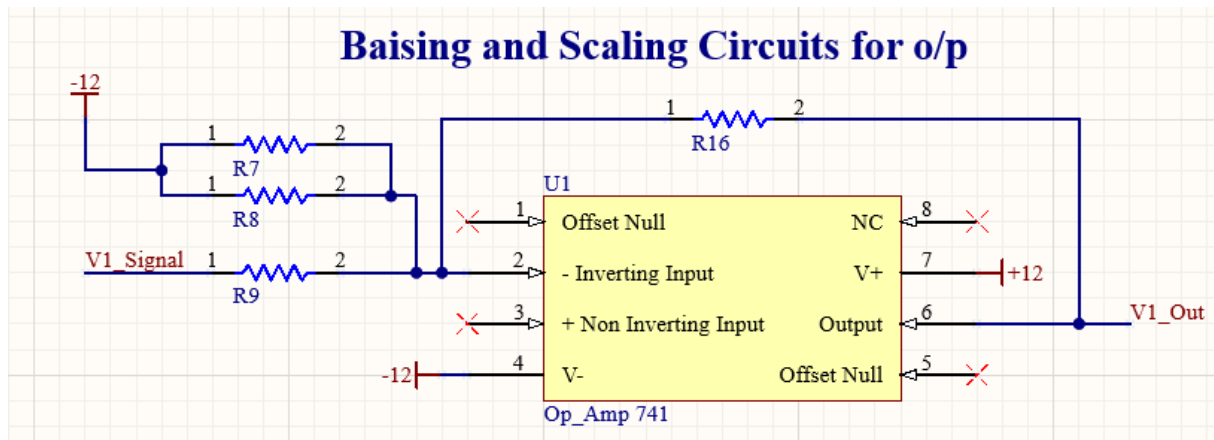


Figure 4.9: The schematic of the op-amp circuit

4.3.4 The Micro-Controller

We have chosen to use DSP LaunchpadF28069M, because it is the easier controller to generate our model on it. We built a DSP interfacing with the inverter using optocoupler circuit to make the suitable isolation. For further references click here: [datasheet](#).

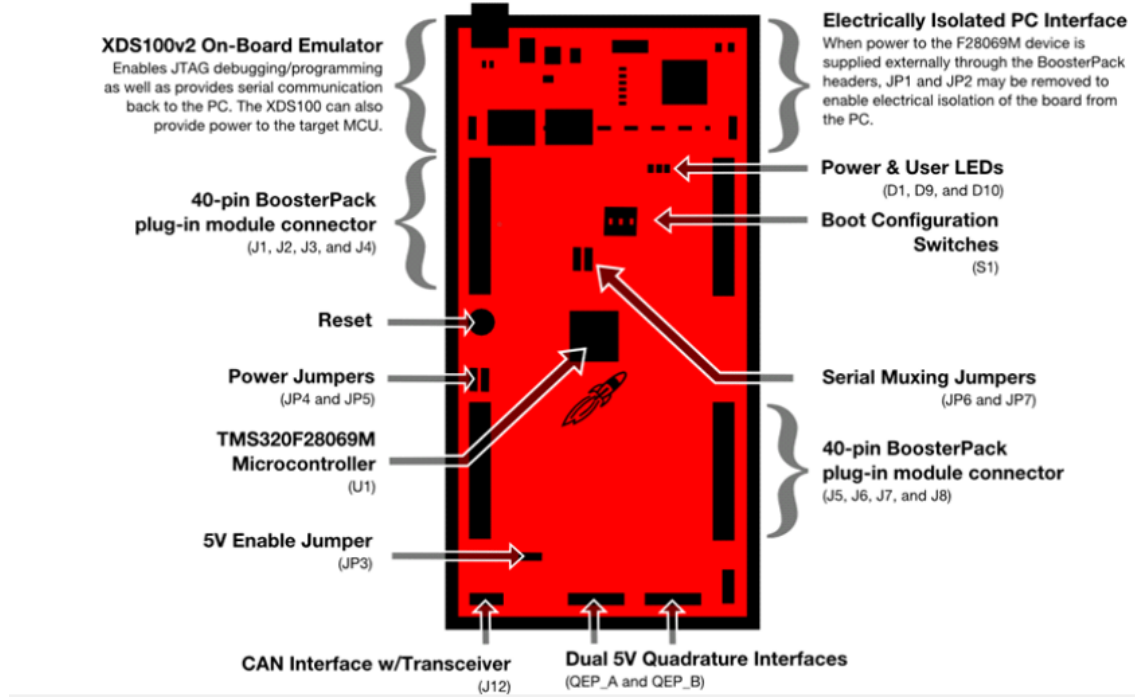


Figure 4.10: DSP LaunchpadF28069M

4.4 Hardware Design

Our hardware design process involved developing five specialized PCBs—Inverter module, DC-link board, current sensors board, voltage sensors board for feedback, and a micro-controller interfacing board. Altium Designer, version 2024, played a pivotal role in this endeavor, chosen over alternatives like Eagle for specific reasons.

Altium Designer's selection hinged on its robust feature set. Its advanced tools facilitated precise design implementation, crucial for our intricate requirements.

Choosing Altium Designer over Eagle was a strategic decision based on its advanced features, multi-board design capabilities, documentation quality, community support, and scalability. This choice streamlined our PCB design for the inverter system efficiently.

4.4.1 The Inverter Module

This board is considered the main board as it interfaces with the micro-controller and the DC-link board, also it interfaces to collect the feedback from the current and the voltage sensors boards. This board has indicating green LED to indicate the power connection, a red LED to indicate faults, several test points, IDC connecting cable to interface with the micro-controller and bootstrap circuits.

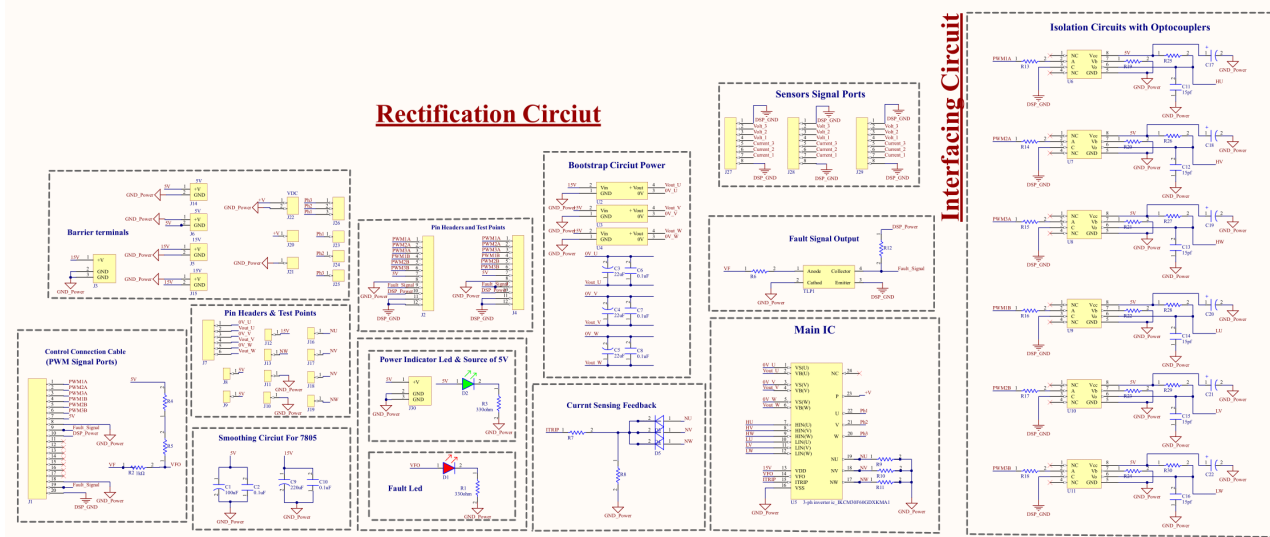


Figure 4.11: The schematic of the inverter module board

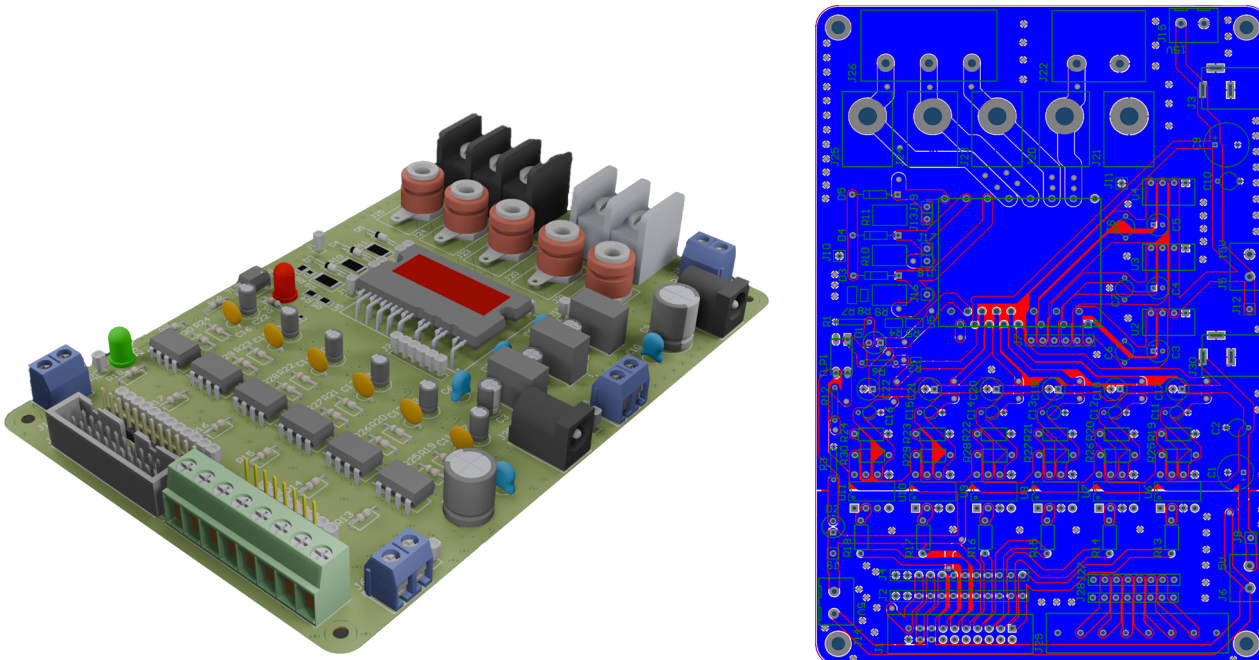


Figure 4.12: Inverter module hardware board design

4.4.2 DC-Link

According to our calculations that we have done in previous sections, we have designed a DC-Link to suit our project to literally link between the AC/DC Conversion and the DC/DC Conversion boards.

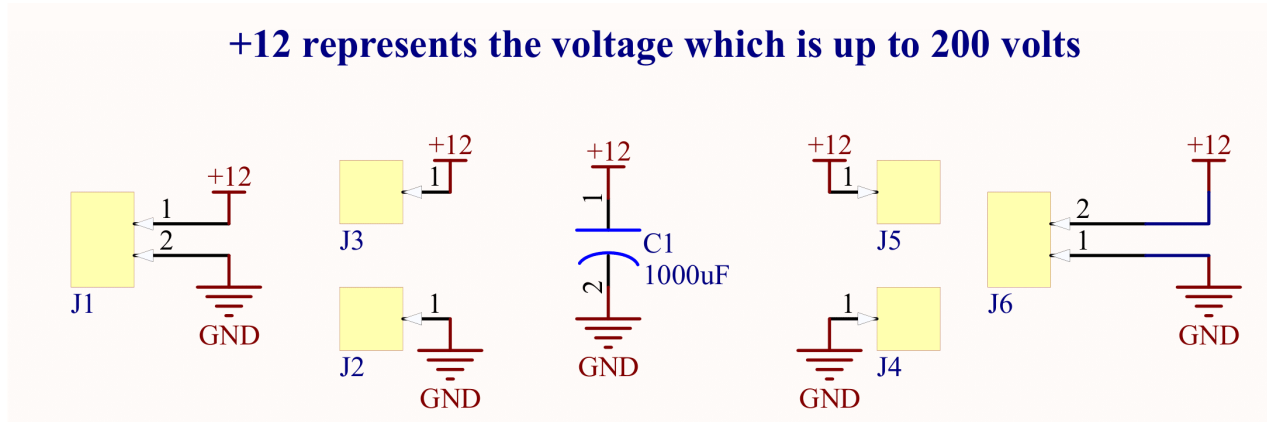
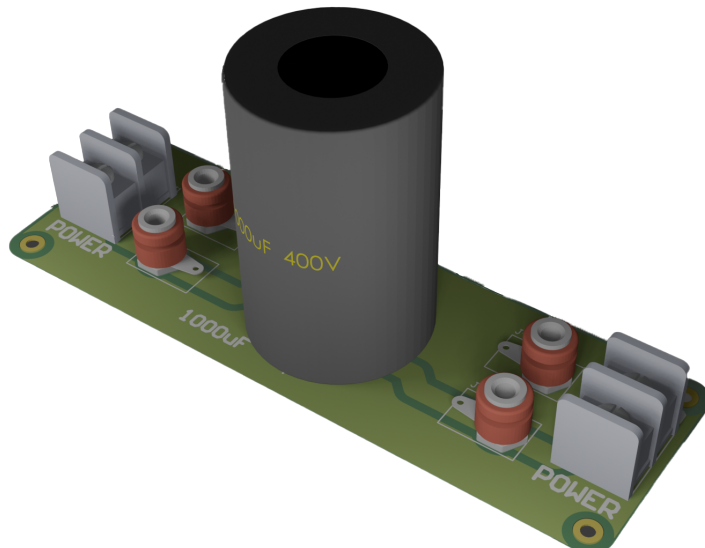
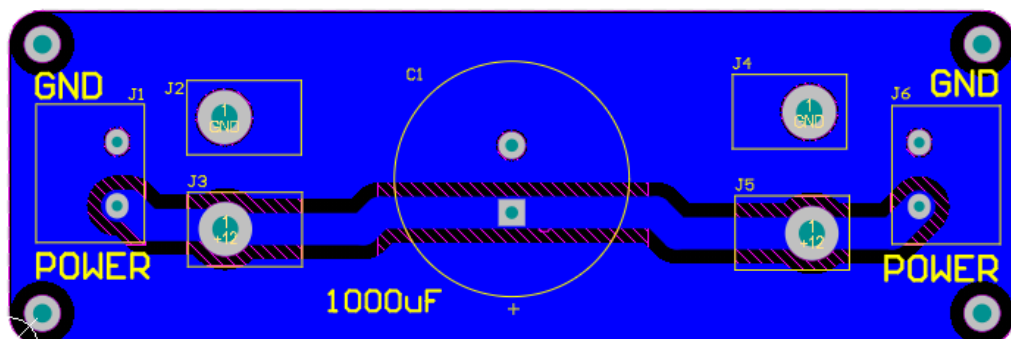


Figure 4.13: The schematic of the DC-link board



(a) DC-link PCB 3D design



(b) DC-link board - bottom layer

Figure 4.14: DC-link hardware board design

4.4.3 Current Sensors

This board is designed for three current sensors. It also has LED indicator to indicate the power connection. It interfaces with the main board to provide current feedback.

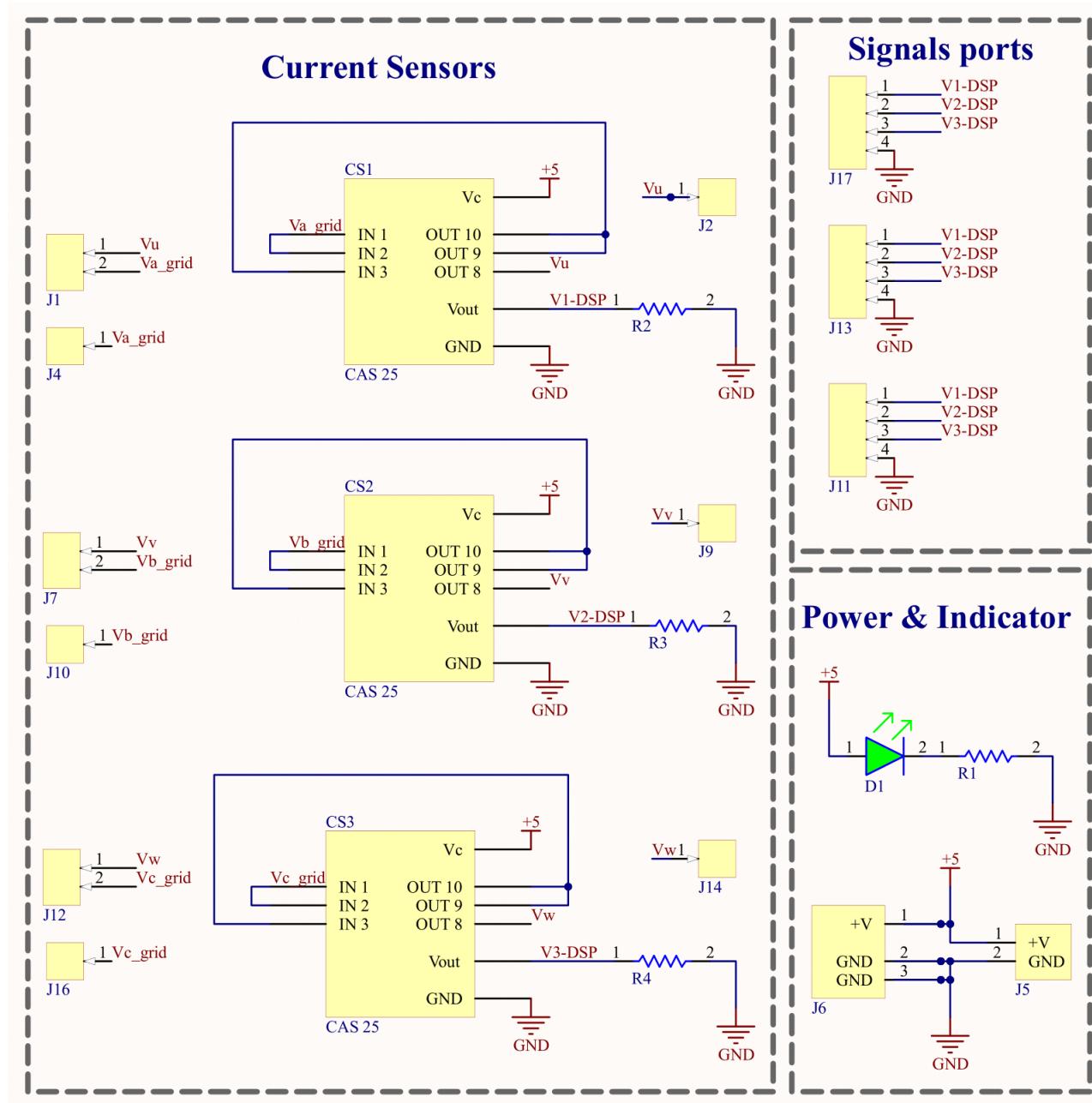


Figure 4.15: The schematic of the current sensors board

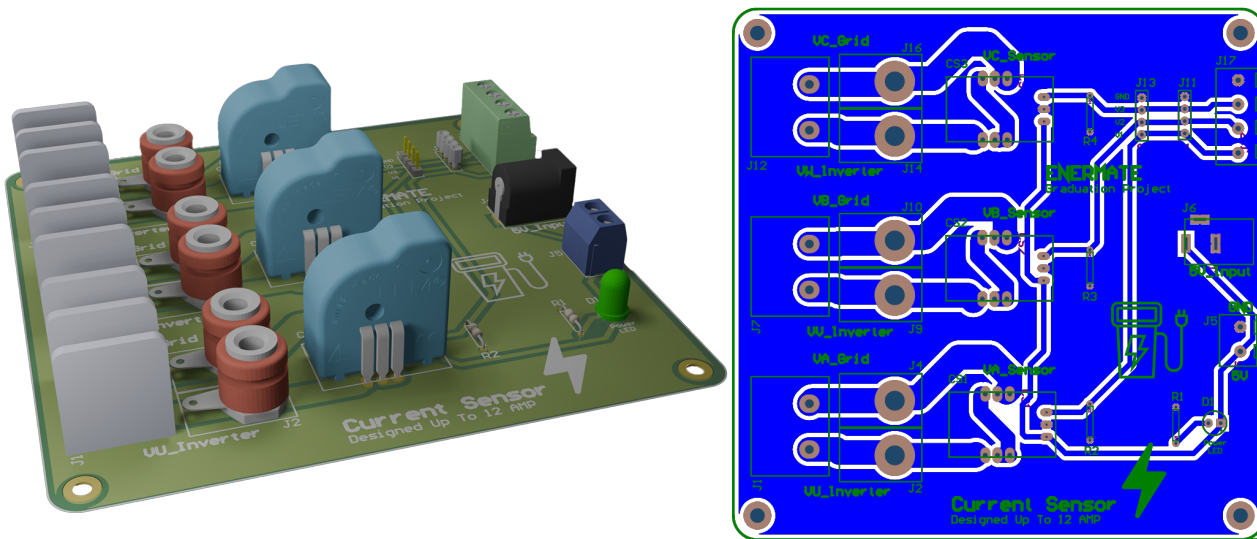


Figure 4.16: Current sensors hardware board design

4.4.4 Voltage Sensors

This board is designed for three voltage sensors, two of them will be used as feedback of the input line voltage and the last one will be used as feedback for the output DC voltage. It also has an LED indicator to indicate the power connection.

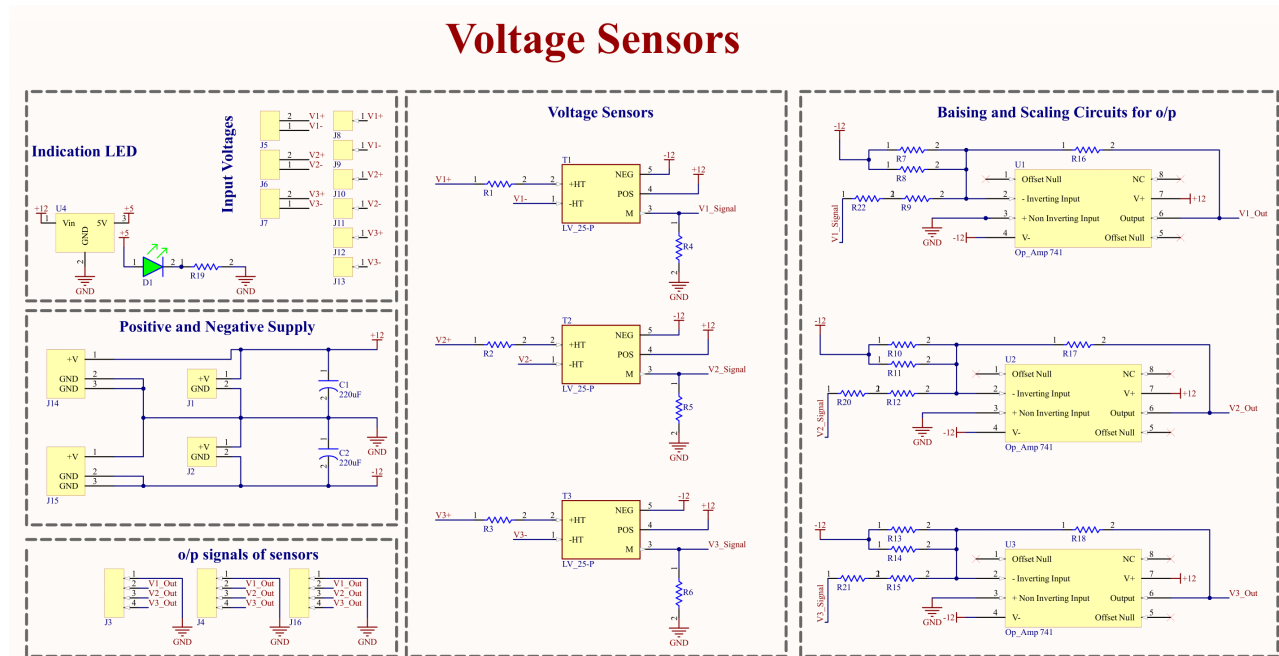


Figure 4.17: The schematic of the voltage sensors board

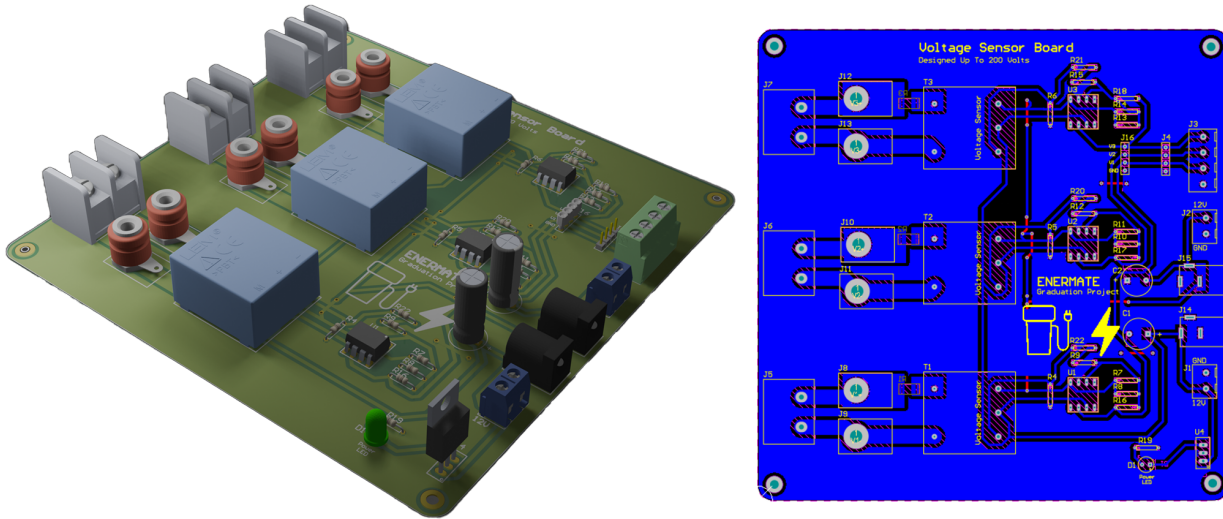


Figure 4.18: Voltage sensors PCB

4.4.5 Micro-Controller Interfacing

This board acts as a shield for the DSP. It has several isolation optocouplers to protect the micro-controller from any fault.

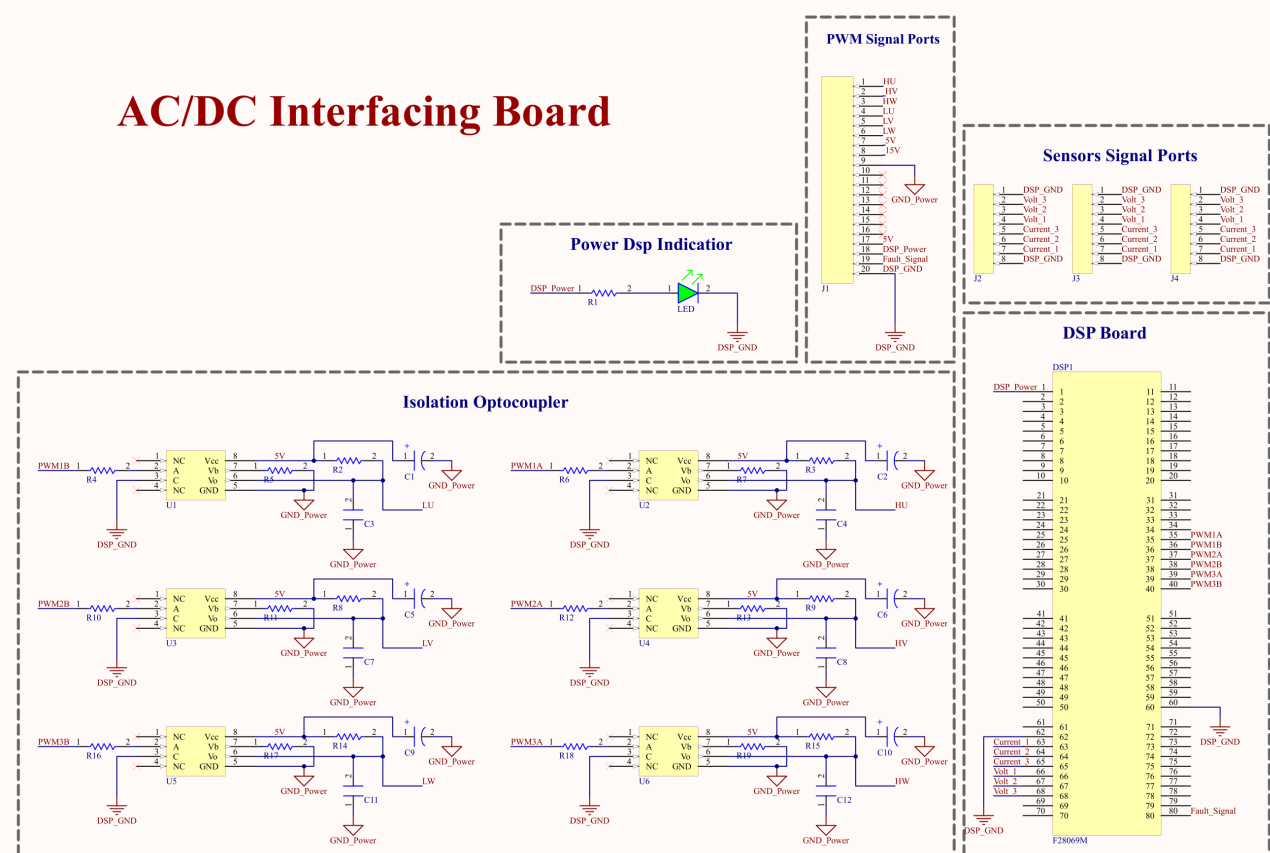


Figure 4.19: The schematic of the DSP interfacing board

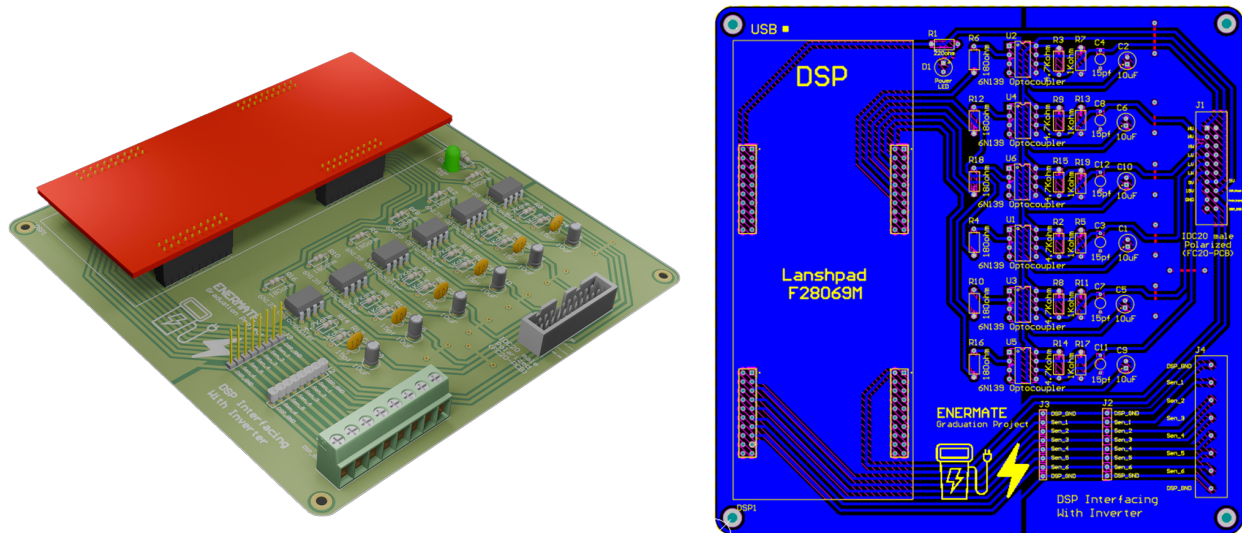


Figure 4.20: DSP interfacing hardware board design

Chapter 5

Hardware Calibration

This chapter includes tests of various components such as voltage sensor, current sensor, etc. Also, it includes the final hardware product and its operation.

5.1 Testing of Voltage Sensor (LV 25-P)

5.1.1 Objective

Evaluate the performance of the voltage sensor, ensuring accurate output and proper biasing within predefined voltage ranges.

5.1.2 Equipment

- Voltage sensor LV 25-P.
- Designed R_{in} , R_m values of the sensor.
- Op-amp circuit with calculated resistor values.
- Single-phase auto-transformer.
- Micro-controller (DSP LaunchPad F28069M).

5.1.3 Procedure

1. Voltage Circuit Setup:

- Connect the voltage circuit with designed R_m value for required output voltage of the transducer. This will regulate the output voltage feeding into the op-amp circuit.
- Design R_{in} for the required ratings of the measured voltage.

2. Op-Amp Biasing Circuit Construction:

- Build the biasing circuit using the op-amp adder configuration with pre-calculated resistor values. This sets the desired output voltage delivered to the DSP (including biasing and gain adjustments for the op-amp input signal).

3. Primary Side Connection:

- Connect the primary side of the sensor to the auto-transformer.

4. Biasing Verification:

- With 0V input, measure the output voltage. This should correspond to the predetermined op-amp biasing value.

5. Output Voltage Verification:

- Apply various input voltage values.
- Compare measured output voltages with pre-calculated values for accuracy.
- Ensure the maximum output voltage never exceeds 3.3V.

6. Sensor Calibration:

- Connect the sensor circuit output (output of op-amp circuit) to the DSP.
- Utilize the DSP's ADC block to convert the analog signal to a digital reading.
- Set the pin name corresponding to the connected output.
- Expect the analog reading to match the digital reading after multiplying by (3.3/4095) (considering 12-bit ADC with reference voltage of 3.3V).
- Account for the biasing value shifting the signal above the x-axis in the analog domain.
- Subtract the measured practical shift from the signal to center it around the x-axis.
- Determine the actual maximum value achieved.
- Apply a gain factor to scale the measured input voltage to match the sensor's expected output range.

5.1.4 Documentation

- Record all measured data (input voltages, output voltages, biasing values).
- Calculate discrepancies between measured and expected values.
- Note any observations regarding sensor behavior or circuit limitations.

5.1.5 Notes

- Exercise caution when handling high voltage. Ensure proper safety procedures are followed.
- Double-check all connections and resistor values before applying power.

5.2 Testing of Current Sensor (LTS 25-P)

5.2.1 Objective

Evaluate the performance of the voltage sensor, ensuring accurate output and proper biasing within predefined voltage ranges.

5.2.2 Equipment

- Current sensor LTS 25-P.
- R_l "10KΩ".
- AC & DC current controlled power supplies.
- Micro-controller (DSP LaunchPad F28069M).

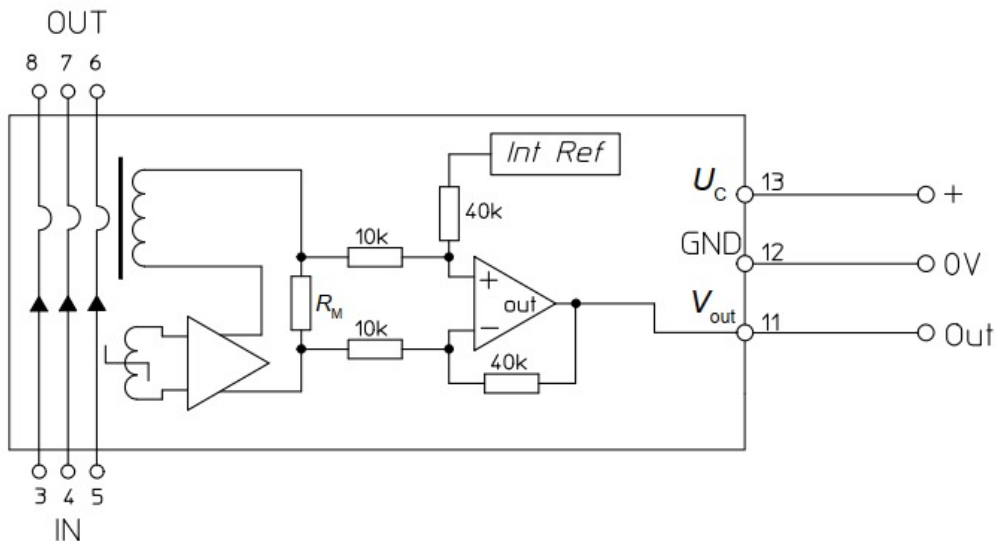


Figure 5.1: The schematic of the current sensor

5.2.3 Connection

- The 6 pins of input and outputs are connected in different ways according to the current rating..
- GND: connected to gnd of power supply.
- Vout: connected to micro-controller and it's value is corresponding to the current flow through the sensor.
- R_l: resistor to limit output current and typically equal to 10KΩ.

5.2.4 Procedure

1. Connect the Uc to a 5V DC supply.
2. Check the output voltage of the sensor at no input current using oscilloscope “typically 2.5V”.
3. Connect the sensor to DC current controlled power supply and start with 1Ampere.
4. Connect the sensor output to an ADC input pin of micro-controller “DSP”.
5. Convert the output of ADC to an equivalent volt by multiplying the output by gain.”gain = $3.3/4095$ in case of DSP F28069M”
6. Subtract the output by the measured Voltage value at no input.
7. Convert this measured value to a corresponding current value using a gain equal to $(\text{max current} / (3.3 - 2.5))$ “typically equals 20”. Where 3.3 is the output voltage at maximum current flowing through the sensor.
8. Change the input current to 2Amp then 3amp ... and notice the sensor response.
9. Monitor the output of and begin to change the gain slightly until making the sensor output equal to the actual applied current.
10. Repeat the steps with AC current controlled supply.

5.3 Open Loop Test Procedure

5.3.1 Objective

As in the industry we wanted to take the tests gradually till we reach the closed loop voltage control which is the endpoint purpose.

5.3.2 Equipment

- DC Voltage Supply.
- Micro-controller (DSP LaunchPad F28069M).
- Three-Phase motor.

5.3.3 Procedure

1. Hardware interfacing with the Micro controller:

- Connect the DC supply to input of the board with the inverter module to operate as an inverter.

- Connect the output to a 3-phase motor as to a load to be fed from the inverted signals coming from the inverter module.

2. Loading the Software to the Micro controller:

- As there is no control it's just needed to apply PWMs to the inverter module with the desired duty cycle.
- Build a model like the one showing in the following figure.

5.3.4 Documentation

- Observe the Motor reaction to the applied voltage.
- Note the applied voltage out from the inverter Board.
- Note any observations regarding Motor behavior or circuit limitations.

5.3.5 Notes

- Be cautious not to apply a very high voltage from the DC supply.
- check connections and make sure every component is well-handled.

5.4 Phase Locked Loop Test

5.4.1 Objective

Phase Locked Loop plays an important role in Grid Synchronization so we first need to make sure of the phase angle produced is proper before going into the upcoming step which is integration of the system with the grid.

5.4.2 Equipment

- Voltage sensor LV 25-P.
- Three-phase auto-transformer.
- Three-phase high power resistor.
- Micro-controller (DSP LaunchPad F28069M).

5.4.3 Procedure

1. Hardware adjustment:

- Connect the Three-Phase Transformer with the Grid then, in series with the inputs of the Voltage Sensors add the Three-Phase Resistor.
- Connect the previously determined analog pins of the Micro-Controller to the Voltage Sensors.
- Upload the already built simulink model to the Micro-Controller.

2. Loading the Software to the Micro controller:

- The model mainly consists of measuring the line voltages across the grid (VUV and VUW) and then, calculating the phase voltages.
- The measured phase voltages (in per-unit) are inputs the Three-Phase PLL Block.
- Build a model like the one showing in the following figure.

5.4.4 Documentation

- Observe the angle signal as it should be a saw-tooth.
- make sure of the grid sequence as any outage leads to a phase change from the grid.
- any phase change will lead to undesired results as instead of the two quadrature components cancel each other they would be added so the result won't be zero.

5.4.5 Notes

- any phase change will lead to undesired results as instead of the two quadrature components cancel each other they would be added so the result won't be zero.
- check connections and make sure every component is well-handled.

5.5 Current-Controlled Inverter

5.5.1 Objective

This test is performed to control the output current. It consists of two main parts: Connection to star-connected inductive load and connection to the grid. the first part of the test is done as an essential procedure before connecting the converter to the grid.

5.5.2 Equipment

- DC Voltage Supply.
- Micro-controller (DSP LaunchPad F28069M).
- Three-Phase inductive load.
- Current sensors.
- Voltage sensors.

5.5.3 Procedure

Part 1: Star-Connected Inductive Load Connection

1. Hardware Interfacing with the Micro-Controller:

- Perform the PLL test to have the required ω_t signal.
- Connect the DC supply to input of inverter module (dc side) to operate as an inverter.
- Connect the output of the inverter module (ac side) to the input of the current sensors.
- Connect the output of the current sensors to the three-phase star-connected inductive load.
- The ADC pins of the micro-controller should be connected to the current sensors.
- And finally the PWM pins should be connected to the gating signals in the inverter module.

2. Loading the Software to the Micro-Controller:

- Download the Simulink model to the micro-controller which is as shown in the following figure.

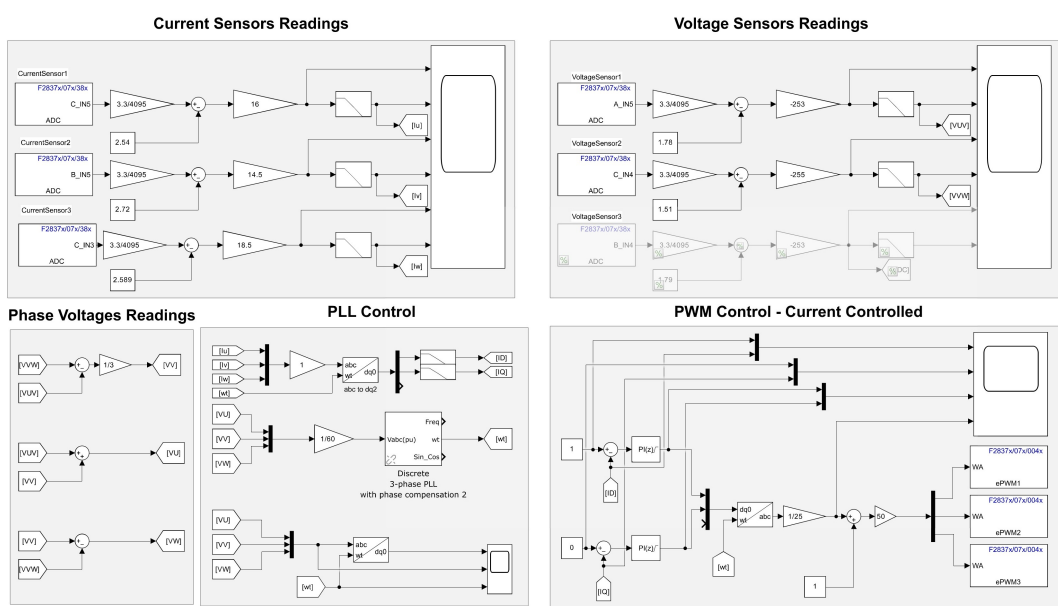


Figure 5.2: Current-controlled inverter - Simulink model

3. Operation:

- Start from zero voltage after making sure that the PLL test is performed correctly.
- Set the current to be controlled to one ampere and increase the voltage gradually.
- Monitor the current scope to make sure that the current reaches the required limit.
- Change the reference current to ensure the operation of the system.

Part 2: Grid Connection

4. Hardware Modifications:

- Disconnect the electricity from the whole circuit and stop the simulation.
- Disconnect the current sensors from the inductive load and connect them to the grid.
- Perform the operation procedure once more.

5.5.4 Documentation

- Note any observations regarding the DC supply current.

5.5.5 Notes

- Make sure that the connection with the current sensors is configured correctly in order to control the flow of the current.

5.5.6 Results

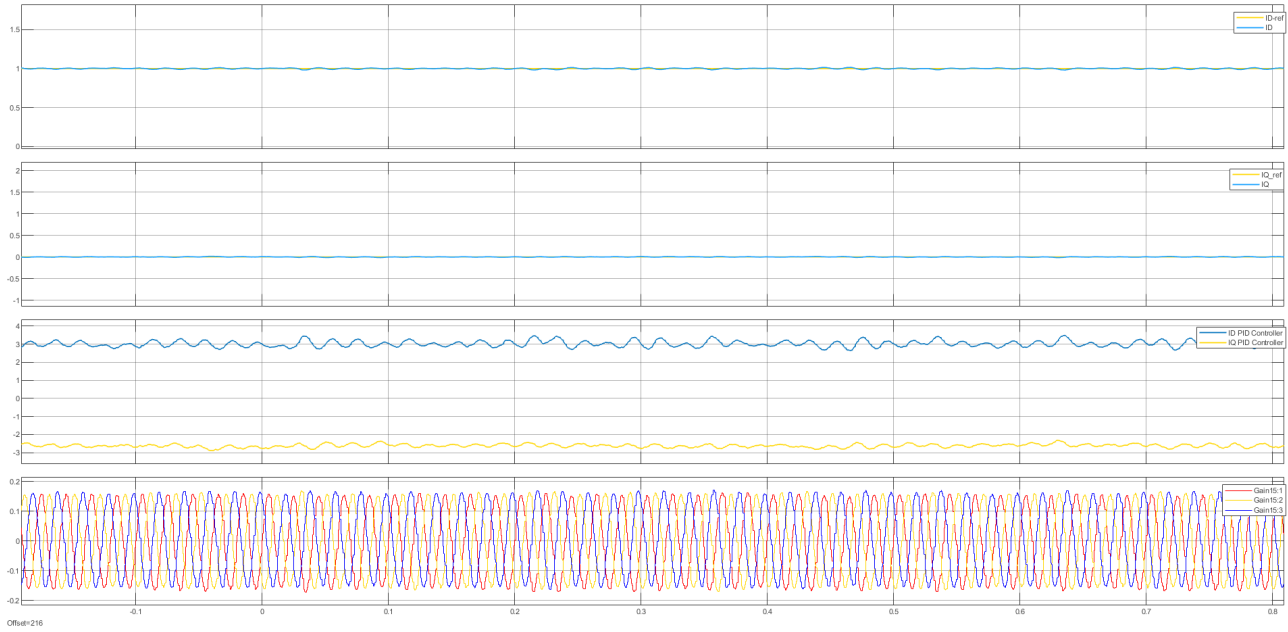


Figure 5.3: Current behavior during normal operation with inductive load

Figure 5.3 shows the current behavior during normal operation with inductive load. The current is controlled to maintain a steady value as specified by the reference current setting. The waveform indicates stable operation under nominal conditions.

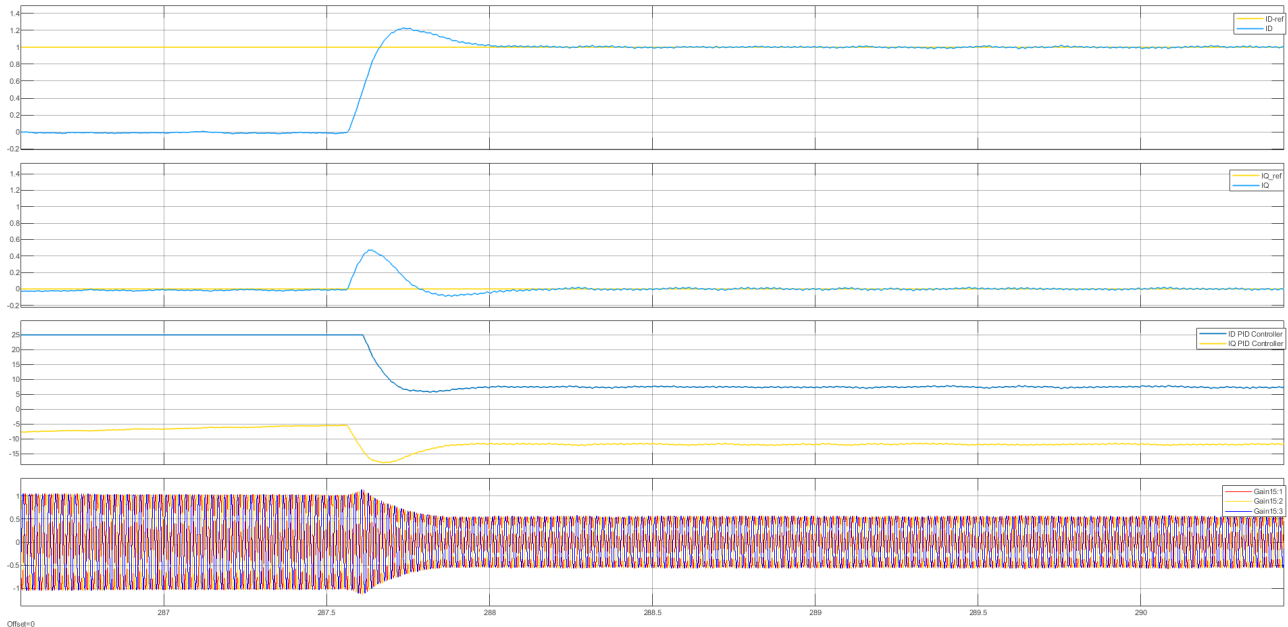


Figure 5.4: Current behavior when DC supply voltage changes

Figure 5.4 illustrates the current response when the DC supply voltage is changed. The current controller adjusts to maintain the desired current, showcasing the system's robustness against supply voltage variations.

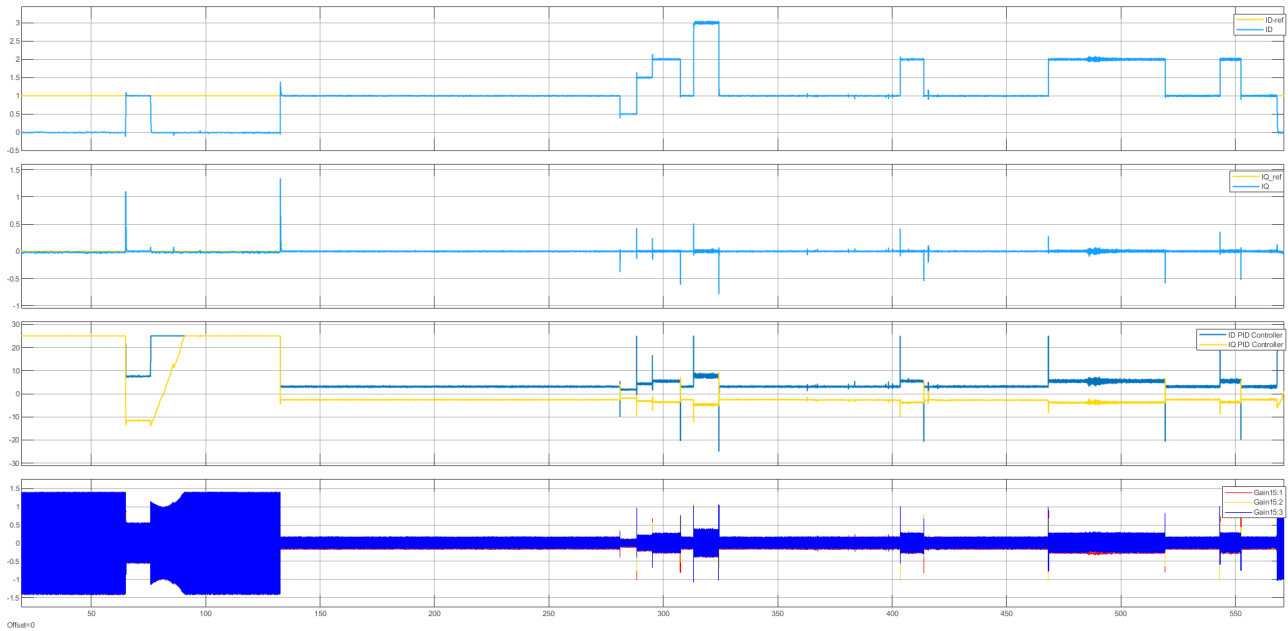


Figure 5.5: Current behavior when reference current is changed

Figure 5.5 demonstrates the current behavior when the reference current is altered. The system responds by adjusting the output current to match the new reference value, verifying the dynamic response and accuracy of the current control mechanism.

5.6 VOC Controlled Rectifier

5.6.1 Objective

This test is performed to control the output current. It consists of two main parts:

1- Connection to a DC Supply

2- Connection to a Battery.

the first part of the test is done as an essential procedure to tuning the inner PI controller. the second part is done as an essential procedure to tuning the outer PI Controller.

5.6.2 Equipment

- Three-Phase Power Supply.
- DC Voltage Supply.
- Micro-controller (DSP LaunchPad F28069M).
- Current sensors.
- Voltage sensors.

5.6.3 Procedure

Part 1: Current Control Rectifier connected to DC Supply

1. Hardware Interfacing with the Micro-Controller:

- Perform the PLL test to have the required ω_t signal.
- Connect the DC supply to the input of the inverter module (DC side) to operate at a constant voltage.
- Connect the output of the inverter module (AC side) to the output of the current sensors.
- Connect the input of the current sensors to the three-phase Supply.
- The ADC pins of the micro-controller should be connected to the current sensors.
- And finally the PWM pins should be connected to the gating signals in the inverter module.

2. Operation:

- Start from zero voltage after making sure that the PLL test is performed correctly.
- Set the current to be controlled to one ampere and increase the voltage gradually.
- Monitor the current scope to make sure that the current reaches the required limit.
- Change the reference current to ensure the operation of the system.

Part 2: Voltage Control rectifier with Charging the battery

3. Hardware Modifications:

- Disconnect the electricity from the whole circuit and stop the simulation.
- Disconnect the DC supply from the inverter module.
- Connect DC load to the inverter module.

5.6.4 Documentation

- Note any observations regarding the DC supply current in part 1.
- Note any observations regarding the DC output voltage in part 2.

5.6.5 Notes

- Make sure that the connection with the current sensors is configured correctly in order to control the flow of the current.

Part II

DC/DC Conversion

Chapter 6

Introduction to DC-DC Converters

DC-DC converters are essential components in modern electronic systems, facilitating the efficient conversion of one DC voltage level to another. These converters play a pivotal role in a wide array of applications, ranging from portable electronic devices to large-scale power distribution systems. By altering voltage levels, DC-DC converters enable the optimization of power delivery, enhancing energy efficiency and system performance.

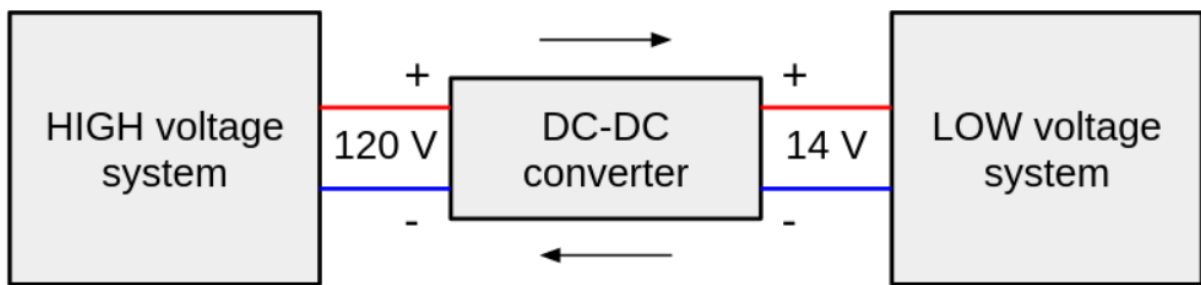


Figure 6.1: DC-DC Conversion from one voltage level to another

Furthermore, DC-DC converters are essential electronic circuits that play a critical role in modern power management systems. Their primary function is to convert the voltage of a direct current (DC) source from one level to another, ensuring stable and efficient power delivery to various electronic devices and systems. In applications where input voltage levels can fluctuate due to factors such as battery discharging over time or changes in load conditions, DC-DC converters maintain a constant output voltage, providing reliable power to the system's components.

One significant advantage of DC-DC converters is their superior power conversion efficiency. By using switching techniques, DC-DC Converters can minimize power losses associated with resistive elements, such as transformers or linear regulators, which typically generate heat and waste energy. This results in better overall efficiency and prolonged battery life in portable devices. Moreover, DC-DC converters offer the flexibility to step up or down voltage levels, allowing for efficient power distribution management in electronic systems. They can also provide galvanic isolation, separating the input and output grounds to reduce the risk of ground loops and safeguard sensitive components from voltage spikes and noise.

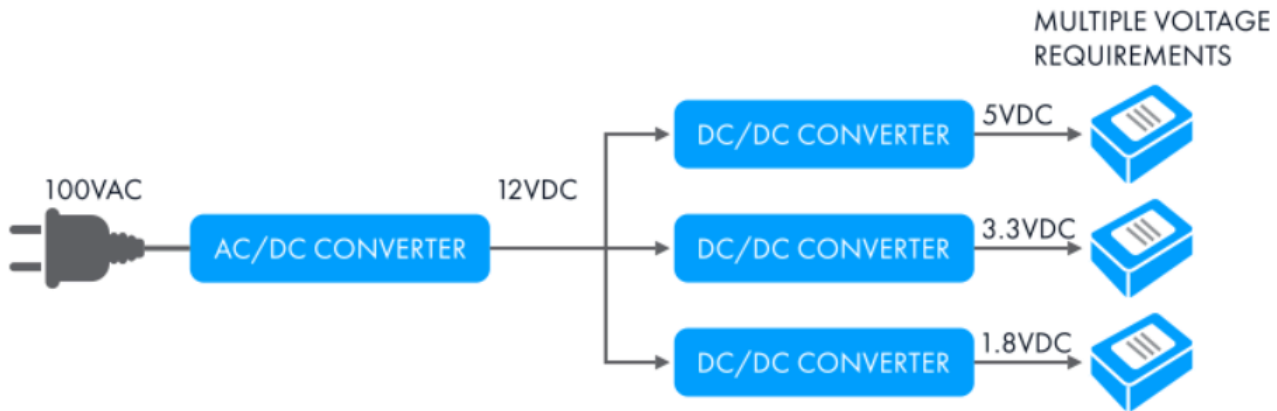


Figure 6.2: DC-DC Converters for Multiple Voltage Requirements

Another noteworthy feature of DC-DC converters is their precise voltage regulation. Some converters can maintain output voltage accuracy within a narrow range, typically with less than a 1 percent deviation. This level of precision is vital for ensuring the proper operation of electronic devices and systems that require stable power supplies.

DC-DC converters come in various topologies and configurations, catering to a broad range of applications and power requirements. They can be designed as standalone devices, integrated into larger power management systems, or embedded into individual components, such as microprocessors or micro-controllers.[7]

6.1 Principle of Operation

The fundamental principle behind DC-DC converters is the conversion of electrical energy from one voltage level to another. This conversion is achieved through the manipulation of electrical components such as semiconductor switches (transistors), inductors, capacitors, and diodes.

DC-DC converters operate on the principle of energy storage and transfer. They utilize switches to control the flow of electrical current through inductive and capacitive elements, thereby altering the voltage levels while maintaining the continuity of power delivery.

The operation of DC-DC converters involves switching cycles where the input voltage is modulated to produce the desired output voltage. Control mechanisms such as pulse-width modulation (PWM), voltage regulation feedback loops, and control algorithms ensure precise voltage regulation and efficient power conversion.

Power supply designers often use isolated DC/DC converters to realize galvanic isolation, meet safety requirements and enhance noise immunity. When designing an isolated DC/DC converter, output voltage regulation accuracy is one of many design objectives to consider and the required level can vary from one application to the next. Better than ± 5 percent overall voltage regulation is adequate in some while ± 10 percent might be necessary for others.

The many power management topologies and regulating schemes for isolated DC/DC converters differ widely in voltage regulation accuracy. For example, the feedback and control of a closed-loop isolated DC/DC converter is shown in Figure 6.3. [8]

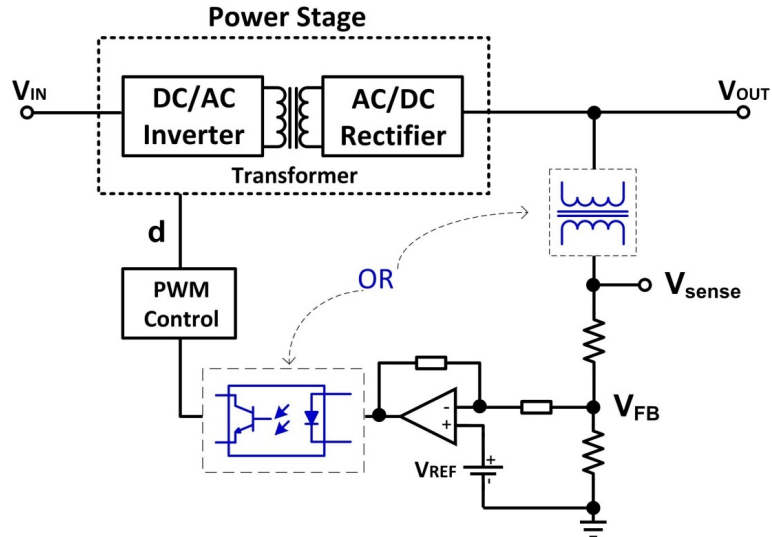


Figure 6.3: Feedback and Control of a Closed-loop Isolated DC/DC Converter

In this example, a transformer is used to electrically isolate the output from the input of the power stage. In a closed-loop isolated DC/DC converter, the feedback circuitry senses the output voltage and generates an error by comparing the sensed voltage with a voltage reference. The error is then used to adjust the control variable, for example, duty cycle, to compensate for the output deviation. Galvanic isolation between control circuitry on the primary side and secondary side is also essential. Such isolation can be achieved by utilizing either a transformer or an optocoupler. Assuming the reference voltage is precise and stable over temperature changes, regulation accuracy mainly depends on output voltage sensing accuracy. In other words, how well V_{SENSE} resembles V_{OUT} . [8]

6.2 Types of DC-DC Converters

Buck Converter (Step-Down Converter): The buck converter is a widely used DC-DC converter that produces an output voltage lower than the input voltage. It achieves this by intermittently connecting the input voltage source to the output load through a semiconductor switch (usually a MOSFET). The energy stored in the inductor during the ON state of the switch is transferred to the output during the OFF state, resulting in a lower output voltage. [7]

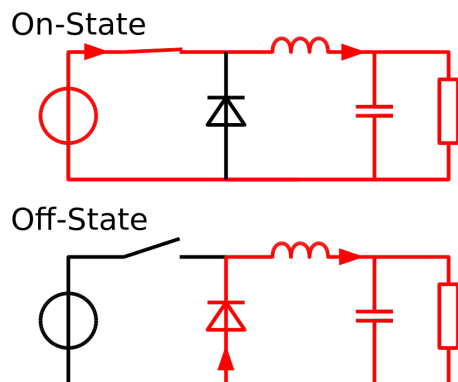


Figure 6.4: ON and OFF States of Buck Converter

Boost Converter (Step-Up Converter): The boost converter increases the output voltage level compared to the input voltage. It operates by storing energy in an inductor while the switch is ON and releasing it to the output during the OFF state. This continuous energy transfer results in an output voltage higher than the input voltage. [7]

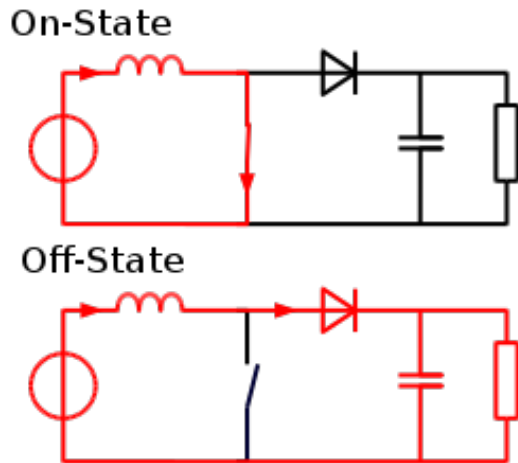


Figure 6.5: ON and OFF States of Boost Converter

Buck-Boost Converter: The buck-boost converter is capable of producing an output voltage either higher or lower than the input voltage. It combines the principles of both buck and boost converters by intelligently controlling the duty cycle of the switch. The buck-boost converter is ideal for applications requiring versatile voltage regulation capabilities. [7]

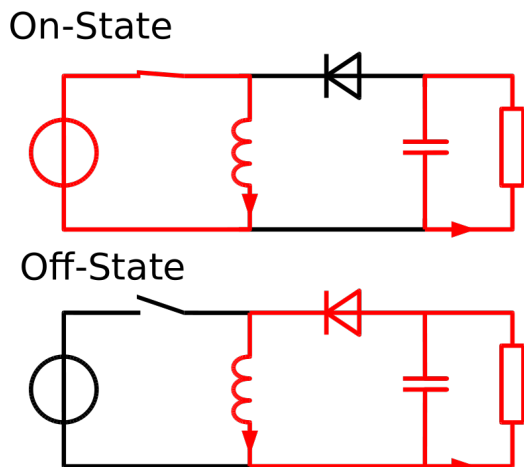


Figure 6.6: ON and OFF States of Buck-Boost Converter

6.3 Applications

There are many DC-DC converters applications across a wide range of industries and systems:

Portable Electronics: Mobile phones, laptops, tablets, and other battery-powered devices rely on DC-DC converters to efficiently manage power consumption and extend battery life.

Renewable Energy Systems: Solar photovoltaic systems and wind turbines employ DC-DC converters to interface with the electrical grid and efficiently convert variable DC voltages into usable power.

Automotive Electronics: Electric vehicles (EVs), hybrid vehicles, and onboard electronics utilize DC-DC converters for voltage regulation, battery charging, and power distribution.

Industrial Automation: Robotics, motor drives, PLCs (Programmable Logic Controllers), and factory automation systems benefit from DC-DC converters for precise voltage regulation and power efficiency.

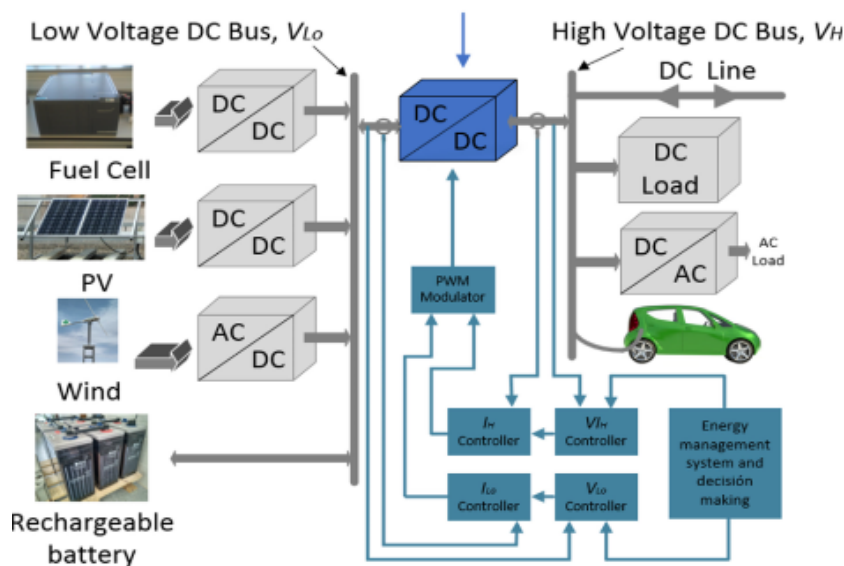


Figure 6.7: Applications of DC-DC Converters

In addition, DC-DC Converters can be used in many other applications like Medical Devices, Smart Lightning and other small-scale electronic appliances.[9]

Chapter 7

Dual Active Bridge

7.1 Introduction

The isolated bidirectional DC-DC converters have become so popular. These converters find applications in various fields, including uninterruptible power supplies (UPS), energy storage management systems, and electric vehicles which is exactly our concern in this book.

Several DC-DC converter topologies have been explored to meet this growing need. Among them, the dual-active bridge (DAB) converter stands out. Since its introduction, it has gained popularity, particularly for high-power applications, due to its high power density, simple implementation, minimal passive components, and zero-voltage-switching (ZVS) characteristic which will be discussed in details throughout this chapter. [10]

The DAB DC-DC converter, with its electrical isolation, high power density, and modularity, is well-suited for such high-power applications. However, input voltage fluctuations and load changes can cause instability, making the development of control strategies for the DAB DC-DC converter to enhance energy storage performance a critical area of research. [11]

7.2 Structure

A DAB is basically composed of two converters which are coupled together with the help of High Frequency (HF) transformer. That's why it's called dual. In other words, dual means using two converters together, inverter on one side and a rectifier on the other side. The two converters, either inverter or rectifier are Full Bridge (FB). Figure 7.1 illustrates DAB diagram. [12]

A DAB is a bidirectional DC-DC converter as it allows the power transfer or flow between the 2 sides or converters. It's an isolated DC-DC converter because there is a HF transformer between the two converters. hence, the two converters are isolated from each other. Consequently, this converter has the advantages of electrical isolation and large boost range making it widely used in important applications with high power and high reliability requirements like railway and all electric ships.[11]

A parallel capacitor at both sides or converters is used for filtration, fixation, stabilizing, regulating and smoothing the required voltages especially the output voltage which can be used with a load or a battery to be charged.

There should be an inductor as shown in Figure 7.1 which is essential for:

- **Energy Storage and Transfer:** The auxiliary inductor stores and transfers energy between the primary and secondary sides of the converter. It helps in shaping the current waveform and ensuring efficient power transfer between the two bridges.
- **Soft Switching:** The auxiliary inductor facilitates Zero-Voltage Switching (ZVS) or Zero-Current Switching (ZCS) by providing the necessary conditions for the switches to turn on and off with minimal losses. This reduces switching losses and improves the overall efficiency of the converter.
- **Regulating Power Flow:** By adjusting the phase shift between the primary and secondary bridges, the auxiliary inductor helps regulate the amount of power transferred. It works in conjunction with the control strategy to manage the power flow and maintain stable operation.
- **Reducing Circulating Current:** The auxiliary inductor helps minimize circulating currents within the converter, which can otherwise lead to increased losses and reduced efficiency. Proper design and placement of the inductor can significantly improve the converter's performance.
- **Handling Load Variations:** In applications with varying loads, the auxiliary inductor helps maintain stable operation by smoothing out fluctuations in the input and output currents. This contributes to the converter's ability to handle dynamic load conditions effectively.

Hence, the auxiliary inductor is a key component and indispensable in this converter.

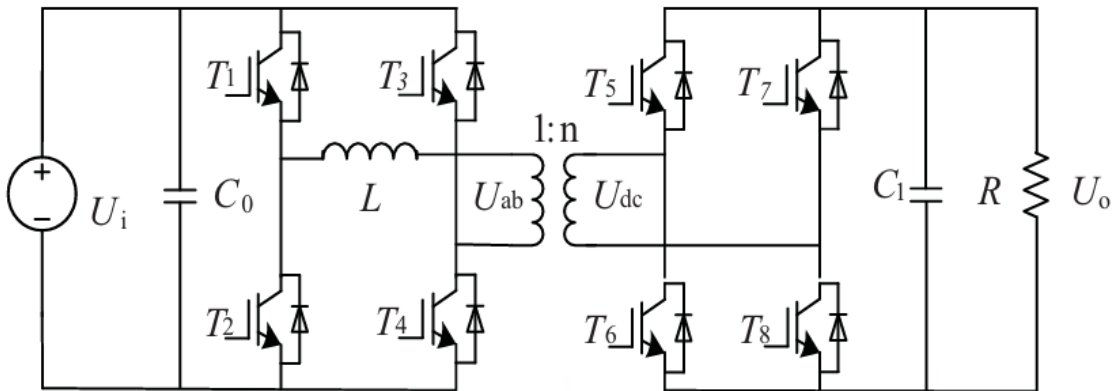


Figure 7.1: Diagram of a DAB DC-DC Converter

7.3 Simplified Circuit Model

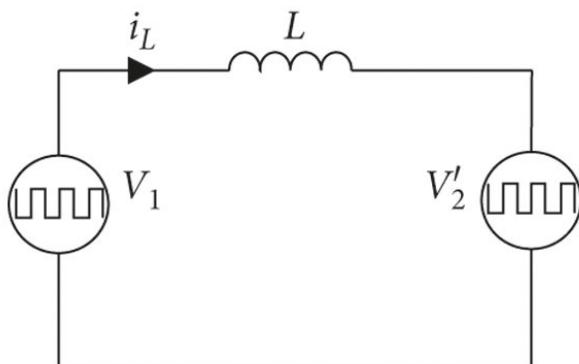
A DAB can be modelled in a simplified manner to be two AC voltage sources and an inductor representing line reactance in between. The voltage source V_1 is the output of the first converter (inverter in this case) and V'_2 is the secondary voltage after being referred to the primary side whereas V_2 is the AC input voltage to the other converter (rectifier in this case).

$$V'_2 = \frac{V_2}{N} \text{ where } N \text{ is the number of turns of the HF transformer (For turns ratio 1:N)}$$

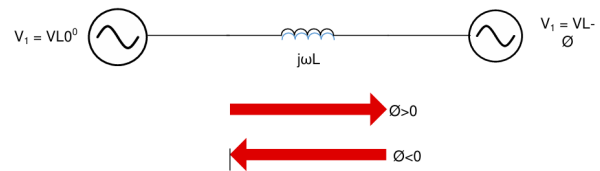
For the power to be transferred between the two AC sources V_1 and V'_2 , the voltage which leads the other will be the sending end, while the one which lags will be the receiving end. This emphasizes that in AC system, the voltage magnitudes don't matter that much while the phase angle between the two voltages matters V_1 and V'_2 in the power transfer issue.

For example, if V_1 leads V'_2 by angle δ , therefore:

- V_1 is the sending end.
- V'_2 is the receiving end.
- Power is transferred from V_1 side to V'_2 side.
- And vice versa.



(a) Simplified Circuit Model for a DAB converter



(b) Power Transfer Between Voltage Bus

Figure 7.2: DAB Simplified Circuit Model

$$P = \frac{V_1 V_2 \sin(\Phi)}{wL} \quad (7.1)$$

Similarly, power transfer happens in a dual-active bridge where two high-frequency square waves are created in the primary and secondary side of the transformer by the switching action of MOSFETs. These high-frequency square waves are phase shifted with respect to each other. Power transfer takes place from the leading bridge to the lagging bridge, and this power flow direction can be easily changed by reversing the phase shift between the two bridges. [13]

This simplified circuit model will make it easy to understand the principle of operation of the DAB converter.

7.4 Principle of Operation

Assuming the converter on the left to be an inverter and the one on the right to be a rectifier, the principle of operation of the converter can be described as follows:

- **A DC Source** -which is the input to the whole converter- is converted to **high frequency AC** with the help of the **inverter**.

- The **AC output** of the first converter "FB inverter on the left" is then transformed to a **higher or a lower voltage** with the help of the **HF transformer**.
- The **stepped up or down** AC output Voltage is again converted to **DC** with the help of the second converter "**FB rectifier on the right**".
- The previous operation allows the **power flow** from the converter on the left "FB Inverter" to the converter on the right "FB Rectifier". However, the power flow can be **reversed** whereas the converter on the right will be a FB inverter and the one on the left will be a FB rectifier. That's why a **DAB** converter is a **bidirectional** DC-DC converter. This is based on the idea of power transferred between two AC sources previously explained in the **Simplified Circuit Model** Section.
- The **rate of change of current** passing across the inductor depends upon the kind of **voltage across the inductance** which in turns is decided by the **status of the switches** $T_1, T_2, T_3, T_4, T_5, T_6, T_7$ and T_8 . That's the reason the power flow could be controlled quite easily by controlling these switches.
- **To sum up**, each bridge is controlled with constant **duty cycle (50%)** to generate a high-frequency square-wave voltage at its transformer terminals ($\pm V_i, \pm V_o$). **Considering** the presence of the leakage inductance of the transformer, with a controlled and known value, the two square waves can be appropriately **phase shifted** to control the power flow from one DC-source to the other, so **bidirectional power transfer** can be achieved. Power is delivered from the bridge which generates the leading square wave. [13]

7.5 Control Techniques

- There are many modeling techniques and control methods for a DAB[14]:
 - Feedback-only control. Linearisation Control, Feed-forward Plus Feedback, Disturbance-Observer-Based Control, Feed-forward Current Control, Model Predictive Current Control (MPC), Sliding Mode Control (SMC) and Moving Discretized Control Set Model Predictive Control.
 - Phase Shift Control (PSC) **which is our concern** and it includes:
 - * Single-Phase Shift (SPS) Control.
 - * Dual-Phase Shift (DPS) Control.
 - * Triple-Phase Shift (TPS) Control.
 - * Extended Phase-Shift (EPS) Control.
- These techniques represent a broad spectrum of control strategies for DAB converters, each suited to different application requirements and performance goals. The choice of control method depends on the specific needs of the application, such as desired efficiency, response time, complexity, and robustness.

7.5.1 Phase Shift Control PSC

- Phase Shift Control is a general term that encompasses several specific techniques, including Single-Phase Shift, Dual-Phase Shift, and Triple-Phase Shift control.

- The primary idea is to control the phase difference between the voltages of the primary and secondary bridges to regulate the power transfer.
- The phase shift control (PSC) technique can be done by applying a **delay of angle theta** θ between the two sides by applying a **firing delay** between the switches of the inverter T_1 and T_4 and these of the rectifier T_5 and T_8 shown in Figure 7.1.
- The output voltages of primary and secondary side (U_{ab} and U_{dc}) form square wave with 50% duty ratio and have shifted-phase between two sides. The average transferring power is controlled by adjusting the phase-shift angle. This control strategy is very intuitive and easy to implement. However, this method can only manage the average output power, because it has only one degree of freedom. Other variables are not considered in deciding the phase-shift angle, such as circulating reactive power, current flowing on the transformer, which can deteriorate the system performance. [10]

7.5.2 Single Phase Shift Control SPS

- Single-Phase Shift Control is a specific implementation of PSC where only a single phase shift angle is adjusted. It is the simplest form of PSC with limited control capabilities and involves shifting the phase of one of the bridges relative to the other.
- In SPS, only one degree of freedom (the phase shift angle) is used to control the power flow.
- Since only one phase shift is adjusted, SPS may not be able to optimize other performance aspects, such as minimizing circulating currents or improving efficiency under varying load conditions. So, SPS is limited to some applications.
- In this phase shifted mode of operation and concerning the firing of the first bridge (the one on the left), gate signal for Q_2 should be 180 degrees out of phase with respect to Q_1 to prevent shoot through.
- The firing of Q_4 is the same as that of Q_1 and that of Q_3 is the same as of Q_2 . Hence, Q_1 and Q_4 work at the same time interval and Q_2 and Q_3 work at the same time interval.
- For the second bridge (The one on the right), there should be some phase shift from these for the the first bridge. Both Q_5 and Q_8 have the same firing. Similarly, Q_6 and Q_7 have the same firing. However, there is a shift between between the firing of Q_1 and that of Q_5 and the same shift between the firing of Q_2 and that of Q_6 .
- Figure 7.3 illustrates the waveform of these these gate signals or firing.
- If Q_1 and Q_4 are ON, the output voltage on the primary side is the voltage U_i . If Q_2 and Q_3 are ON, the primary output voltage will be $-U_i$.
- Similarly, for the secondary side, if Q_5 and Q_8 are On, the output voltage is the voltage U_i . While, if Q_6 and Q_7 are On, the output voltage is the voltage $-U_i$.
- In this way, the obtained voltages on both primary and secondary sides will be square waves but with some phase shift as previously mentioned. The diagonal switches turn on and turn off together so that the output of each bridge is a square wave. The switching sequence is divided into four intervals based on the inductor current waveform and phase shift between the voltages at the primary and secondary of the transformer as shown in Figure 7.3 [13].

- From the DAB simplified circuit model shown in Figures 7.2a and 7.2b, the voltage across the inductor can be determined as the voltage difference between the primary voltage and secondary voltage referred to primary side ($V_L = V_1 - V'_2$ or $V'_1 - \frac{V_2}{N}$).
- For interval 1, the term ($V_1 - V'_2$) is large since V_1 has a max positive value and V'_2 has a large negative value. Hence, the voltage across inductor is large. Similarly, for interval 3, the voltage across inductor is large but with a negative value.
- For both intervals 2 and 4, the term ($V_1 - V'_2$) becomes smaller which leads to smaller voltage across inductor either of a positive or a negative value.
- The inductor current waveform for intervals 1 and 3 is **rising or decaying quickly** due to large value of V_L . For both intervals 2 and 4, it's **rising or decaying a little bit** due to small value of V_L .

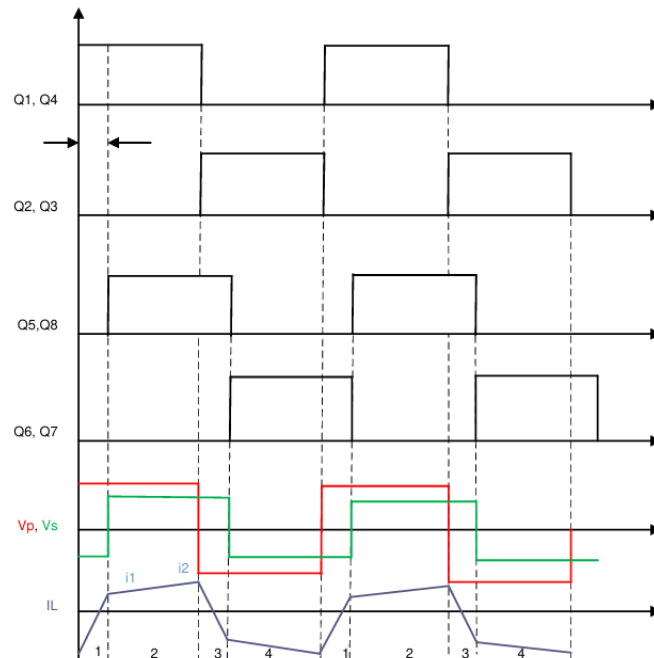


Figure 7.3: Gate Signals, Transformer Primary and Secondary Voltages, and Inductor Current

7.6 Some Considerations and Design Parameters

7.6.1 Zero Voltage Switching (ZVS)

During the transition from interval one to two, there exists a small dead time where the inductor-stored energy discharges the output capacitances of the MOSFETs and holds them close to zero voltage before they are turned on. This phenomenon, where the voltage across the MOSFET is close to zero at turn on, is referred to as zero voltage switching (ZVS). This is a major advantage with this topology, where due to the natural lagging current in one of the bridges, the inductive stored energy causes ZVS of all of the lagging bridge switches and some of the switches of the leading bridge.

[13] This depends on the stored inductive energy E_L available to charge and discharge the output capacitances of MOSFETs:

$$E_L = \frac{1}{2}LI^2 \quad (7.2)$$

$$E_c = \frac{1}{2}CV^2 \quad (7.3)$$

When transition happens from interval one to two, the primary side switches Q_1 and Q_5 continue conduction, whereas in the secondary, Q_6 and Q_7 turn off and Q_5 and Q_8 turn on. Initially the voltage across Q_6 and Q_7 is zero when they are conducting, and Q_5 and Q_8 block the entire secondary voltage. During dead time, when all of the switches in the secondary are off, the inductor-stored energy circulates current which discharges the capacitor across MOSFETs Q_5 and Q_8 to zero and charges the capacitor across MOSFETs Q_6 and Q_7 to the full secondary voltage. [13]

7.6.2 Switching Frequency

Switching frequency is important design parameter which affects the efficiency and power density of power converter. The input and the output voltage levels primarily determine the type of switches used in the power stage. Operating at higher switching frequencies enables reduced size of magnetics which helps in improved thermal solution, thereby improving the power density of the converter. [13]

By increasing switching frequency, the size of leakage inductor used will be smaller and easier to be implemented in DAB converter. However, we should choose the optimal switching frequency as the selection of switching frequency is primarily a trade-off between the allowable heat sink solution and transformer size for a given efficiency target. [13]

7.6.3 Filter Circuit Design

The output parallel capacitor used for filtration and smoothing the converter output must be designed based on the following procedures:

- **First:** determine some parameters required to be achieved like:

- Input and Output Voltages V_i , V_o .
- The output Current and Power I_o , P_o .
- The Switching Frequency F_{sw} .
- The Voltage and Current Ripples Percentage Allowed.

- **Secondly:** Calculate the Duty Ratio D from the relation:

$$D = \frac{1}{2} * \frac{\text{RequiredOutputVoltage}(V_o)}{\text{MaximumOutputVoltage}} \quad (7.4)$$

Where, the maximum output voltage should be greater than the required output voltage by the voltage drop across the transistors (the bridges' MOSFETs), diodes, transformer and the inductor.

- **Thirdly:** Calculate the Ripple Current I_{ripple} from the relation:

$$I_{\text{ripple}} = \frac{\text{CurrentRipplesPercentageAllowed}}{100} * I_o \quad (7.5)$$

- **Fourthly:** Calculate the Ripple Voltage V_{ripple} from the relation:

$$V_{\text{ripple}} = \frac{\text{VoltageRipplesPercentageAllowed}}{100} * V_o \quad (7.6)$$

- **Finally:** Calculate the output Capacitance C_o of the filter from the relation:

$$C_o = I_{\text{Ripple}} * \frac{D * T_{\text{sw}}}{V_{\text{ripple}}} \quad (7.7)$$

Where, T_{sw} is the switching time which is the reciprocal of the switching frequency F_{sw} .

7.6.4 HF Transformer Turns Ratio

The turns ratio of the transformer (N) must be chosen in a way to make sure that the output voltage meets the application requirements.

That's why the voltage drops across transistors, diodes, transformer itself and inductor should be taken into consideration. There should be margin depending on the application for the voltage. Hence, we can't use the required output voltage directly to get the turns ratio. Instead, the voltage after a margin from 20 to 30 percent or whatever depending on the application should be taken into consideration:

$$N = \frac{N_p}{N_s} = \frac{V_o}{V_i} \quad (7.8)$$

Where, V_o = Actual Required Output voltage * (100 + Margin) %

However, the turns ratio of the HF transformer used will be discussed in detail in **High Frequency (HF) Transformer Design** Chapter.

7.6.5 Leakage Inductance Design

The following equation is considered the main design criteria required to find the leakage inductance of the HF transformer, as it is the main element in the DAB:

$$L_{\text{leakage}} = \frac{NV_iV_oD(1 - D)}{2F_{\text{sw}}P_o} \quad (7.9)$$

7.7 Simulation

Simulation Parameters:

- Input voltage: 800V.

- Output battery 400V (nominal voltage).
- Switching frequency 100KHz.
- Inductance 42uH.

Control method used is single phase shift. There are two parameters to be controlled output voltage (constant voltage charging mode) and current control (constant current charging mode).

CC Phase: Fast charging with constant current until the battery reaches its maximum safe voltage.

CV Phase: Tapering off the current while maintaining constant voltage until the battery is fully charged.

7.7.1 MATLAB Model

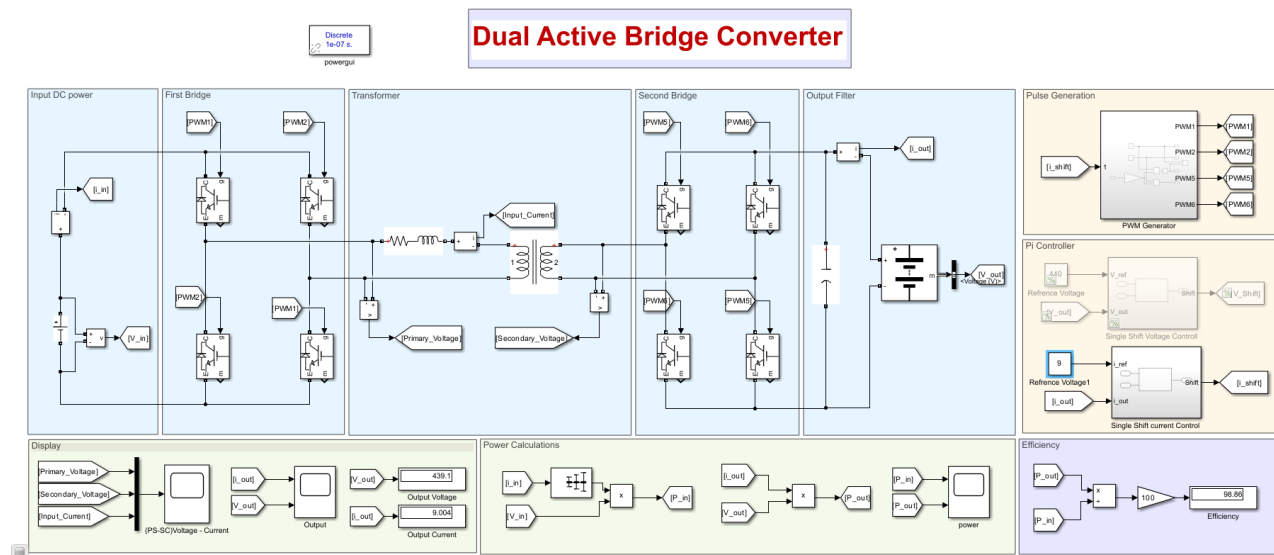


Figure 7.4: Dual Active Bridge DC-DC Converter Simulation Model

7.7.2 PWM Generator

The main function of this subsystem is to generate pulses for the two bridges. The PWM signal of Second bridge is shifted by an angle ($0 - 90^\circ$) degree as shown in figure 7.5.

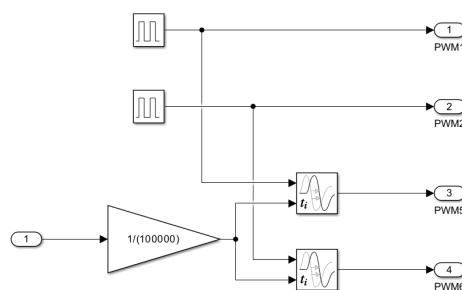


Figure 7.5: PWM Generator for Single Shift Control For DAB

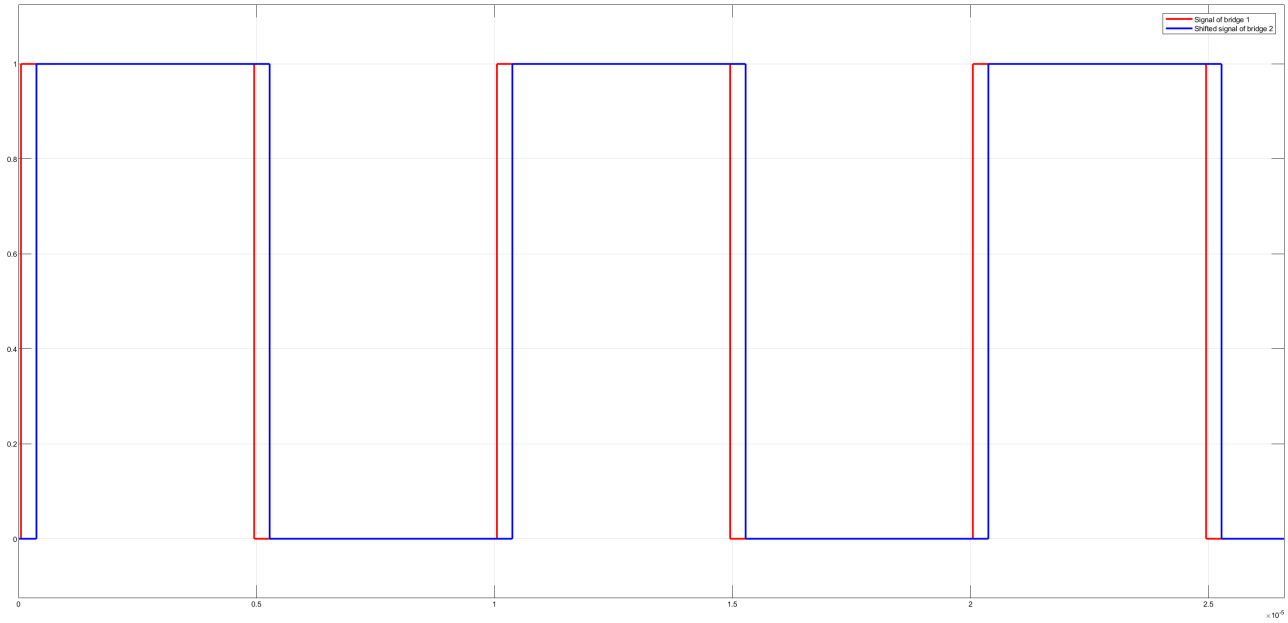


Figure 7.6: Shifted PWM Signal Between First and Second Bridge

7.7.3 PI Controller

Controlling Current and controlling voltage required PI controller its input is the error in current or voltage and its output is the shift angle that used in PWM pulse generator to shift the firing of second bridge than the first bridge. the control loop shown in figure 7.7.

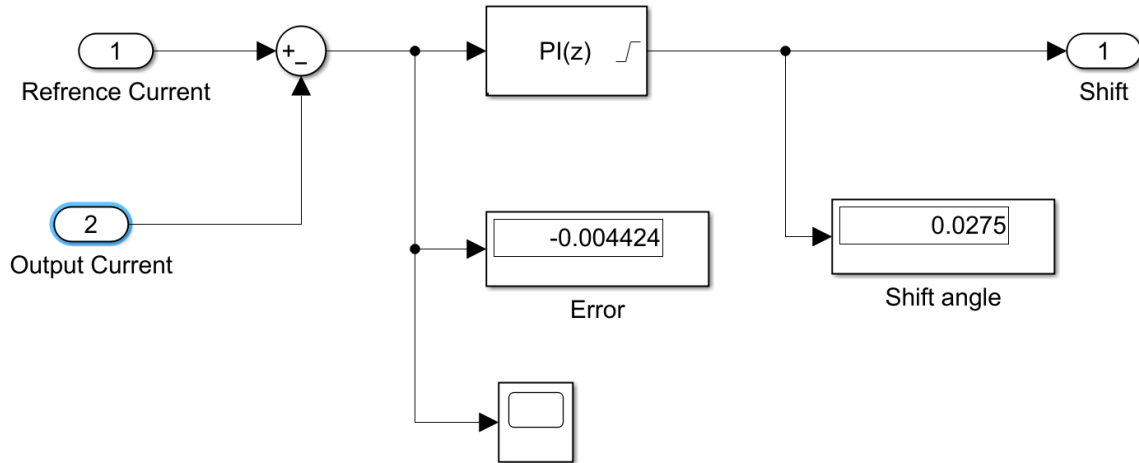


Figure 7.7: PI Controller for DAB converter

7.7.4 The Results of Current Control

The figure 7.8 shown the controlling on current that charges the battery and shown the variation of output current due to change in current reference.

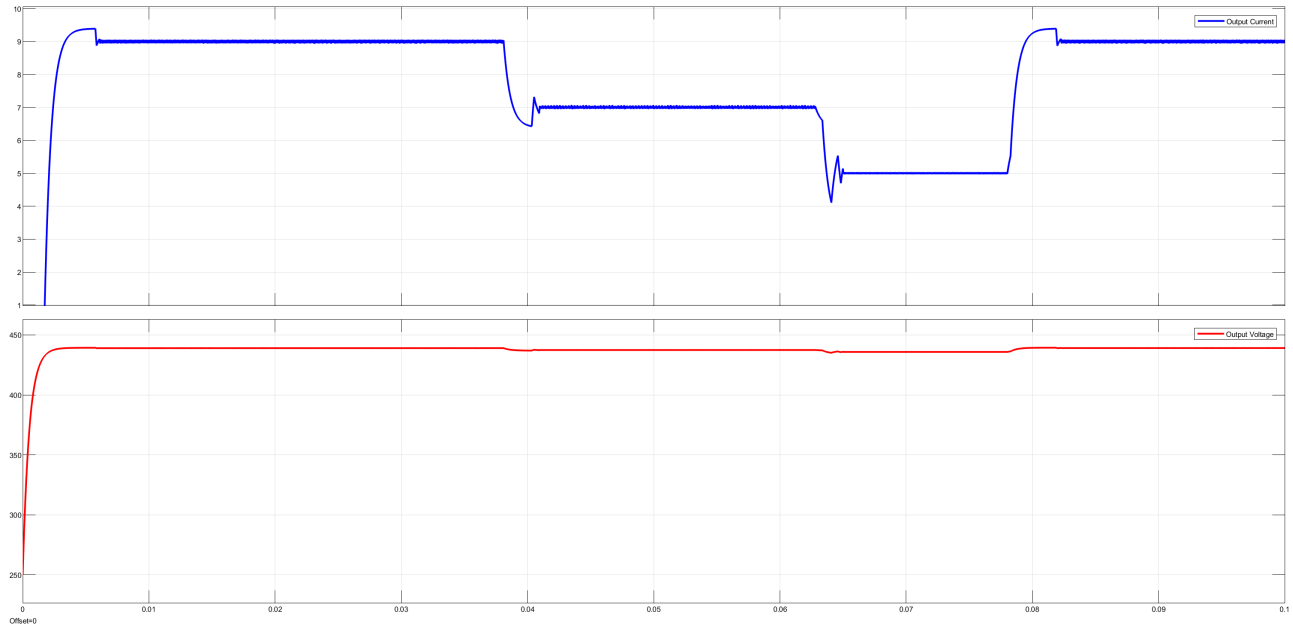


Figure 7.8: Output Current and Voltage Using CC for DAB

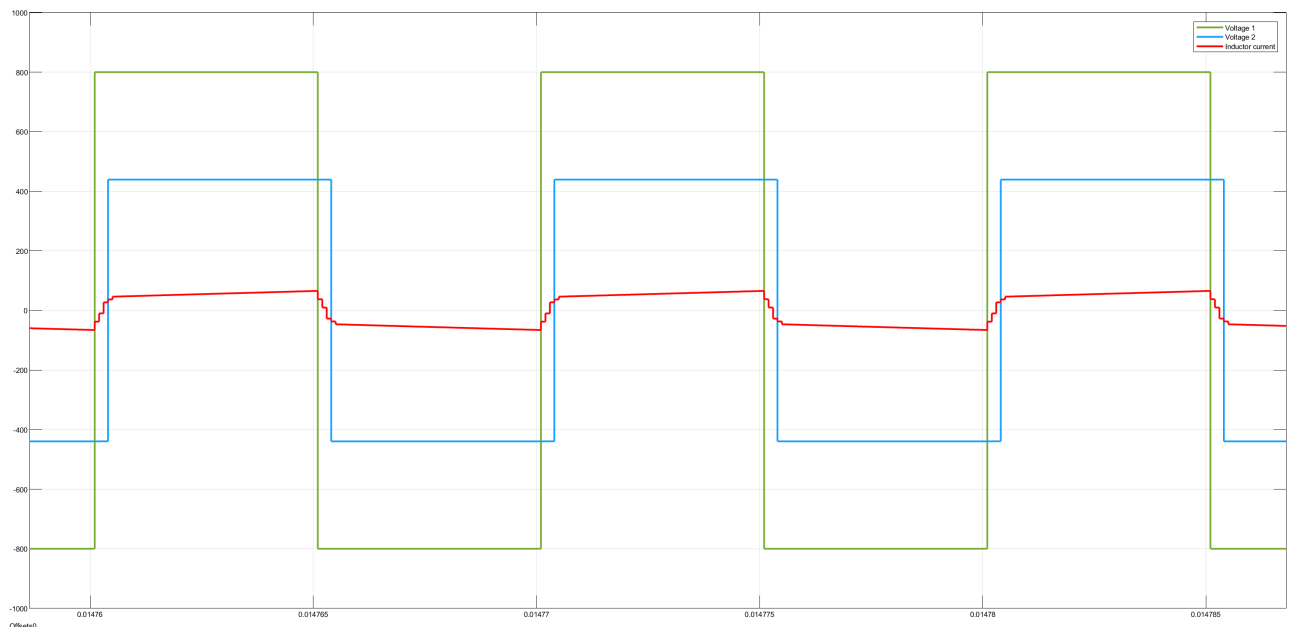


Figure 7.9: Relation between The Primary Voltage, Secondary voltage and The Inductor Current

Note: inductor current multiplied by 10 to show the shape of wave form.

7.7.5 The Results of Voltage Control

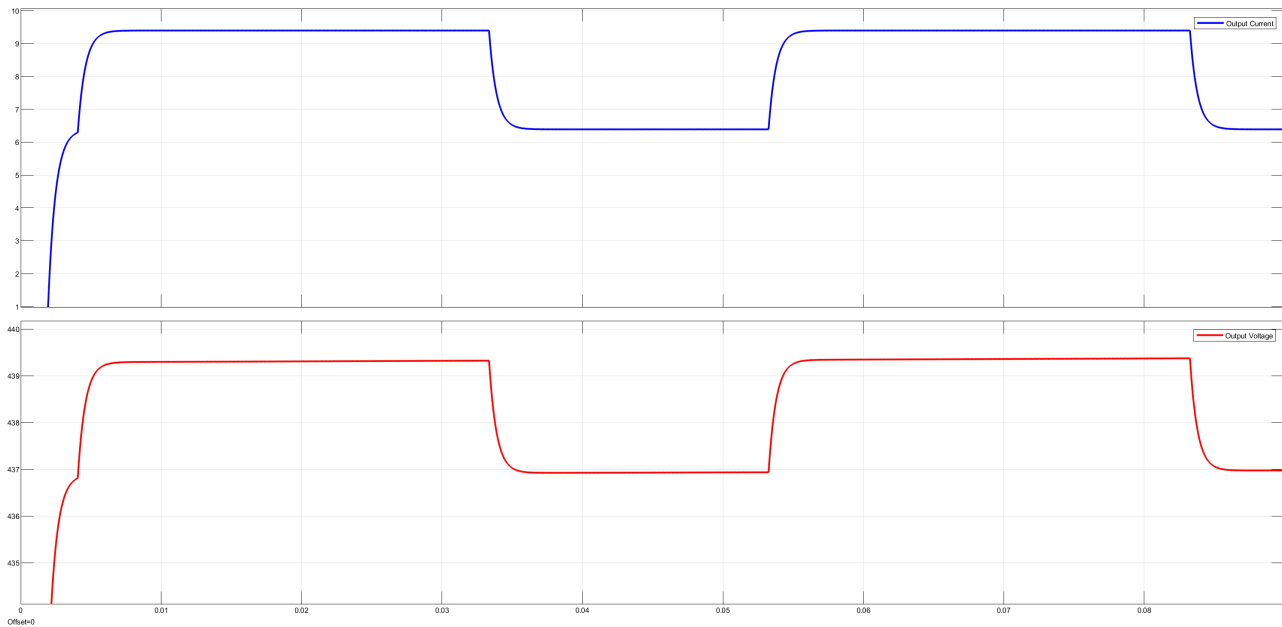


Figure 7.10: Output Current and Voltage Using CV for DAB

The figure 7.10 shown the controlling on voltage that applied on the battery and shown the variation of output voltage due to change in voltage reference.

7.7.6 Converter Efficiency

The efficiency is around 97% for the rated designed state. By controlling the current, the efficiency decreases and it can reach to around 60%. This is one of the main disadvantages of this converter.

7.8 Hardware Implementation

The setup mainly consists of six main boards:

- Power circuit.
- Gate drive circuit.
- High frequency transformer
- Coil
- Current sensor.
- F28069M LaunchPad™.

7.8.1 Power Circuit

Power circuit is the circuit which includes the two bridges and an input for external coil. The main component of this circuit is the MOSFET (IRFP460 N-Channel MOSFET). Rating at 500V and 20A. Shown in figure 7.11 the bottom layer design of the circuit and 3D model for it.

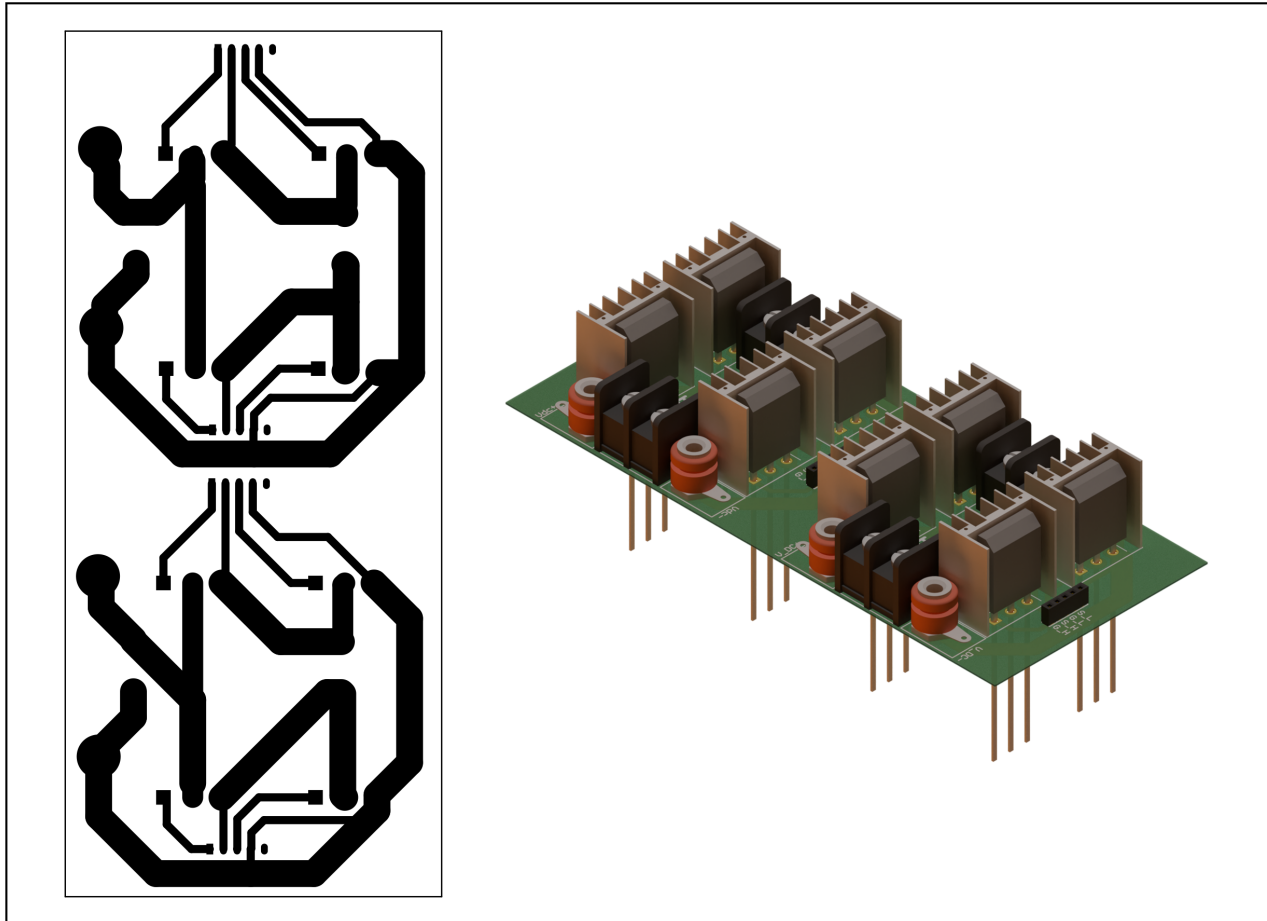


Figure 7.11: DAB Power Circuit Design and 3D Model

7.8.2 Gate Drive Circuit

Gate drive circuit provide protection and isolation for the MCU and isolate it from the power circuit using optocoupler 6N139. It also drive the MOSFET on power board using IC IR2111 that generate a signal and its complement to drive a leg of H bridge. So four signals only from controller are needed to control the two bridges.

Shown in figure 7.12 the bottom layer design of the circuit and 3D model for it.

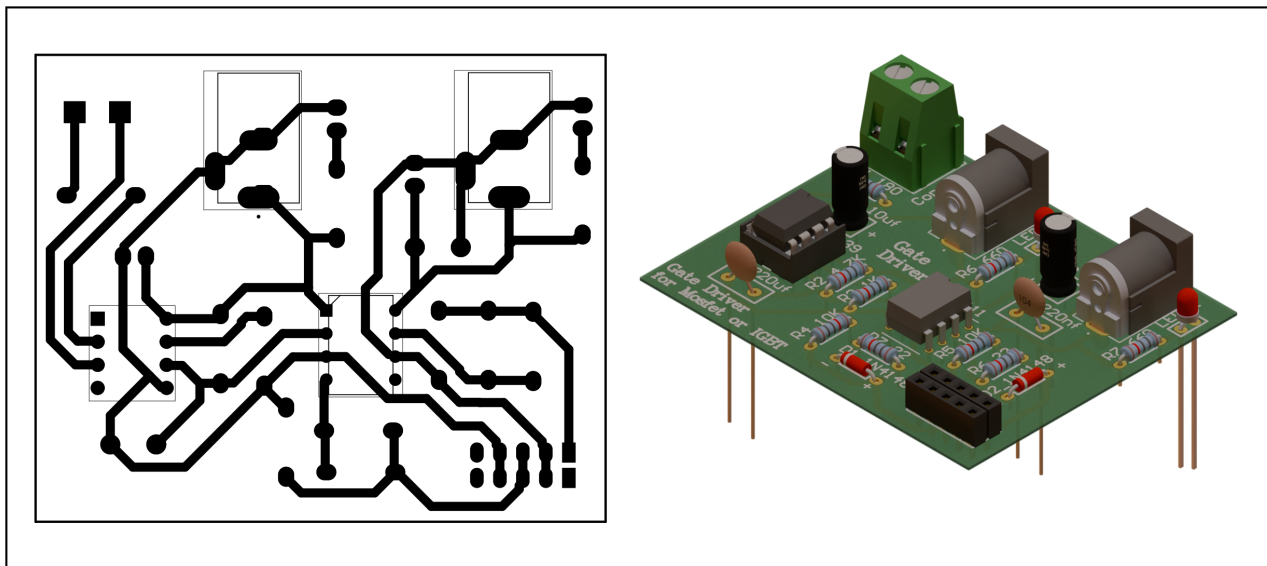


Figure 7.12: Gate Drive Circuit Design and 3D Model

7.8.3 Current Sensor

Controlling the output current of DAB needs a current sensor. Current Sensor Module ACS712 30A is a good selection for reading the value of the output current and convert it to analogue signal that can be used by controller to control the current at reference value.



Figure 7.13: Current Sensor Module ACS712

7.8.4 MCU

Generating shifted PWM with high switching frequency needs an efficient MCU so using DSP F28069M LaunchPad™ is suitable for our application. It can generate PWM with specific duty cycle and switching frequency. It also can delay the PWM signal of bridge 2 from bridge 1 by a specific angle. It also has a simple interfacing with MATLAB simulink.

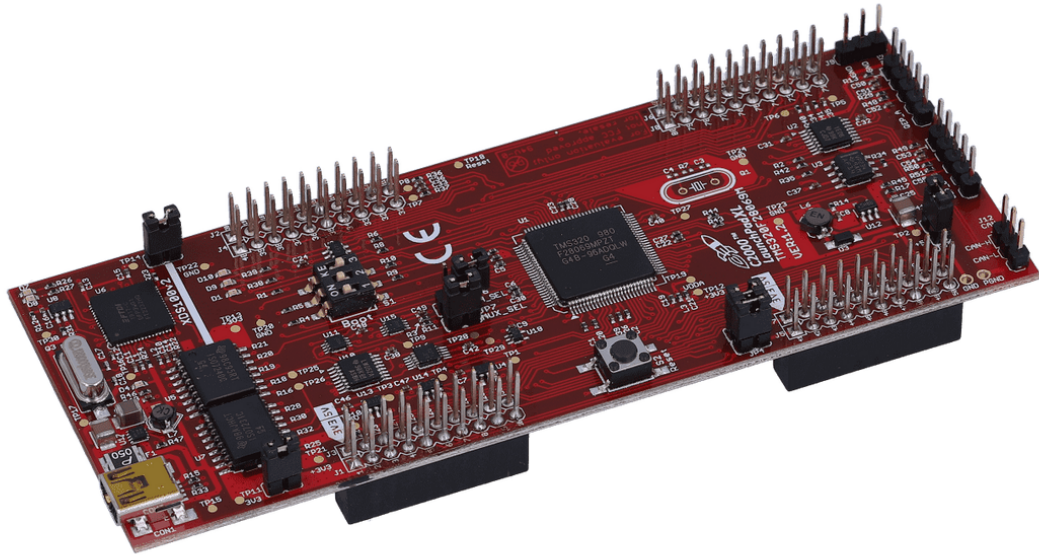


Figure 7.14: F28069M LaunchPad™

Chapter 8

LLC Converters

8.1 Introduction

LLC resonant converters have become an important topic in power electronics because they can meet the demanding performance requirements set by modern power supply designs. The LLC is one of a significantly larger family of resonant converter topologies, all of which are based on resonant tanks. Resonant tanks are circuits made up of inductors and capacitors that oscillate at a specific frequency, called the resonant frequency. Because they allow for higher switching frequencies (f_{SW}) and reduce switching losses, these switch-mode DC/DC power converters are often used in high-power, high-efficiency applications.

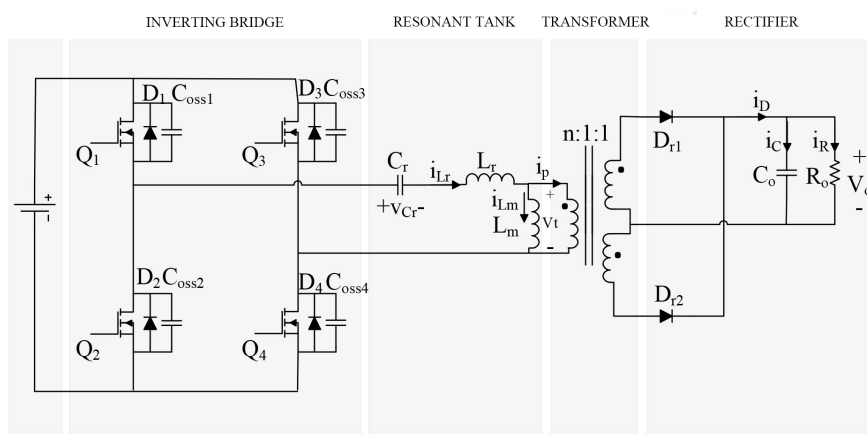


Figure 8.1: LLC Resonant Converter circuit

An LLC converter is made up of 4 blocks: the power switches, resonant tank, transformer, and diode rectifier. First, the MOSFET power switches convert the input DC voltage into a high-frequency square wave. This square wave then enters the resonant tank, which eliminates the square wave's harmonics and outputs a sine wave of the fundamental frequency. The sine wave is transferred to the secondary of the converter through a high-frequency transformer, which scales the voltage up or down, according to the application. Lastly, the diode rectifier converts the sine wave into a stable DC output.

$$\text{Gain} = \text{bridge gain} * \text{resonant tank gain} * \text{turns ratio } (N_s/N_p) \quad (8.1)$$

N_s: Secondary side turns ratio

N_p: Primary side turns ratio

The bridge can be full bridge or half bridge. Full bridge gain = 1 and half bridge gain = 0.5. Full bridge consists of 4 switches but half bridge consists of only two switches. in our design we will use full bridge inverter as shown in Figure 8.1 so the bridge gain equals 8.1.

8.2 Resonant Tank

The resonant tank is made up of a resonant capacitor (CR) and two inductors: the resonant inductor (LR), in series with the capacitor and transformer, and the magnetizing inductor (LM), in parallel. The tank's role is to filter out the square wave's harmonics, outputting a sine wave of the fundamental switching frequency to the input of the transformer.

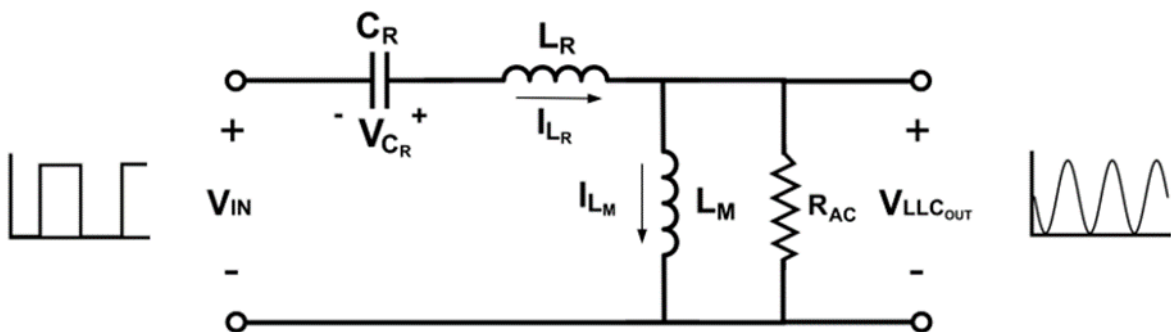


Figure 8.2: resonant tank

The resonant tank has a gain that varies according to the frequency and the load applied to the secondary side and the ratio between L_m and L_r (L_n). Designers must tune these parameters to ensure that the converter efficiently operates across a wide range of loads by designing the tank's gain to exceed 1 for all load values. This Figure shows the resonant tank's gain for a range of loads if the resonant tank were only composed of the resonant capacitor and the magnetizing inductor. At light loads, there is a clear peak in the resonant tank's gain. However, the gain for the heavy load does not peak — instead, it has a damped response and only achieves unity gain at very high frequencies. If the resonant tank is only made up of the resonant inductor (LR) in series with the resonant capacitor, the behavior is different. The gain does not exceed 1, but when the load is heaviest, the tank reaches unity gain much more quickly than it would with the parallel inductor.

By implementing both inductors in the resonant tank, the resulting frequency gain response ensures that the converter can adequately respond to a much larger range of loads —in addition, it can enable stable control for the entire load range

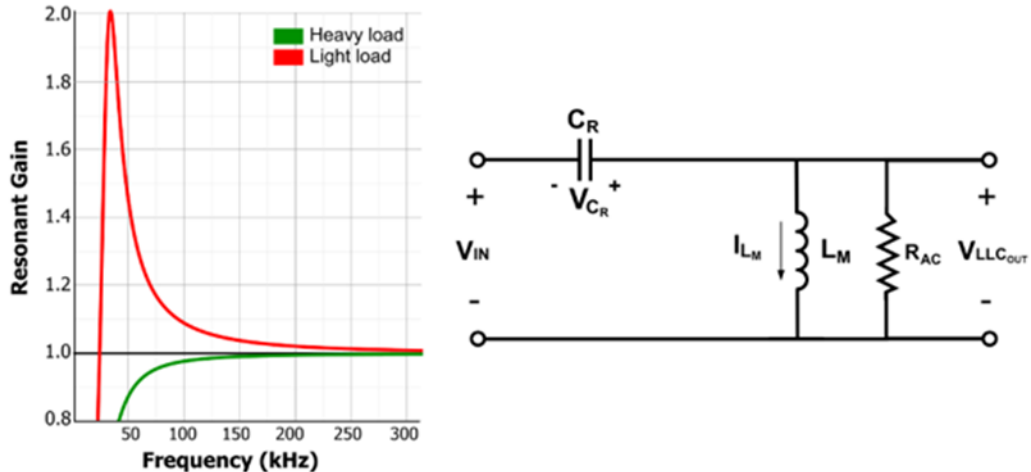


Figure 8.3: parallel resonant tank response

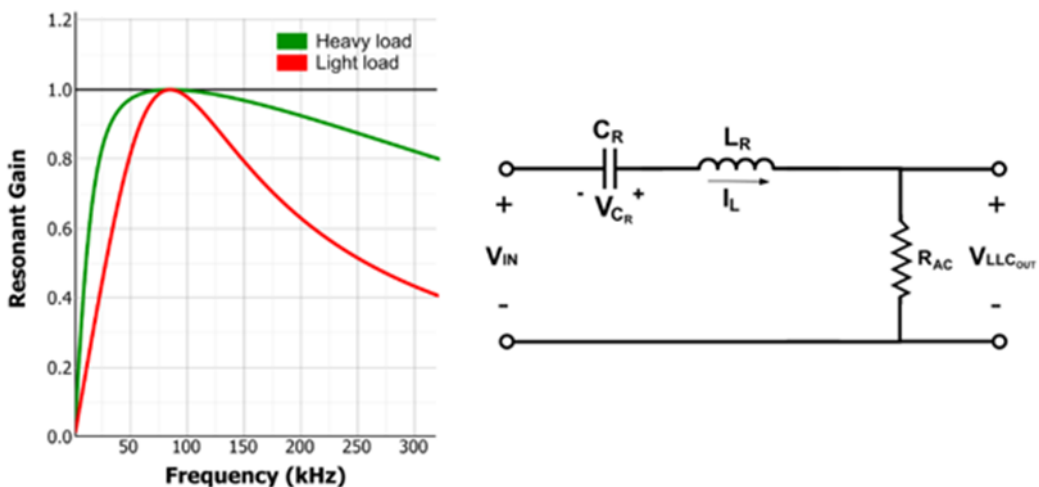


Figure 8.4: series resonant tank response

8.3 Behavior of the Voltage-Gain Function

The voltage-gain function expressed by Equation

$$M_G(Q, L_N, F_N) = \frac{V_{OVT}}{V_{IN}} = \frac{f_N^2 \times (L_N - 1)}{(f_N^2 - 1)^2 + f_N^2 x (f_N^2 - 1) \times (L_N - 1)^2 \times Q^2} \quad (8.2)$$

the quality factor (Q), which is dependent on the load connected to the output. However, using the value of the load is not accurate, since there is a transformer and a rectifier between the output of the resonant tank and the load. Therefore, we must use a primary-referenced value for the load, called RAC. RAC and Q can be estimated with these two equations respectively

$$R_e = \frac{V_{oe}}{I_{oe}} = \frac{8 \times n^2}{\pi^2} \times \frac{V_o}{I_o} = \frac{8 \times n^2}{\pi^2} \times R_L \quad (8.3)$$

$$Q_e = \frac{\sqrt{L_r/C_r}}{R_e} \quad (8.4)$$

it is necessary to understand how Mg behaves as a function of the three factors f_n , L_n , and Q . In the gain function, frequency f_n is the control variable. L_n and Q are dummy variables, since they are fixed after their physical parameters are determined Mg is adjusted by f_n after a design is complete. As such, a good way to explain how the gain function behaves is to plot Mg with respect to f_n at given conditions from a family of values for L_n and Q

Regardless of which combination of L_n and Q is used, all curves converge and go through the point

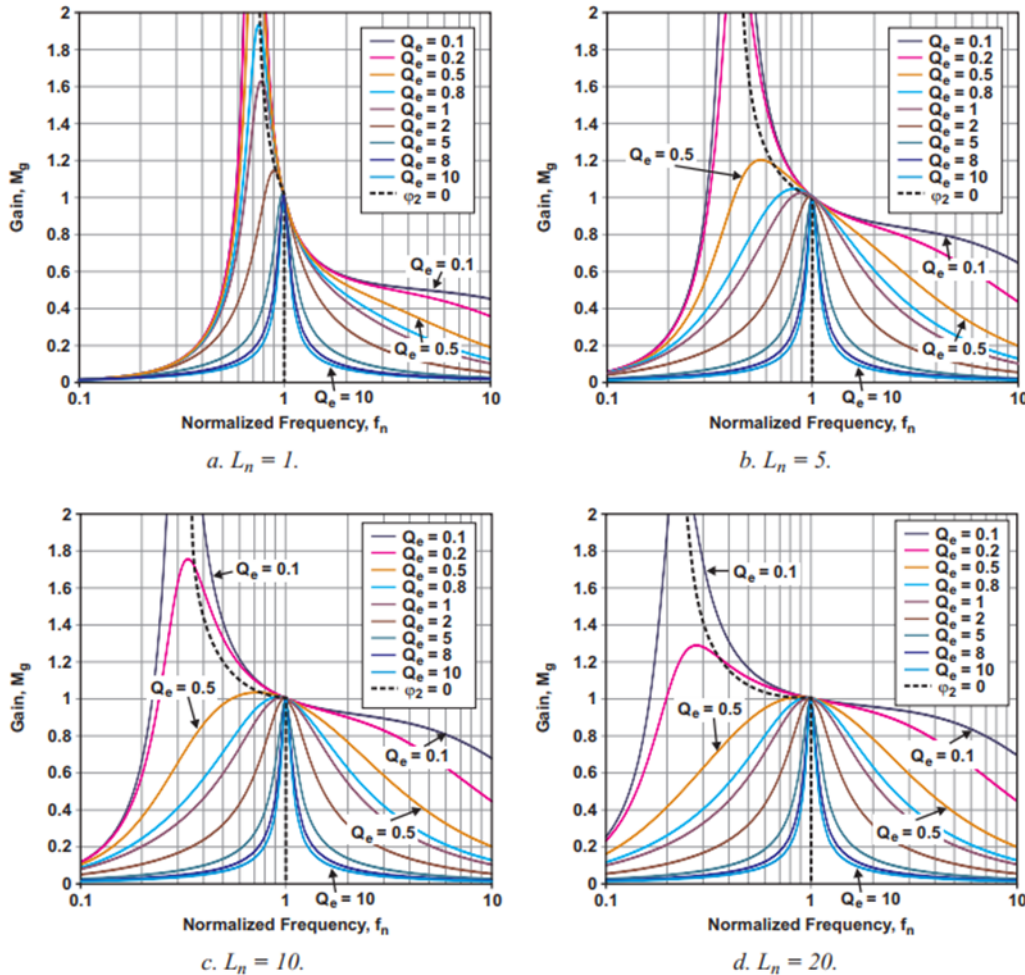


Figure 8.5: Plots of voltage-gain function (M_g) with different values of L_n

of $(f_n, Mg) = (1, 1)$. This point is at $f_n = 1$, or $f_{sw} = f_0$. By definition of series resonance, $XL_r - XC_r = 0$ at f_0 . In other words, the voltage drop across L_r and C_r is zero, so that the input voltage is applied directly to the output load, resulting in a unity voltage gain of $Mg = 1$.

It is obvious that lower values of L_n can achieve higher boost gain, in addition to the narrower range of the frequency modulation, meaning more flexible control and regulation, which is valuable in applications with wide input voltage range. Nevertheless, low values of L_n for the same quality factor Q and resonant frequency f_r means smaller magnetizing inductance L_m , hence, higher magnetizing peak-peak current ripple, causing increased circulating energy and conduction losses.

For summarize, After analysis of the tank circuit, the resonant tank gain equation:

$$K(Q, m, F_x) = \frac{F_x^2(m-1)}{\sqrt{(m \cdot F_x^2 - 1) + F_x^2(F_x^2 - 1)^2 \cdot (m-1)^2 \cdot Q^2}} \quad (8.5)$$

where,

$$Q = \frac{\sqrt{L_r/C_r}}{R_{ac}} \quad (\text{Quality factor}) \quad (8.6)$$

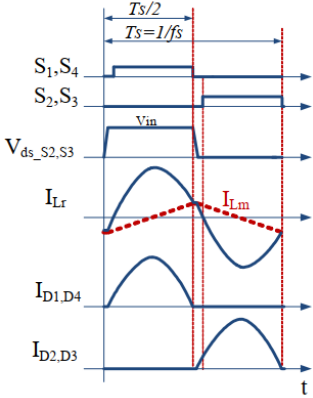
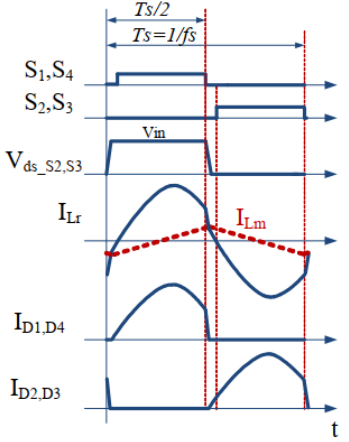
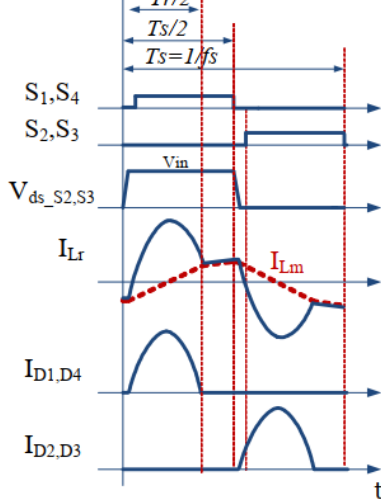
$$R_{ac} = \frac{8}{\pi^2} \cdot \frac{N_p^2}{N_s^2} \cdot R_o \quad (\text{Reflected load resistance}) \quad (8.7)$$

$$F_x = \frac{f_s}{f_r} \quad (\text{Normalized switching frequency}) \quad (8.8)$$

$$f_r = \frac{1}{2\pi\sqrt{L_r \cdot C_r}} \quad (\text{Resonant frequency}) \quad (8.9)$$

$$m = \frac{L_r + L_m}{L_r} \quad (\text{Ratio of total primary inductance to resonant inductance}) \quad (8.10)$$

using previous equations we can design our resonant tank by assuming variable with a constant value then start to calculate other parameters.

At Resonant frequency operation $f_s=f_r$	Above resonant frequency operation $f_s>f_r$	Below resonant frequency operation $f_s<f_r$
<p>Each half of the switching cycle contains a complete power delivery operation (described above), where the resonant half cycle is completed during the switching half cycle. By end of the switching half cycle, the resonant inductor current I_{Lr} reaches the magnetizing current I_{Lm}, and the rectifier current reaches zero. The resonant tank has unity gain and best optimized operation and efficiency, therefore, transformer turns ratio is designed such that the converter operates at this point at nominal input and output voltages</p> 	<p>Each half of the switching cycle contains a partial power delivery operation (described above), similar to the resonant frequency operation, but it differs in that the resonant half cycle is not completed and interrupted by the start of the other half of the switching cycle, hence primary side MOSFETs have increased turn off losses and secondary rectifier diodes have hard commutation. The converter operates in this mode at higher input voltage, where a step down gain or buck operation is required.</p> 	<p>Each half of the switching cycle contains a power delivery operation (described above), at the time when resonant half cycle is completed and resonant inductor current I_{Lr} reaches the magnetizing current, the freewheeling operation (as described above) starts and carries on to the end of the switching half cycle, hence primary side have increased conduction losses due to the circulating energy. The converter operates in this mode at lower input voltage, where a step up gain or boost operation is required.</p> 

8.4 Design Steps and Considerations

Line regulation is a requirement needs to be considered , it is defined as the maximum output voltage variation caused by an input voltage variation over a specified range, at a given output load current.A minimum and maximum output voltage, $V_{o_{min}}$ and $V_{o_{max}}$, respectively, will be assumed. To simplify the discussion, it will also be assumed that all parasitic voltage drops—for example, from PCB traces, the MOSFET's $R_{ds_{on}}$, the diode's forward voltage, etc.—are already converted or lumped into a part of the output-voltage range Mg should be designed to meet the conditions which says that all possible Mg values must contain the value of both Mg_{min} and Mg_{max} within the fn limits.

$$M_{g_min} = \frac{n \times V_{o_min}}{V_{in_max}}, M_{g_max} = \frac{n \times V_{o_max}}{V_{in_min}} \quad (8.11)$$

1. Selecting the Transformer Turns Ratio (n)

Initially the gain can be set at unity ($Mg = 1$) for the output voltage at its middle value between $V_{o_{min}}$ and $V_{o_{max}}$. This middle value can be called the output voltage's nominal value, $V_{o_{nom}}$, Similarly, the input voltage's nominal value can be called $V_{in_{nom}}$. Then the transformer turns ratio.

$$n = \frac{M_g \times V_{in_{nom}}}{V_{o_{nom}}} \quad (8.12)$$

2. Selecting L_n and Q

there is two ways for selecting these values

first method :

first we need to select Q_{max} , it depends on the load current. Heavy load conditions operate at high Q values, while lighter loads have lower Q values. It is important to set a value for the Q_{max} associated with the maximum load point

To illustrate the effect of the Q value on voltage regulation, Figure below shows an example voltage gain plot for different Q values. Let's assume that the resonant tank gain is required to range from 0.8 to 1.2 for example, we can see that the low Q value curve ($Q=0.3$) can reach higher boost gain, but it is less sensitive to frequency modulation in the “above resonance f_s, f_r ” region, hence, switching frequency has to increase much in order to reach the minimum voltage gain ($K=0.8$), causing extra switching losses, while the higher Q value curve ($Q=1$) can reach the minimum gain ($K=0.8$) with less switching frequency increase, but unable to reach the maximum gain ($K=1.2$). Therefore, a moderate Q value of around 0.5 seems to satisfy the voltage gain requirement in this specific case.

and then we can assume a suitable value for L_n which is around 6 and then plot gain curve , Mg_{max} can be plotted to the gain curves to obtain cross point between Q_{max} and Mg_{max} it will define the minimum frequency to operate to make sure that we operate in inductive region Because the gain curves are dependent on L_n and Q, several gain curves may need to be drawn to find a proper point This is certainly one way to make the initial selection of L n and Q, but it is a difficult way and most likely will require some wild guess.

second method : A more desirable approach is to create a common tool to represent the gain curves that can be shared and reused by different designs. Since the attainable peak gain (Mg_{ap}) corresponding to Qg_{max} is the highest gain of concern for a design, gain-curve plots can be created beforehand to show Mg_{ap} with different values of L_n and Q. Then L_n and Q can be selected to achieve $Mg_{ap} > Mg_{max}$ based on a common tool—the Mg_{ap} curves. How this method is used will be described after a discussion of how the Mg_{ap} curves are obtained. the created Mg_{ap} curves are shown in Fig. a The horizontal axis is Q and the vertical axis is Mg_{ap} with

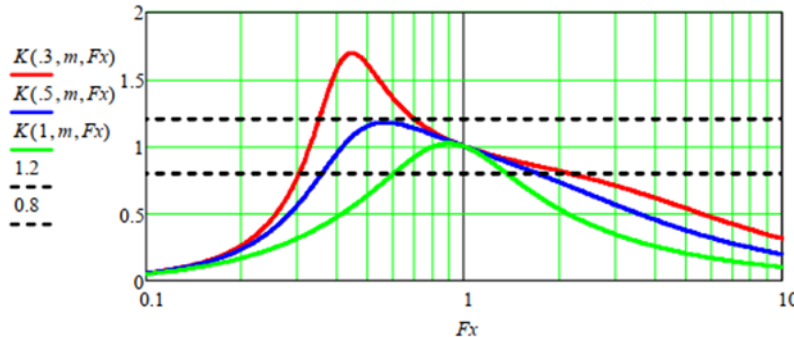
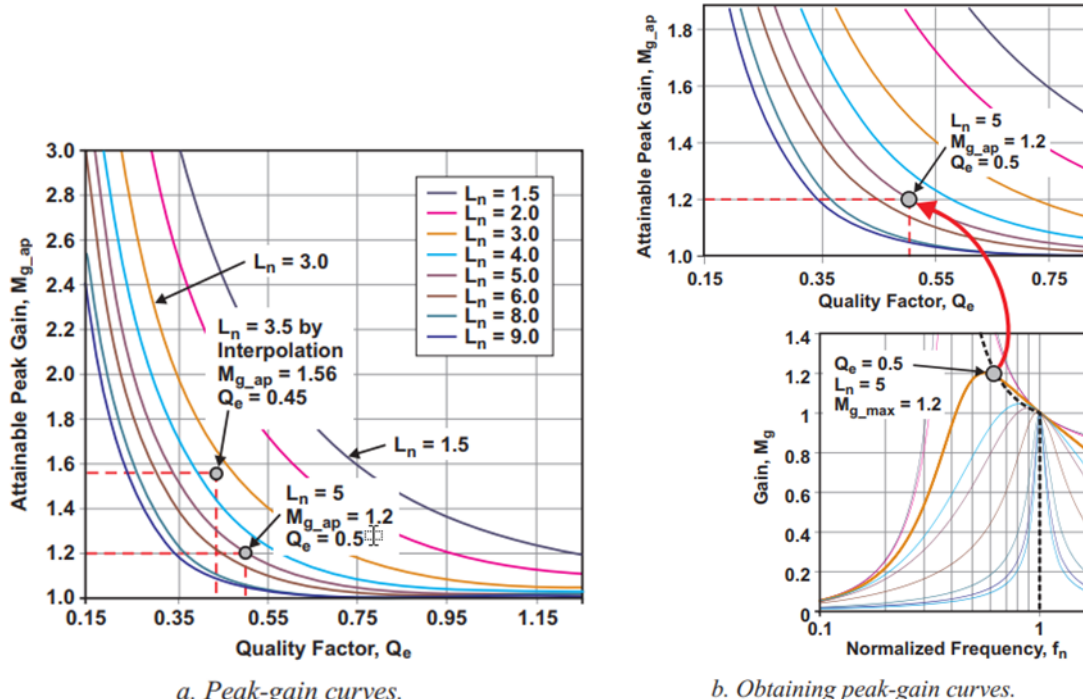


Figure 8.6: voltage gain

Figure 8.7: The created Mg_{ap} curves

respect to a family of fixed values for L_n . Fig. b is used to illustrate how Fig. a is formed. From a plot of gain curves, for example from Fig. b, which is partially copied to the lower half of Fig. b, one attainable peak-gain value, $Mg_{ap} = 1.2$, can be located at the curve with $(L_n, Q) = (5, 0.5)$. This point can be plotted to Fig. a at $(Mg_{ap}, Q) = (1.2, 0.5)$. (Note that $L_n = 5$ at this point.) Because all curves in Fig. b have a fixed $L_n = 5$, that figure can be used to repeat the process with different Q values. Then a peak-gain curve can be formed as a function of Q with a fixed $L_n = 5$.

With Mg_{max} already determined, Mg_{max} can be plotted as a horizontal line on Fig. a. Any Mg_{ap} values above this line are greater than Mg_{max} , so the designed converter should operate in the inductive region. For example, for $Mg_{max} = 1.2$, any values of Mg_{ap} can be selected that are greater than 1.2, as shown in Fig. a. Then the selected value meets the maximum-gain requirement. From the selected Mg_{ap} value, L_n and Q values can then be selected. For example, selecting a value from the curve of $L_n = 5$ provides the L_n value right away. Since a gain value greater than Mg_{max} needs to be selected, Q would have to be less than 0.5, based on Fig. a.

Similarly, a smaller L_n provides more gain and L_n can be selected by interpolating as shown in Fig. a. For example, if a value of 0.45 is selected for Q , the corresponding Mg_{ap} value with $L_n = 3.5$ would be $1.56 > Mg_{max}x = 1.2$, which satisfies the design requirements

3. determining R_e and resonant circuit parameters.

$$C_r = \frac{1}{2\pi \times Q_e \times f_0 \times R_e}, \quad L_r = \frac{1}{(2\pi \times f_0)^2 C_r}, \quad L_m = L_n \times L_r \quad (8.13)$$

8.5 Design Using MATLAB Script

This MATLAB Script used to find the values of components of resonant tank.

```
%----- DC Input -----
Vin = 700; % operating input voltage
Vin_rated = 700; % rated input voltage
Vin_min = 650; % minimum input voltage
Vin_max = 800; % maximum input voltage
%----- Output Load -----
Vo = 450; % operating output voltage
Vo_rated = 450; % rated output voltage
Vo_min = 400; % minimum output voltage
Vo_max = 600; % maximum output voltage
Po_rated = 7000; % rated output power
% load percentage with respect to the rated load
K_load = 1;
Q_rated = 0.3; % Q factor at the rated condition
%----- Operating Conditions -----
f_res = 70000; % resonant frequency
K_ind = 6; % parallel-to-series inductance ratio
% relative frequency factor for open-loop operation
K_rel_freq = 0.75;
%*****
%
% Parameters from Calculation
%
%*****
fsw = f_res*K_rel_freq; % switching frequency fsw
%----- Transformer and Load -----
a_sp = (Vo_max+Vo_min)/(2*Vin_rated); % Ns/Np ratio
a_sp2 = a_sp*a_sp;
% rated load resistance
Ro_rated = Vo_rated*Vo_rated/Po_rated;
% Ro_rated referred to the primary side
Ro_rated_pri = Ro_rated/a_sp2;
% load resistance at the operating conditions
```

```

Ro = Ro_rated / K_load ;
%----- Resonant Circuit -----
% Minimum gain and maximum gain required
G_dc_min = Vo_min/(a_sp*Vin_max); % minimum gain
G_dc_max = Vo_max/(a_sp*Vin_min); % maximum gain
% resonant inductance
Ls = (Q_rated*Ro_rated_pri)/(2*pi*f_res);
% resonant capacitance
Cs = 1/(2*pi*f_res*Q_rated*Ro_rated_pri);
% transformer magnetizing inductance
Lm = K_ind*Ls;
% Q value at the operating conditions
%Q = Zo / R; Zo = sqrt(Ls/Cs);
Q = sqrt(Ls/Cs)/(Ro/a_sp2);

```

8.6 LLC Resonant Converter Closed Loop Control

In any DC-DC converter, it's important to keep the value of the output voltage constant. The change in load leads to a change in output voltage in the case of open-loop control. Using closed-loop control is necessary, so LLC converter closed-loop control can be achieved by the cascaded control loop, as shown in the Figure 8.8.

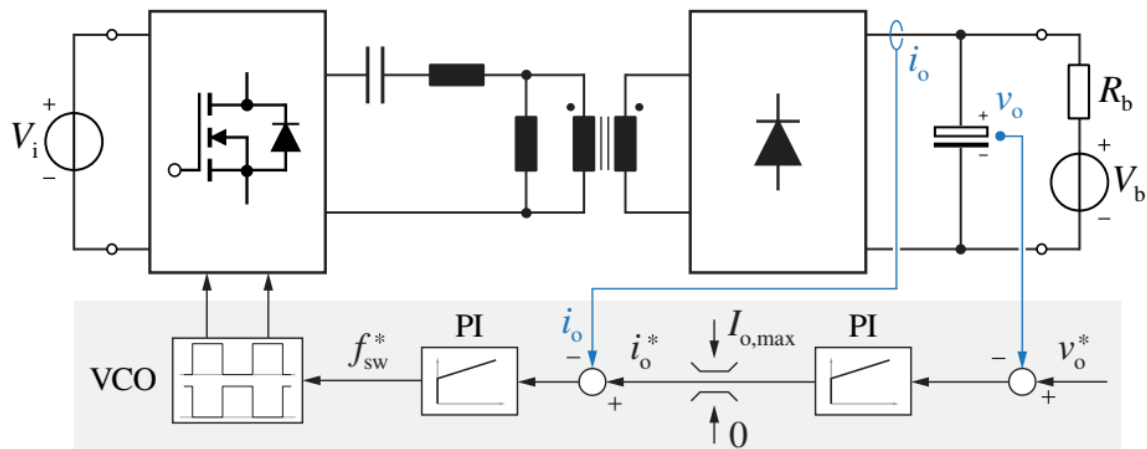


Figure 8.8: Cascaded Closed Loop Control for LLC Resonant Converter

The cascaded control loop is used to control both the output voltage and the current value. If the control loop consisted of a single PI controller that only controls the output voltage, during the transient of the circuit, the current value may become too high, potentially exceeding the rated switch current. There are two PI controllers used in this setup. The first PI controller's input is the voltage error (the reference value minus the measured value), while the second PI controller's input is the current error (the output of the first PI controller minus the measured current value), as shown in the Figure 8.8.

8.7 Matlab Model

The simulation ratings:

- Input voltage: 650 - 800 volt rated 700 Volt.
- Output voltage: 350 - 500 volt rated 400 Volt.
- Transformer turns ratio $N_p/N_s = 700/400$.
- Frequency 70K Hz.
- Rated power: 7000 watt.
- L_r : 3.8e-05 H.
- L_m : 2.32e-04 H.
- C_r : 1.3e-07 F.

The MATLAB Simulink model:

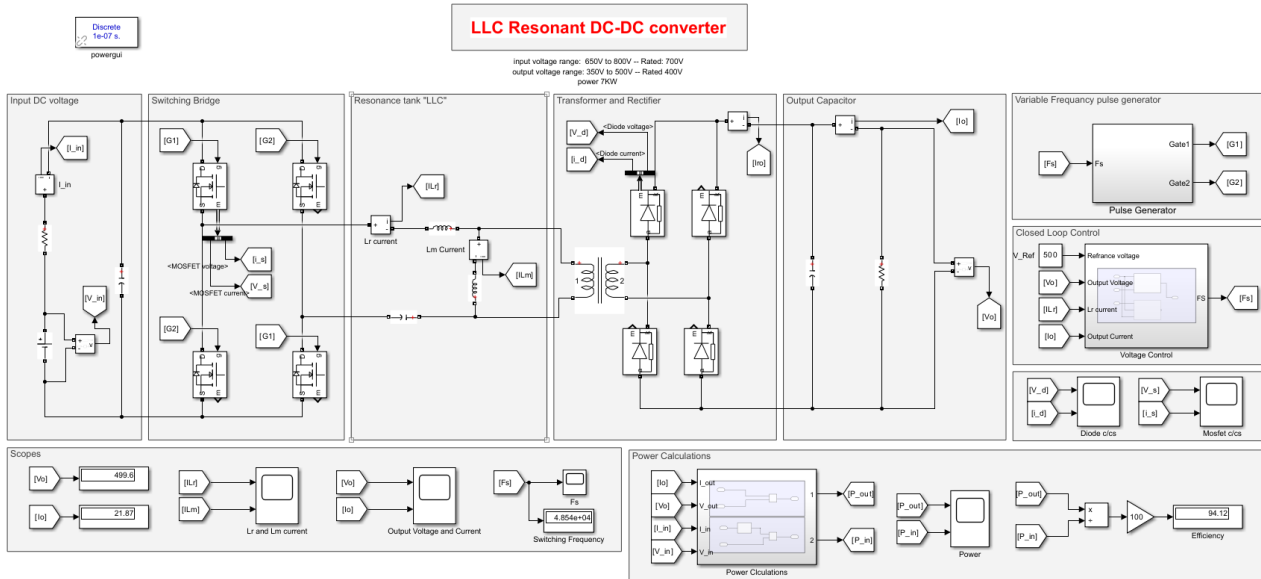


Figure 8.9: MATLAB Simulink Model For LLC Resonant Converter

This model consists of three main sections:

- The power circuit [8.10].
- Voltage controller [8.11].
- Variable frequency pulse generator [8.12].

The power circuit has input DC source, active bridge, resonant tank, transformer, diode bridge and output DC link.

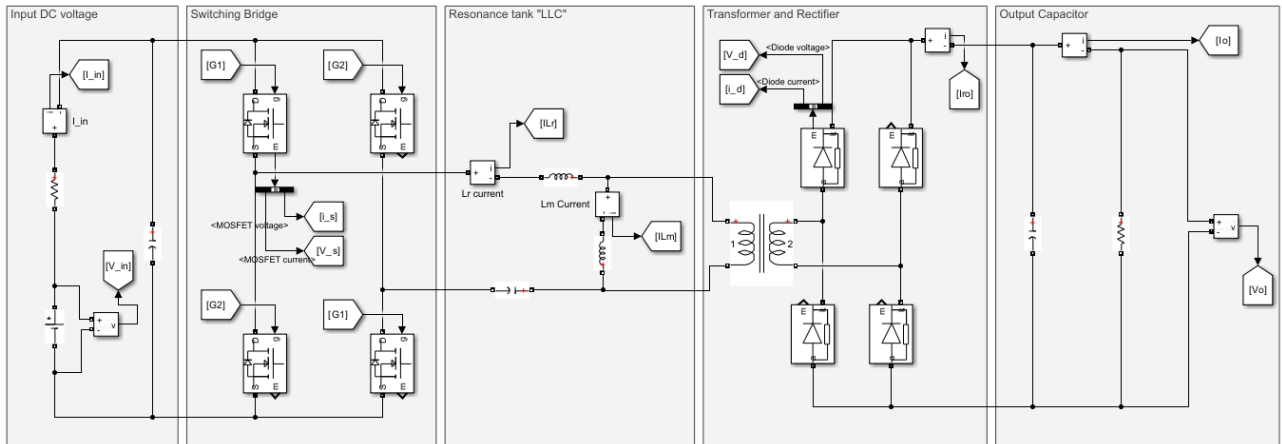


Figure 8.10: LLC Resonant Converter Power Circuit

The voltage controller is a cascaded control "multi loop control" using PI controller. It controls the output voltage and limit the transient current.

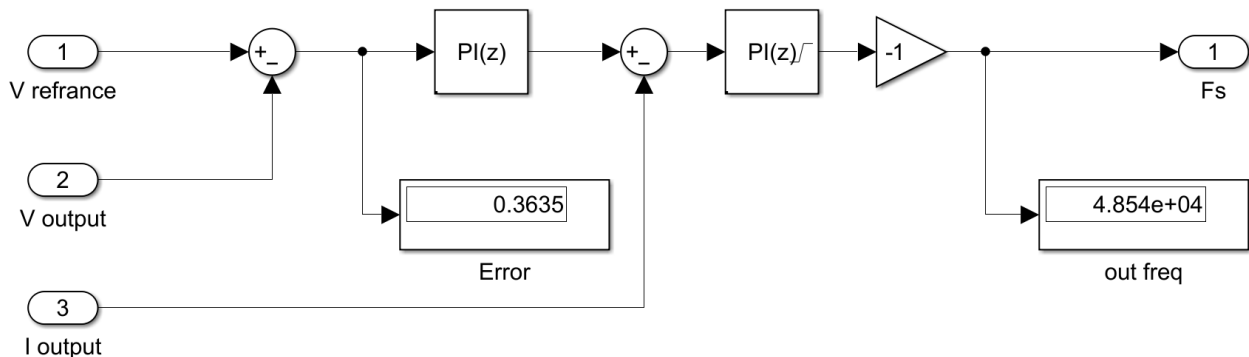


Figure 8.11: Cascaded Control for LLC Resonant Converter

Variable frequency pulse generator is used to generate pulses with specific duty cycle (in this model the duty cycle = 0.5) with variable frequency.

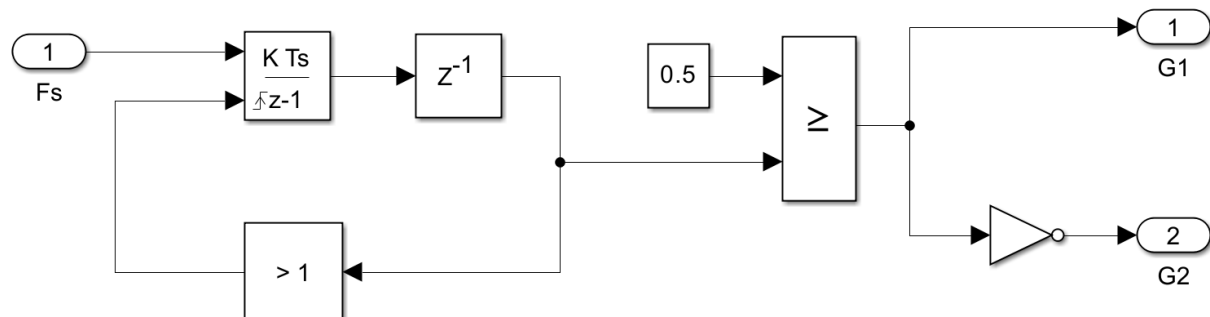


Figure 8.12: Variable Frequency Pulse Generator

This is the result of simulation in case of the reference voltage is 350V so the converter operates as a buck converter.

The figure 8.13 shows the results of simulation and shows the output voltage, the waveform of leakage inductor current and magnetizing inductor current and the change in frequency.

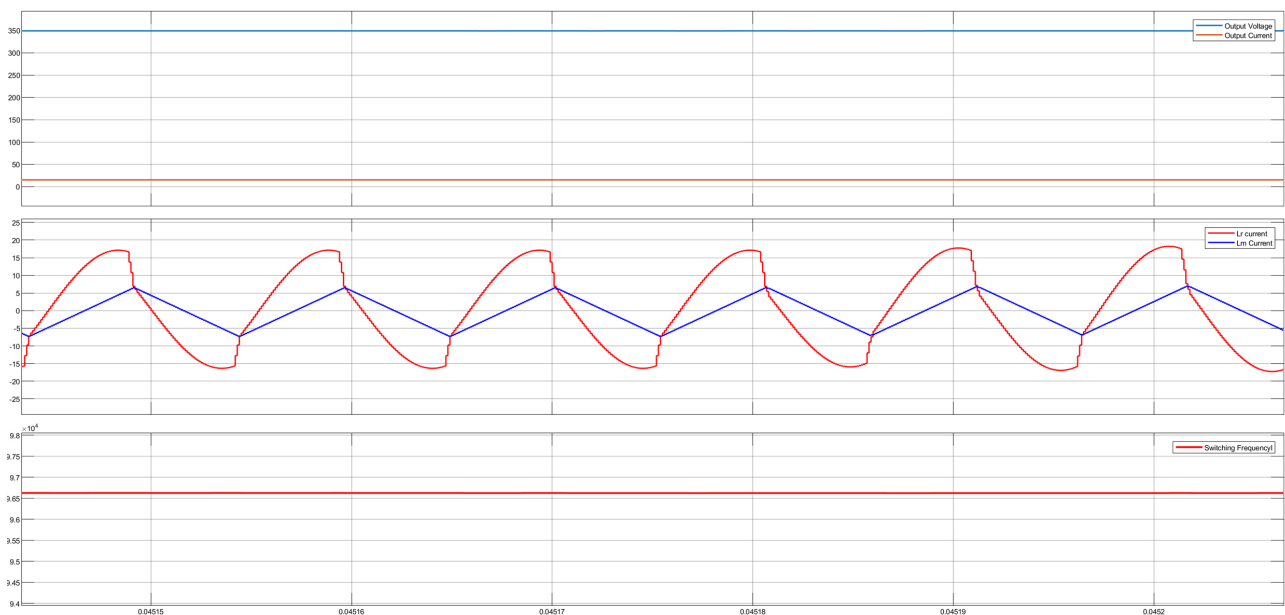
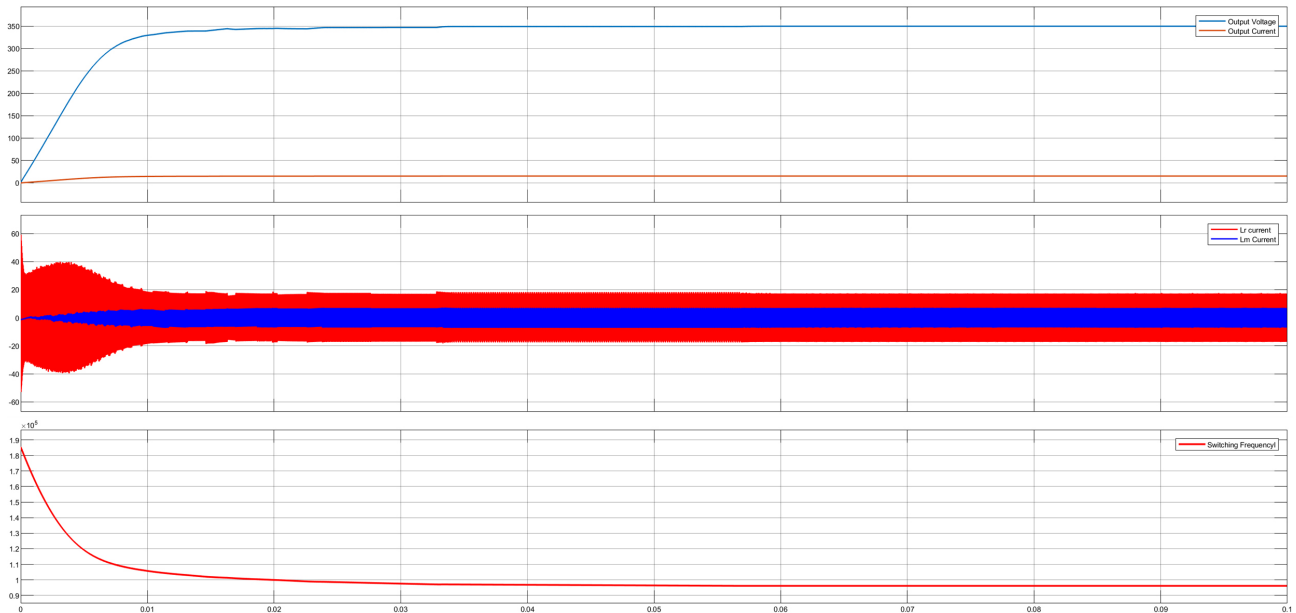
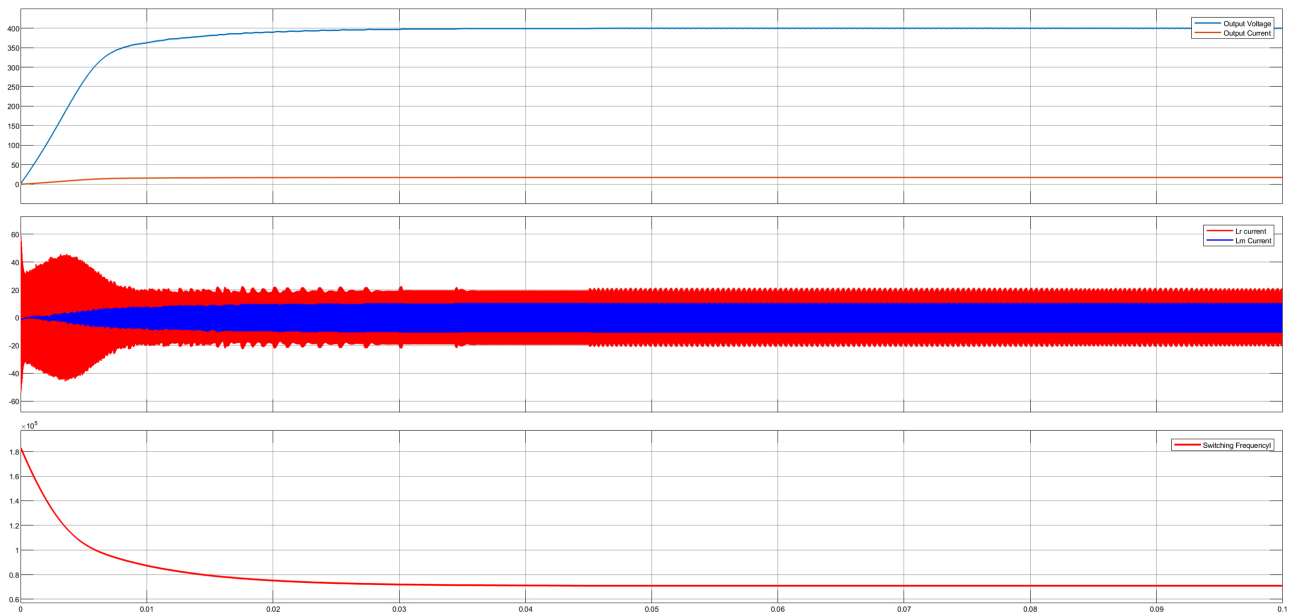


Figure 8.13: Results in case of Reference voltage equal 350V

This is the result of simulation in case of the reference voltage is 400V. The figure 8.14 shows the results of simulation and shows the output voltage, the waveform of leakage inductor current and magnetizing inductor current and the change in frequency.



At Steady State

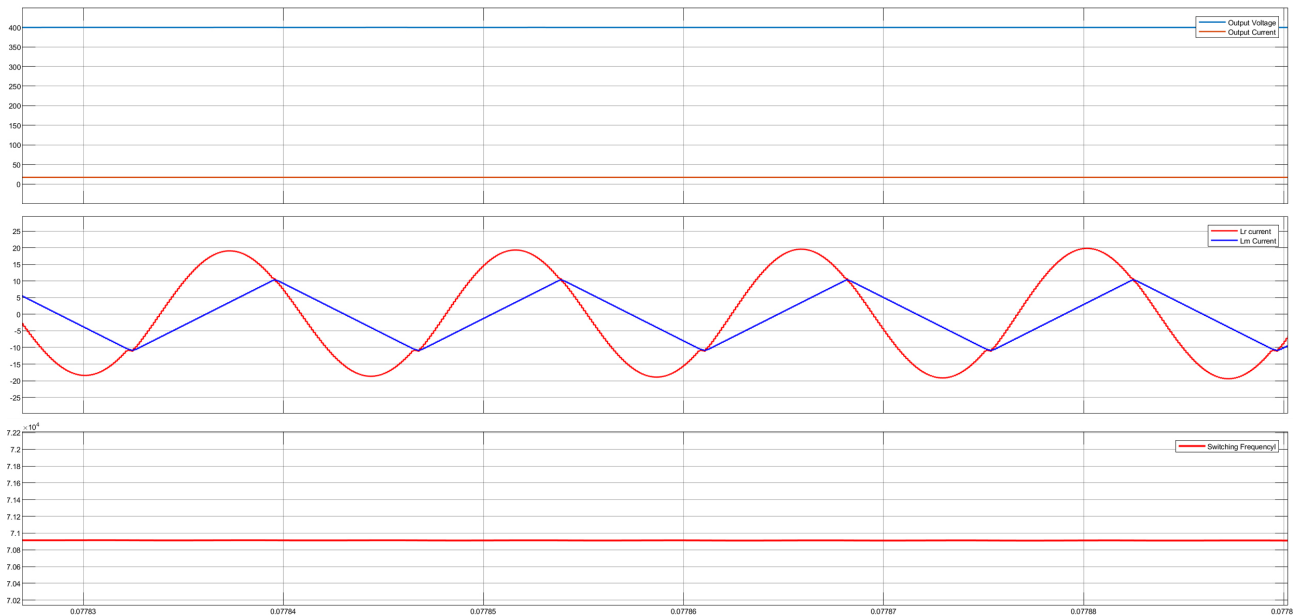
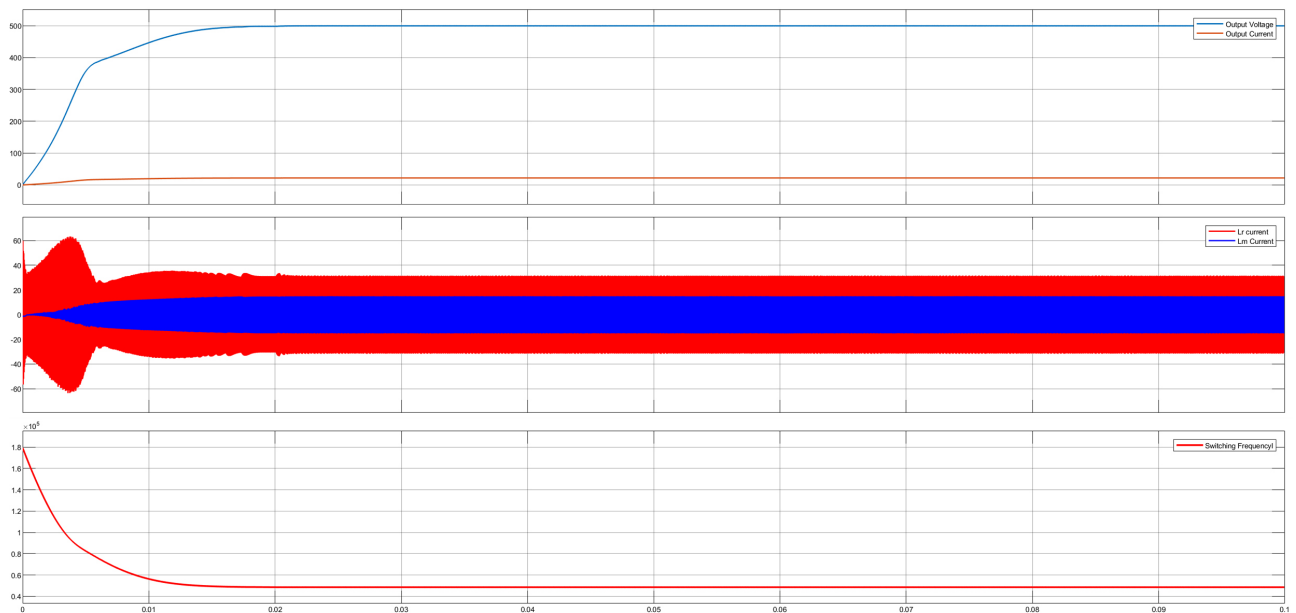


Figure 8.14: Results in case of Reference voltage equal 400V

This is the result of simulation in case of the reference voltage is 350V so the converter operates as a boost converter.

The figure 8.15 shows the results of simulation and shows the output voltage, the waveform of leakage inductor current and magnetizing inductor current and the change in frequency.



At Steady State

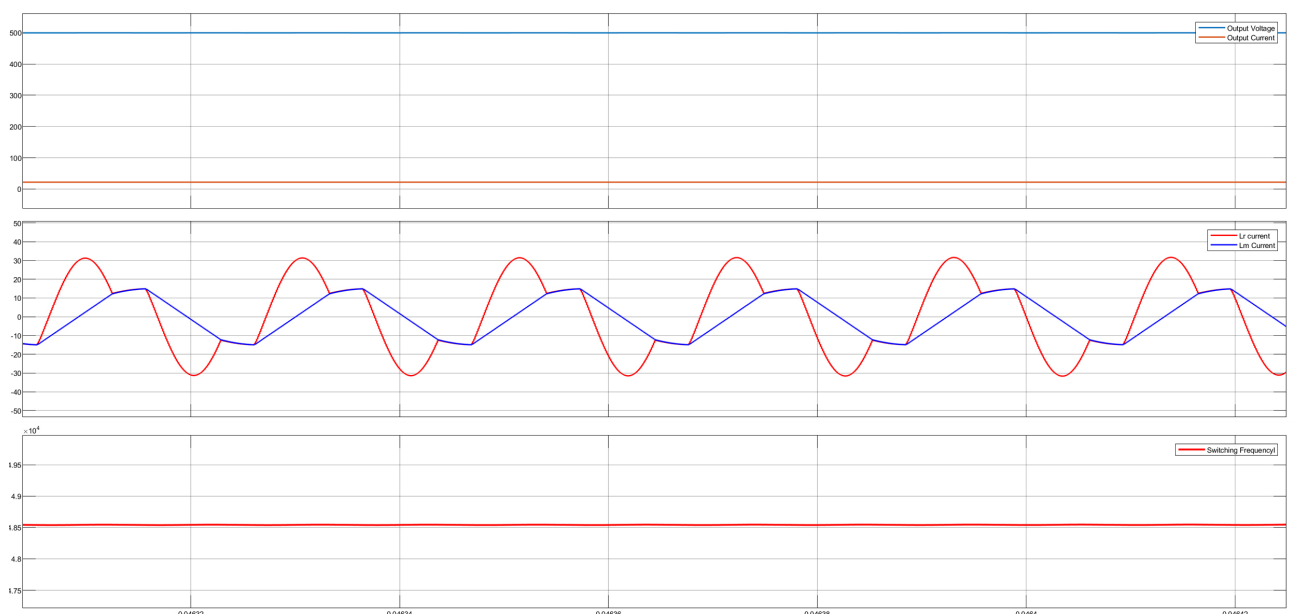


Figure 8.15: Results in case of Reference voltage equal 500V

8.8 Conclusion

The LLC resonant converter is an isolated DC-DC converter with high efficiency, around 96%. It can be used for bucking or boosting the input voltage. The LLC resonant converter can be controlled by adjusting the switching frequency of its inverting bridge, allowing it to operate in three modes. It finds application in various fields such as electrical vehicles, solar panels, and more.

Chapter 9

High Frequency (HF) Transformer Design

9.1 Introduction to HF Transformer

High-frequency transformers are vital components in various electronic systems, especially in power electronics, telecommunications, and high-frequency switching applications. Unlike conventional transformers operating at line frequencies (50 Hz or 60 Hz), high-frequency transformers are designed to operate at frequencies ranging from several kHz to MHz.[15]

9.1.1 Operating Frequency

High-frequency transformers operate at frequencies higher than those of traditional transformers. They are commonly used in applications such as switch-mode power supplies (SMPS), DC-Dc converters (the application used in our project), inverters, and radio frequency (RF) circuits.

9.1.2 Core Materials

High-frequency transformers often use ferrite cores rather than traditional iron cores. Ferrite materials have low losses at high frequencies, making them ideal for high-frequency applications. Other materials like powdered iron, amorphous metals, and some specialty materials are also used based on specific design requirements.

9.1.3 Winding Configurations

Transformers designed for high frequencies may have specialized winding configurations to minimize leakage inductance and inter-winding capacitance. Techniques such as interleaving, layering, and other techniques may be employed to achieve desired electrical characteristics.

9.1.4 Wire and Insulation

High-frequency transformers often use specialized wire types with thin enamel insulation to minimize skin effect losses and maximize packing density. Insulation materials are carefully selected to withstand the high voltages and minimize parasitic capacitances.

9.1.5 Losses and Efficiency

Efficiency is critical in high-frequency transformers due to the increased switching losses at higher frequencies. Design considerations include minimizing core losses (hysteresis and eddy current losses), and copper losses (resistive losses in windings).

9.1.6 Magnetic Design

Magnetic design involves selecting core materials, determining core geometry, calculating the number of turns, and optimizing magnetic flux density to achieve desired performance.

9.1.7 Electromagnetic Interference (EMI)

High-frequency transformers should be designed to minimize electromagnetic interference (EMI) emissions and susceptibility. Techniques such as shielding, grounding, and layout optimization are used to mitigate EMI issues.

9.1.8 Temperature Rise and Cooling

High-frequency transformers may experience significant temperature rise due to increased losses. Cooling methods such as conduction, convection, and liquid cooling may be employed to manage temperature rise.

9.2 HF Transformer Design

High-frequency transformer design requires a deep understanding of core materials, winding configurations, losses, efficiency, electromagnetic properties, and thermal management techniques. The design process involves careful consideration of these factors to meet the performance requirements of modern electronic systems operating at high frequencies.

9.2.1 General Procedures

1. Select system requirements including:

- Switching Frequency.
- Power Supply in Watt.

- Output Voltage and Current and Input Voltage.
2. Choose the suitable and most appropriate core material.
 3. Determine number of turns.
 4. Test the obtained output and compare it with the required one to be obtained.
 5. Determine diameter of wire.
 6. Determine number of layers.
 7. Determine length of wire.

9.2.2 Procedures in Detail

Starting with the Primary Side:

- **First:** The Choice of Core Material:

The choice of the core and its material is done through the intersection between the power rating, the switching frequency, and the selected shape from Typical Power Handling Chart shown in Figure 9.1:

Typical Power Handling Chart

Power in Watts				Pot, RS, DS	E Cores	RM, PQ, EP	UU, UI, UR	ETD, EER, EC	EFD, Planar	Toroid
20 kHz	50 kHz	100 kHz	250 kHz							
2	3	4	7	41811 RS DS PC	41205 EE 41707 EE	41313 EP 41812 RM 41912 RM			42107 EE 41805 EE	40907 TC 41406 TC 41303 TC 41435 TC 41304 TC 41206 TC 41506 TC 41407 TC 41405 TC 41305 TC
5	8	11	21	41814 PC 42311 RS DS HS	41808 EE	41717 EP 42013 RM 42016 PQ 42610 PQ			42019 EFD 42216 EI 42214 EI 43208 EI	41306 TC 41607 TC 41450 TC 41410 TC 41605 TC 41610 TC 41606 TC
12	18	27	52		41810 EE 42510 EE	42316 RM				
13	20	29	56	42213 PC		42614 PQ				
15	22	32	62	42318 RS DS HS					42214 EE	
18	28	40	78			42020 PQ			42523 EFD	
19	30	42	83	42616 RS DS HS	42513 EE 42515 EI	42120 EP 43214 PQ	42515 UI		42216 EE 43618 EI 42217 EE 44008 EI	42106 TC 41809 TC
26	42	58	113						43208 EE	42206 TC
28	45	63	122		42520 EE				43030 EFD	
30	49	67	131	42616 RS PC		42620 PQ				42109 TC
33	53	74	144		42515 EE	42819 RM				42207 TC
40	61	90	175		42526 EE 43007 EE					42506 TC
42	70	94	183	43019 HS		42625 PQ			43618 EE	
48	75	108	210	42823 PC 43019 RS DS PC	43009 EE		42512 UU 42515 UU	42929 ETD	44008 EE	42507 TC

Figure 9.1: Typical Power Handling Chart

- **Second:** Checking or Testing the Power:

$$Power = \frac{AP_c * f}{754} \quad (9.1)$$

Where $AP_c = A_e * W_c$,

AP_c is calculated in cm^4 ,

A_e is the effective area of the core (from datasheet) in cm^2 ,

W_c is the winding window of copper.

OR

$$Power = Area * (5.6)^2 \quad (9.2)$$

Where Area is the product of core length and width or total area of core in cm^2 .

- **Third:** Calculating the Number of Turns:

$$N_p = \frac{V_{peak} * 10^8}{4 * B_{MaxGauss} * A_e * f} \quad (9.3)$$

Where, $B_{MaxGauss}$ is the flux density that depends on core material choice in Gauss,

$$1000 \text{ Gauss} = 0.1 \text{ Tesla}$$

V_{Peak} is the peak input voltage to the primary side of transformer in Volt (V),

A_e is the effective area of the chosen core in cm^2 ,

N_p is the required Number of primary side turns,

f is the switching frequency in Hz.

Another Rule:

$$N_p = \frac{V_{in} * D * 10^8}{B_{max\text{ Gauss}} * A_e * f} \quad (9.4)$$

Where, D is the Duty Cycle (Since we are dealing with square wave),

V_{in} is the input voltage.

OR

$$N_p = \frac{V_{in} * t_{on}}{B_{max\text{ Tesla}} * A_e} \quad (9.5)$$

There is an important check to take into account which is:

For the calculated N_p , check the flux density obtained (B) to make sure that it still suited the chosen core material by substituting in the following rule:

$$B_{max\text{ Gauss}} = \frac{V_{peak} * 10^8}{4 * N_p * A_e * f} \quad (9.6)$$

Fourth: Calculating the Diameter of Wire:

We should determine Current in Primary Side by:

- a. Finding output power from the relation: $P_o = V_o * I_o$
- b. Finding input power from the relation: $P_{in} = P_o + 0.05 * P_o$ where $0.05 * P_o$ are some assumed losses.
- c. Finding current in primary side from the relation: $I_p = \frac{P_p}{V_p} = \frac{P_{in}}{V_{in}}$

Using the AWG (American Wire Gauge) and entering with the value of I_p which is approximately the maximum current in such table, we get the suitable diameter of wire.

However, there are well-known diameters like 0.4 mm and 0.6 mm.

So, there are some other checks to determine whether to use the standard diameters or the one obtained from table after calculating I_p :

- a. Check for Max Frequency (Make sure you choose diameter that has maximum frequency greater than the input switching frequency).
- b. Check the resistance from the table (Make sure that the chosen diameter has resistance (ohm/km) that causes an acceptable voltage drop. However, Voltage Drop Calculation is more effective in Secondary than in Primary).
- c. Check for maximum current, max frequency, and resistance per km if you decide to use a standard diameter like 0.4 mm and 0.6 mm.

Fifth: Calculating the Number of Layers:

- a. Calculate the vertical distance of the area subjected to the winding.
- b. Calculate the number of wires: Number of wires = $\frac{\text{Distance Calculated in a}}{\text{Diameter of Wire}}$

Note: There will be a margin to prevent the presence of high voltage at the terminals in the case of E-core for example (The margin is between 1 mm and 2 mm).

- c. Calculate the number of layers from the relation:

$$\text{Number of Layers} = \frac{\text{Number of Turns}}{\text{Number of Wires}}$$

There is another check here which is the guarantee that the area of the chosen core will be enough for or compatible with the winding and number of layers:

This check is done by:

- a. If Number of Layers * diameter of 1 wire < Area occupied by the wires by acceptable value. Therefore, proceed to the next step of design.
- b. If Number of Layers * diameter of 1 wire \geq Area occupied by the wires. Therefore, there should be some suggested modifications either:

1. Change Core to a larger one.
2. Or Increase Switching Frequency to decrease the Number of turns and hence decrease the number of layers.

$$N_p = \frac{V_{\text{peak}} * 10^8}{4 * B_{\text{max Gauss}} * A_c * f} \quad \& \text{ Number of Layers} = \frac{\text{Number of Turns}}{\text{Number of Wires}}$$

As N_p is inversely proportional to Switching Frequency and directly proportional to Number of Layers.

Note: Take into consideration that increasing frequency increases the core losses.

Sixth: Calculating the Length of Wire:

Length of Wire = Number of Turns * Length of Complete Turn + Additional 10 or 20 cm (according to design) for the terminals

Checking the Voltage Drop mentioned in **Fourth** is done by:

(Value from Table) ----- 1000 m

? ----- Length of Wire

After that, the Secondary Side:

Many steps are the same as those done in Primary Side but with some differences.

Calculating Number of Turns:

From the relation: $\frac{V_p}{V_s} = \frac{N_p}{N_s}$ ----- $N_s = \frac{N_p * V_s}{V_p}$

Where, V_p is the primary voltage,

V_s is the secondary voltage,

N_p is the number of turns in the primary side,

N_s is the number of turns in the secondary side.

Some Notes and differences for Secondary Design:

- If N_s is decimal, approximate it to the larger or the smaller value then check for V_s from the relation: $\frac{V_p}{V_s} = \frac{N_p}{N_s}$.
- The value of I_s is the same as output current.
- If there is a problem with the diameter of wire with the max frequency when dealing with the AWG Table (as the current in secondary is in Amperes with max frequencies less than the ones used in switching and diameter of wire which is not standard), stranding, or bundling are used in this case. The Number of wires is calculated from the relation:

$$\text{Number of wires} = \frac{I_s}{I_{\text{chosen from table to achieve a standard diameter}}}$$

For Low Rating (Practical):**Givens:**

Switching Frequency = 50KHz

Input and Output Voltage = 200 V

Output Power = 1Kw = 1000 watt

First: The Choice of Core Material:

Typical Power Handling Chart

20 kHz	50 kHz	100 kHz	250 kHz	Pot, RS, DS	E Cores	RM, PQ, EP	UU, UI, UR	ETD, EER, EC	EFD, Planar	Toroid
220	350	495	962		44721 EE		44119 UR			
230	350	550	1073	44229 RS DS		43535 PQ	44121 UR	44013 EER		
260	400	585	1137							43813 TC
280	430	630	1225	44229 PC	44020 EE			44216 EER		
300	450	675	1312					44444 ETD 44818 EER 45224 EC	45810 EI	43615TC
340	550	765	1487		44033 EE		44125 UR			
360	580	810	1575		44022 EE	44040 PQ		45418 EER		43620 TC
410	650	922	1793		44033 EE 45724 EE		44130 UR	44821 EER 44949 ETD	46410 EI	44416 TC 44419 TC 43825 TC
550	800	1237	2406		46016 EE					44015 TC 44715 TC
650	1000	1462	2843			45050 PQ			45810 EE	
700	1100	1575	3062		45528 EE		45716 UR	45454 ETD	46410 EE	44920 TC 44916 TC
900	1500	2000	3900		45530 EE					44925 TC
1000	1600	2250	4375	43428 UG	47228 EE 46022 EE		45917 UR	45959 ETD 47035 EC		46013 TC 46113 TC
1600	2600	3700	7215				46420 UR			44932 TC 46019 TC
2000	3000	4500	8750		46527 EE 47133 EE 48020 EE					46325 TC 46326 TC 47313 TC
2800	4200	6500	12675				49316 UI		49938 EE	48613 TC 48626 TC

Figure 9.2: Typical Power Handling Chart

But here, we don't want to choose these types of cores. We are searching for E cores. Therefore, we head to a power > 1000 watt from this chart.

Checking Powers for E cores with the intersections of 50 KHz and powers: 1100watt, 1500 watt and 1600 watt:

For 1100 watt: 45528 EE (or 45528 EC)

Typical Power Handling Chart

Power in Watts				Pot, RS, DS	E Cores	RM, PQ, EP	UU, UI, UR	ETD, EER, EC	EFD, Planar	Toroid
20 kHz	50 kHz	100 kHz	250 kHz							
220	350	495	962		44721 EE		44119 UR			
230	350	550	1073	44229 RS DS		43535 PQ	44121 UR	44013 EER		
260	400	585	1137							43813 TC
280	430	630	1225	44229 PC	44020 EE			44216 EER		
300	450	675	1312					44444 ETD 44818 EER 45224 EC	45810 EI	43615TC
340	550	765	1487		44033 EE		44125 UR			
360	580	810	1575		44022 EE	44040 PQ		45418 EER		43620 TC
410	650	922	1793		44033 EE 45724 EE		44130 UR	44821 EER 44949 ETD	46410 EI	44416 TC 44419 TC 43825 TC
550	800	1237	2406		46016 EE					44015 TC 44715 TC
650	1000	1462	2843			45050 PQ			45810 EE	
700	1100	1575	3062		45528 EE		45716 UR	45454 ETD	46410 EE	44920 TC 44916 TC
900	1500	2000	3900		45530 EE					44925 TC

Figure 9.3: Typical Power Handling Chart

For 1500 watt: 45530 EE (or 45530 EC)

Typical Power Handling Chart

Power in Watts				Pot, RS, DS	E Cores	RM, PQ, EP	UU, UI, UR	ETD, EER, EC	EFD, Planar	Toroid
20 kHz	50 kHz	100 kHz	250 kHz							
220	350	495	962		44721 EE		44119 UR			
230	350	550	1073	44229 RS DS		43535 PQ	44121 UR	44013 EER		
260	400	585	1137							43813 TC
280	430	630	1225	44229 PC	44020 EE			44216 EER		
300	450	675	1312					44444 ETD 44818 EER 45224 EC	45810 EI	43615TC
340	550	765	1487		44033 EE		44125 UR			
360	580	810	1575		44022 EE	44040 PQ		45418 EER		43620 TC
410	650	922	1793		44033 EE 45724 EE		44130 UR	44821 EER 44949 ETD	46410 EI	44416 TC 44419 TC 43825 TC
550	800	1237	2406		46016 EE					44015 TC 44715 TC
650	1000	1462	2843			45050 PQ			45810 EE	
700	1100	1575	3062		45528 EE		45716 UR	45454 ETD	46410 EE	44920 TC 44916 TC
900	1500	2000	3900		45530 EE					44925 TC

Figure 9.4: Typical Power Handling Chart

For 1600 watt:47228 EE or 46022 EE

Typical Power Handling Chart

20 kHz	50 kHz	100 kHz	250 kHz	Pot, RS, DS	E Cores	RM, PQ, EP	UU, UI, UR	ETD, EER, EC	EFD, Planar	Toroid
220	350	495	962		44721 EE		44119 UR			
230	350	550	1073	44229 RS DS		43535 PQ	44121 UR	44013 EER		
260	400	585	1137							43813 TC
280	430	630	1225	44229 PC	44020 EE			44216 EER		
300	450	675	1312					44444 ETD 44818 EER 45224 EC	45810 EI	43615 TC
340	550	765	1487		44033 EE		44125 UR			
360	580	810	1575		44022 EE	44040 PQ		45418 EER		43620 TC
410	650	922	1793		44033 EE 45724 EE		44130 UR	44821 EER 44949 ETD	46410 EI	44416 TC 44419 TC 43825 TC
550	800	1237	2406		46016 EE					44015 TC 44715 TC
650	1000	1462	2843			45050 PQ			45810 EE	
700	1100	1575	3062		45528 EE		45716 UR	45454 ETD	46410 EE	44920 TC 44916 TC
900	1500	2000	3900		45530 EE					44925 TC
1000	1600	2250	4375	43428 UG	47228 EE 46022 EE		45917 UR	45959 ETD 47035 EC		46013 TC 46113 TC

Figure 9.5: Typical Power Handling Chart

Second: Checking or Testing the Power:

For 45528 EE (or 45528 EC), 45530 EE (or 45530 EC) & 47228 EE or 46022 EE:

TYPE/SIZE	ORDERING CODE	MAGNETIC DATA						HARDWARE
		I _e (mm)	A _e (mm ²)	A _e min (mm ²)	V _e (mm ³)	WaAc (cm ⁴)	Weight (grams per set)	
E 40/17/11	O_44011EC	76.7	127	114	9,780	1.26	49	
E 42/21/9	O_44016EC	98.4	107	106	10,500	1.65	52	
E 43/21/15	O_44020EC	97.0	178	175	17,300	3.55	87	PCB4020N1
I 43/6/15	O_44020IC	67.1	177	176	11,900	1.36	60	PCB4020N1
E 43/21/20	O_44022EC	97.0	233	233	22,700	4.22	114	PCB4022N1
E 42/33/20	O_44033EC	145	236	234	34,200	6.36	164	
E 41/17/12	O_44317EC	77.0	149	142	11,500	1.88	57	PCB4317M1
E 47/20/16	O_44721EC	88.9	234	226	20,800	3.3	103	PCB4721M1
E 56/28/21	O_45528EC	124	353	345	44,000	9.78	212	PCB5528WC
E 56/28/25	O_45530EC	123	420	411	52,000	12.1	255	PCB5530FA
E 56/24/19	O_45724EC	107	337	337	36,000	6.98	179	PCB5724M1
E 60/22/16	O_46016EC	110	248	240	27,200	5.74	135	
E 60/31/22	O_46022EC	139	402	401	55,900	21.0	200	
E 65/32/27	O_46527EC	147	540	530	79,000	23.5	410	00B652701
E 70/33/32	O_47133EC	149	683	676	102,000	23.3	495	
E 72/28/19	O_47228EC	137	368	363	50,300	15.0	250	00B722801
E 80/38/20	O_48020EC	184	392	392	72,300	31.6	357	00B802081
E 100/59/27	O_49928EC	274	738	692	202,000	90.6	980	

Refer to page 62 for additional hardware information.

Figure 9.6: Typical Power Handling Chart

For 1100 watt: 45528 EE (or 45528 EC):

$$\text{Power} = \frac{AP_c * f}{754} = \frac{9.78 * 50 * 10^3}{754} = 648.5411141 \text{ watt} < 1000 \text{ watt}$$

Then, Search in the chart for a core with a higher power (>1100watt)

For 1500 watt: 45530 EE (or 45530 EC):

$$\text{Power} = \frac{AP_c * f}{754} = \frac{12.1 * 50 * 10^3}{754} = 802.3872679 \text{ watt} < 1000 \text{ watt}$$

Then, Search in the chart for a core with a higher power (>1500watt)

For 1600 watt: 47228 EE:

$$\text{Power} = \frac{AP_c * f}{754} = \frac{15 * 50 * 10^3}{754} = 994.6949602 \text{ watt}$$

For 1600 watt: 46022 EE:

$$\text{Power} = \frac{AP_c * f}{754} = \frac{21 * 50 * 10^3}{754} = 1392.572944 \text{ watt}$$

Then we can choose either **47228 EE** or **46022 EE**. We chose **46022 EE**.

Third: Calculating the Number of Turns:

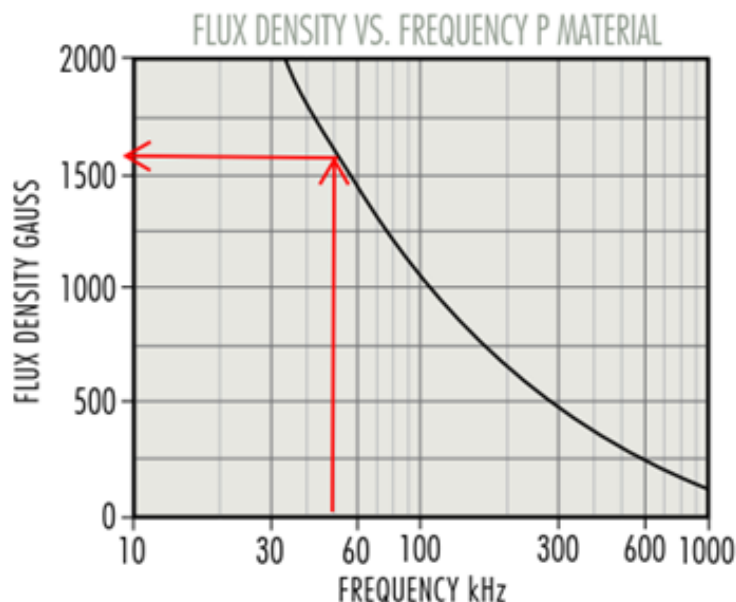


Figure 9.7: Flux Density Vs Frequency (P-Material)

$$N_p = \frac{V_{\text{peak}} * 10^8}{4 * B_{\max} \text{Gauss} * A_e * f} = \frac{200 * 10^8}{4 * 1580 * 402 * 10^{-2} * 50 * 10^3} = 15.74406449 \text{ turns} \approx 16 \text{ turns}$$

Fourth: Calculating the Diameter of Wire:

We should determine Current in Primary Side by:

$$P_o = V_o * I_o = 1000 \text{ watt} = 1\text{Kw}$$

$$P_{\text{in}} = P_o + 0.05 * P_o = 1000 + 0.05 * 1000 = 1050 \text{ watt} = 1.05\text{Kw}$$

$$I_p = \frac{P_p}{V_p} = \frac{P_{\text{in}}}{V_{\text{in}}} = \frac{1050}{200} = 5.25\text{A}$$

From AWG Table: $I_p = 5.25\text{A}$ (I_{max}). However, for 50KHz or 53KHz, the maximum current is 0.729A. So, parallel wires or bundling will be used:

$$\text{Number of parallel wires} = \frac{I_p}{I_{\text{max}}} = \frac{5.25}{0.729} = 7.201646091 \text{ wires} \approx 8 \text{ wires}$$

AWG	Diameter [inches]	Diameter [mm]	Area [mm ²]	Resistance [Ohms / 1000 ft]	Resistance [Ohms / km]	Max Current [Amperes]	Max Frequency for 100% skin depth
0000 (4/0)	0.46	11.684	107	0.049	0.16072	302	125 Hz
000 (3/0)	0.4096	10.40384	85	0.0618	0.202704	239	160 Hz
00 (2/0)	0.3648	9.26592	67.4	0.0779	0.255512	190	200 Hz
0 (1/0)	0.3249	8.25246	53.5	0.0983	0.322424	150	250 Hz
1	0.2893	7.34822	42.4	0.1239	0.406392	119	325 Hz
2	0.2576	6.54304	33.6	0.1563	0.512664	94	410 Hz
3	0.2294	5.82676	26.7	0.197	0.64616	75	500 Hz
4	0.2043	5.18922	21.2	0.2485	0.81508	60	650 Hz
5	0.1819	4.62026	16.8	0.3133	1.027624	47	810 Hz
6	0.162	4.1148	13.3	0.3951	1.295928	37	1100 Hz
7	0.1443	3.66522	10.5	0.4982	1.634096	30	1300 Hz
8	0.1285	3.2639	8.37	0.6282	2.060496	24	1650 Hz
9	0.1144	2.90576	6.63	0.7921	2.598088	19	2050 Hz
10	0.1019	2.58826	5.26	0.9989	3.276392	15	2600 Hz
11	0.0907	2.30378	4.17	1.26	4.1328	12	3200 Hz
12	0.0808	2.05232	3.31	1.588	5.20864	9.3	4150 Hz
13	0.072	1.8288	2.62	2.003	6.56984	7.4	5300 Hz
14	0.0641	1.62814	2.08	2.525	8.282	5.9	6700 Hz
15	0.0571	1.45034	1.65	3.184	10.44352	4.7	8250 Hz
16	0.0508	1.29032	1.31	4.016	13.17248	3.7	11 kHz
17	0.0453	1.15062	1.04	5.064	16.60992	2.9	13 kHz
18	0.0403	1.02362	0.823	6.385	20.9428	2.3	17 kHz
19	0.0359	0.91186	0.653	8.051	26.40728	1.8	21 kHz
20	0.032	0.8128	0.518	10.15	33.292	1.5	27 kHz
21	0.0285	0.7239	0.41	12.8	41.984	1.2	33 kHz
22	0.0254	0.64516	0.326	16.14	52.9392	0.92	42 kHz
23	0.0226	0.57404	0.258	20.36	66.7808	0.729	53 kHz

Table 9.1: AWG Table

Fifth: Calculating the Number of Layers:

The vertical distance of the area subjected to the winding = D dimension = 21.6mm

The number of wires: Number of wires = $\frac{21.6 - 2}{8 * 0.57404} = 4.267995262$ wires ≈ 5 wires

Note: There will be a margin to prevent the presence of high voltage at the terminals in the case of E-core for example (The margin is between 1 mm and 2 mm).

$$\text{Number of Layers} = \frac{\text{Number of Turns}}{\text{Number of Wires}} = \frac{16}{5} = 3.2 \text{ Layers} \approx 4 \text{ Layers}$$

TYPE/SIZE	ORDERING CODE	DIMENSIONS (mm)							
		A	B	C	D	E	F	L	M
E 40/17/11	0_44011EC	40.0 ± 0.51	17.0 ± 0.31	10.69 ± 0.31	10.0 min	27.6 min	10.7 ± 0.31	5.99 ± 0.25	8.86 nom
E 42/21/9	0_44016EC	42.15 ± 0.85	21.1 ± 0.2	9.0 ± 0.25	14.9 min	29.5 min	11.95 ± 0.25	5.94 ± 0.13	8.9 ± 0.25
E 43/21/15	0_44020EC	43.0 +0/-1.7	21.0 ± 0.2	15.2 +0/-0.6	14.8 +0.6/-0	29.5 +1.4/-0	12.2 +0/-0.5	6.75 nom	8.65 nom
I 43/6/15	0_44020IC	43.0 +0/-1.7	5.9 ± 0.2	15.2 +0/-0.6					
E 43/21/20	0_44022EC	43.0 +0/-1.7	21.0 ± 0.2	20.0 +0/-0.8	14.8 +0.6/-0	29.5 +1.4/-0	12.2 +0/-0.5	6.75 nom	8.65 nom
E 42/33/20	0_44033EC	42.0 +1/-0.7	32.8 +0/-0.4	20.0 +1/-0.8	26.0 +1/-0	29.5 +1.4/-0	12.2 +0/-0.5	5.98 ref	9.13 ref
E 41/17/12	0_44317EC	40.6 ± 0.65	16.6 ± 0.2	12.4 ± 0.3	10.4 min	28.6 min	12.45 ± 0.25	6.33 max	7.95 min
E 47/20/16	0_44721EC	46.9 ± 0.8	19.6 ± 0.2	15.6 ± 0.25	12.1 min	32.4 ± 0.65	15.6 ± 0.25	7.54 nom	7.87 min
E 56/28/21	0_45528EC	56.2 +0/-2.1	27.5 ± 0.3	21.0 +0/-0.8	18.5 +0.8/-0	37.5 +1.5/-0	17.2 +0/-0.5	9.35 ref	10.15 ref
E 56/28/25	0_45530EC	56.2 +0/-2.1	27.6 ± 0.38	24.61 ± 0.38	18.5 min	37.5 min	17.2 +0/-0.5	9.35 ref	10.15 ref
E 56/24/19	0_45724EC	56.1 ± 1	23.6 ± 0.25	18.8 ± 0.25	14.6 ± 0.13	38.1 min	18.8 ± 0.25	9.5 nom	9.03 nom
E 60/22/16	0_46016EC	59.99 ± 0.78	22.3 ± 0.3	15.62 ± 0.38	13.8 min	44.0 min	15.62 ± 0.38	7.7 ± 0.25	14.49 ± 0.25
E 60/31/22	0_46022EC	60.3 ± 0.9	30.6 ± 0.3	22.3 ± 0.38	21.6 ± 0.3	42.3 ± 0.78	18.1 ± 0.25	9.0 ref	12.1 ref
E 65/32/27	0_46527EC	65.0 +1.5/-1.2	32.8 +0/-0.6	27.4 +0/-0.8	22.0 +0.8/-0	44.2 +1.8/-0	20.0 +0/-0.7	9.95 ref	12.72 ref
E 70/33/32	0_47133EC	70.5 ± 1	33.2 +0/-0.5	32.0 +0/-0.8	21.9 +0.7/-0	48.0 +1.5/-0	22.0 +0/-0.7	11.25 nom	13.0 nom
E 72/28/19	0_47228EC	72.4 ± 0.76	27.9 ± 0.33	19.0 ± 0.33	17.8 min	52.6 min	19.0 ± 0.38	9.53 ± 0.38	16.9 min
E 80/38/20	0_48020EC	80.0 ± 1.6	38.1 ± 0.3	19.8 ± 0.4	28.2 ± 0.3	59.1 min	19.8 ± 0.4	11.25 nom	19.45 min
E 100/59/27	0_49928EC	100.3 ± 2.0	59.4 ± 0.47	27.5 ± 0.5	46.85 ± 0.38	72.0 min	27.5 ± 0.5	13.75 ± 0.38	22.65 ± 0.5

Table 9.2: Core Dimension

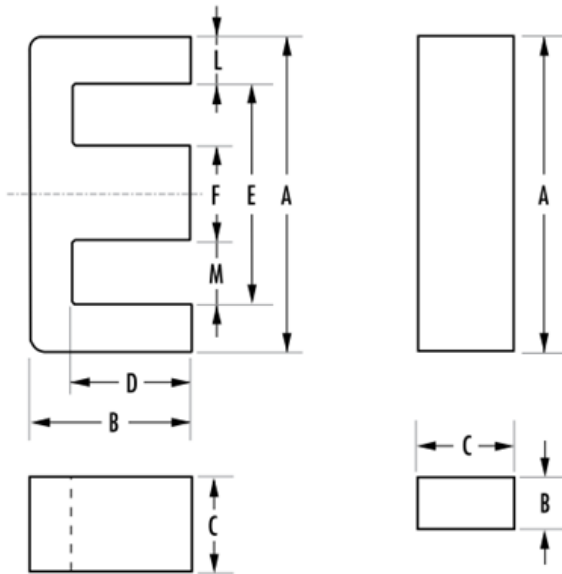
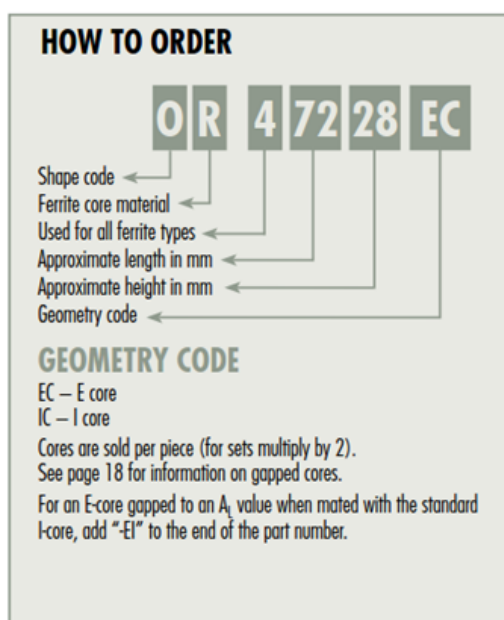


Figure 9.8: Core OR47228EC

Sixth: Calculating the Length of Wire:

Length of Wire = Number of Turns * Length of Complete Turn + Additional 10 or 20 cm (according to design) for the terminals = $16 * (2 * c + 2 * F) + 10 * 10$

$$\begin{aligned} &= 16 * [2 * (22.3 + 0.38) + 2 * (18.1 + 0.25)] + 100 \\ &= 1412.96 \text{ mm} \\ &= 1.41296 \text{ m} \end{aligned}$$

Checking the Voltage Drop mentioned in **Fourth** is done by

$$\begin{array}{rcl} 66.7808 & \text{-----} & 1000 \text{ m} \\ ? & \text{-----} & 1.41296 \end{array}$$

Therefore $R = \frac{66.7808 * 1.41296}{1000} = 0.09435859912 \text{ ohm}$

Therefore $V.D = I_p * R = 5.25 * 0.09435859912 = 0.495382656 \text{ V} \approx 0.5V$

Voltage Drop % = $\frac{0.5}{200} * 100 = 0.25\% < (5\%)$

Therefore, this voltage drop is **accepted**.

After that, the Secondary Side:

Many steps are the same as those done in Primary Side but with some differences.

Calculating Number of Turns:

From the relation: $\frac{V_p}{V_s} = \frac{N_p}{N_s}$

$$N_s = \frac{N_p * V_s}{V_p} = \frac{16 * 200}{200} = 16 \text{ turns (Same as primary)}$$

$$I_s = \frac{P_s}{V_s} = \frac{P_o}{V_o} = \frac{1000}{200} = 5A$$

From AWG Table: $I_s = 5A (I_{max})$. However, for 50KHz or 53KHz, the maximum current is 0.729A. So, parallel wires or bundling will be used:

$$\text{Number of parallel wires} = \frac{I_s}{I_{max}} = \frac{5}{0.729} = 6.858710562 \text{ wires} \approx 7 \text{ wires}$$

The wire used in both primary and secondary is: **AWG 23, 0.57404mm, 0.729A, 53KHz**

- The vertical distance of the area subjected to the winding = D dimension = 21.6mm
- The number of wires: Number of wires = $\frac{21.6 - 2}{7 * 0.57404} = 4.87770887 \text{ wires} \approx 5 \text{ wires}$

Note: There will be a margin to prevent the presence of high voltage at the terminals in the case of E-core for example (The margin is between 1 mm and 2 mm).

- Number of Layers = $\frac{\text{Number of Turns}}{\text{Number of Wires}} = \frac{16}{5} = 3.2 \text{ Layers} \approx 4 \text{ Layers}$

- Length of Wire = Number of Turns * Length of Complete Turn + Additional 10 or 20 cm (according to design) for the terminals = $16 * (2 * c + 2 * F) + 10 * 10$
 $= 16 * [2 * (22.3 + 0.38) + 2 * (18.1 + 0.25)] + 100$
 $= 1412.96 \text{ mm}$
 $= 1.41296 \text{ m}$

- No need to check for voltage drop because $I_s < I_p$ so voltage drop for I_s is less than that of I_p

Same steps will be done for another high ratings:

Givens:

Switching Frequency = 100KHz

Input and Output Voltage = 800 V

Output Power = 10Kw = 10000 watt

9.2.3 Results for both high and low ratings:

<i>POC</i>	<i>Low Rating</i>	<i>High Rating</i>
Core Type and Material	EI Ferrite (P-Material) 46022 EE or 46022 EC	EI Ferrite (P-Material) 49928EE or 49928EC
Effective Area of Core	402 mm ²	738 mm ²
Core Dimension	60/31/22	100/59/27
Number of Turns	16 Turns	26 Turns
Diameter of Wire for Both Sides	0.57404 mm	0.40386 mm
Number of Parallel Wires in Primary Side	8	37
Number of Parallel Wires in Secondary Side	7	34
Number of Layers in Primary Side	4	9
Number of Layers in Secondary Side	4	7
Length of Wire	1.41296 m	3.012 m

Table 9.3: Comparison Between the Results for High and Low Rating

Part III

Charger Integration

Chapter 10

Introduction to Electric Vehicle Chargers

Electric vehicles (EVs) have emerged as a viable alternative to internal combustion engines due to their efficient power delivery, cost-effectiveness, and environmental benefits. However, a key challenge is the availability of adequate charging infrastructure for high-energy-density battery packs and the development of efficient charging topologies. Despite these challenges, the global adoption of EVs is increasing to reduce oil dependency, which faces a 5–7% annual decline post-peak production. The widespread use of EVs, both private and commercial, poses significant challenges for power grids, particularly in maintaining power quality and managing peak load demand.[16]

Battery Electric Vehicles (BEVs) are increasingly gaining attention for their potential benefits. However, advancing their charging systems is challenging due to the need for optimal design, safety, high efficiency, and fast charging. There are two main types of charging technologies: wired (contact charging) and wireless (contactless charging). [17]

10.1 Wired Charging

Wired charging methods, which may be further broken down into AC and DC charging technologies, require a direct cable connection between the EV and the charging equipment to achieve charging. Figure 10.1 shows the overall charging technologies available for BEVs.

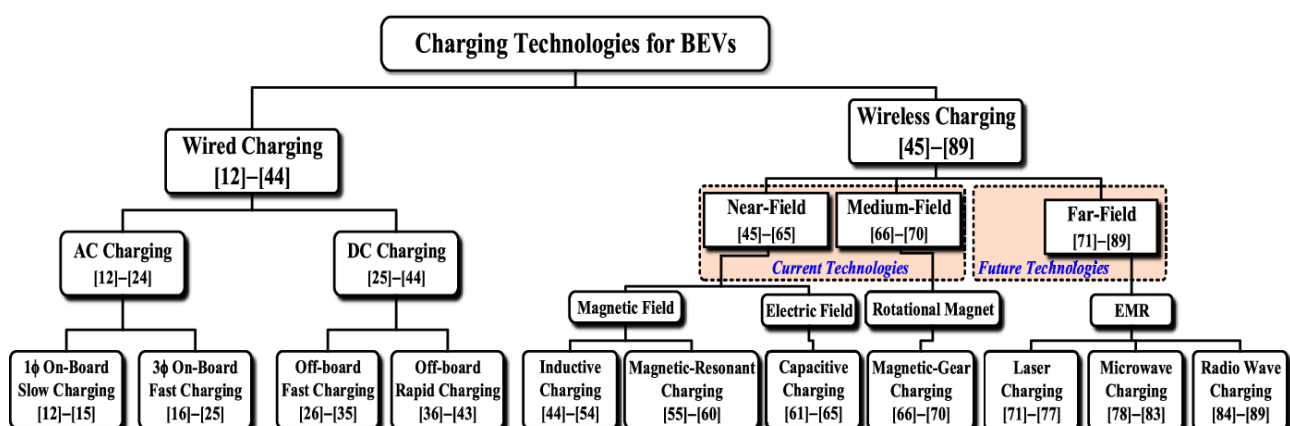


Figure 10.1: Overall charging system for BEVs using wired/wireless

10.1.1 AC Charging

Battery Electric Vehicles (BEVs) are typically charged by an onboard charger (OBC) that converts AC to DC. This adds weight to the vehicle because the conversion unit is housed inside. Charging is done through single-phase slow charging or three-phase fast charging systems. The OBC not only converts AC to regulated DC but also improves current quality by reducing ripples, switching losses, and electromagnetic interference (EMI). AC charging, mostly used in BEVs, operates at power levels below 20 kW, taking 2-6 hours to charge. [17]

10.1.2 DC Charging

Unlike AC methods, DC charging technologies directly charge the battery, enabling faster charging. This includes off-board fast and rapid charging systems, which reduce the vehicle's weight and size by externalizing the conversion unit. DC charging can fully charge high-capacity batteries in under an hour. The system involves an off-board charger at a station that feeds the battery directly, bypassing the onboard charger.

While wired charging systems have made significant progress, they are limited by their inflexibility in charging locations. Additionally, the installation of a battery management system (BMS) is costly and poses challenges in safety and reliability. [17]

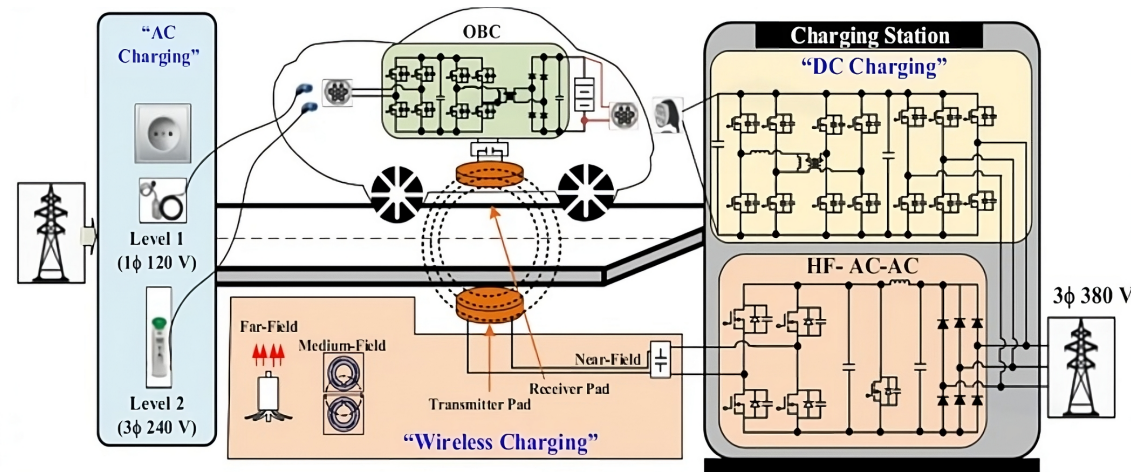


Figure 10.2: AC Vs DC Charging

10.2 Wireless Charging

On the other hand, the problems with wired charging technologies, such as the need for charging cables, maintenance, and safety concerns, have led to research into wireless charging technologies. In these kinds of technologies, the BEV has to park above the charging system to get the high-frequency charging current. Wireless charging technologies can be divided into three categories: near-field, medium, and far-field. However, these technologies are out of our scope. [17]

10.3 EV Charging Stages

10.3.1 AC-DC Rectifier

The AC-DC rectifier is the first power stage in an EV charging station that takes ac voltage of 250-480Vac from the grid and delivers stable dc link voltage of approximately 800V. The rectifiers are connected to the utility grid and so, they can inject harmonics which degrades power quality. Power factor correction (PFC) techniques are employed to address this concern. Utilization of these PFC strategies ensures that input currents are sinusoidal and are in phase with the sinusoidal voltages. Low THD (less than 5 percent), sinusoidal input current, high power factor, bidirectional power flow capability, high efficiency and power density, simple modulation and control, reactive power compensation, and stable output dc voltage are the expected features of an AC-DC rectifier.[18]

10.3.2 DC-DC Converter

The DC-DC back-end converter is the second power conversion stage of an off-board charger that takes rectified input voltage from the first power stage and then, adjusts it according to the EV battery. Input voltage of the dc-dc stage is the dc link voltage and output voltage can vary between 100V and 1000V. The task of constant current (CC) and constant voltage (CV) charging of the battery is accomplished by the DC-DC converter. High efficiency, high frequency operation, high power density, bidirectionality, low output voltage ripple, soft switching capabilities, stable voltage regulation, and wide range of output voltage are the key characteristics of the DC-DC converter.[18]

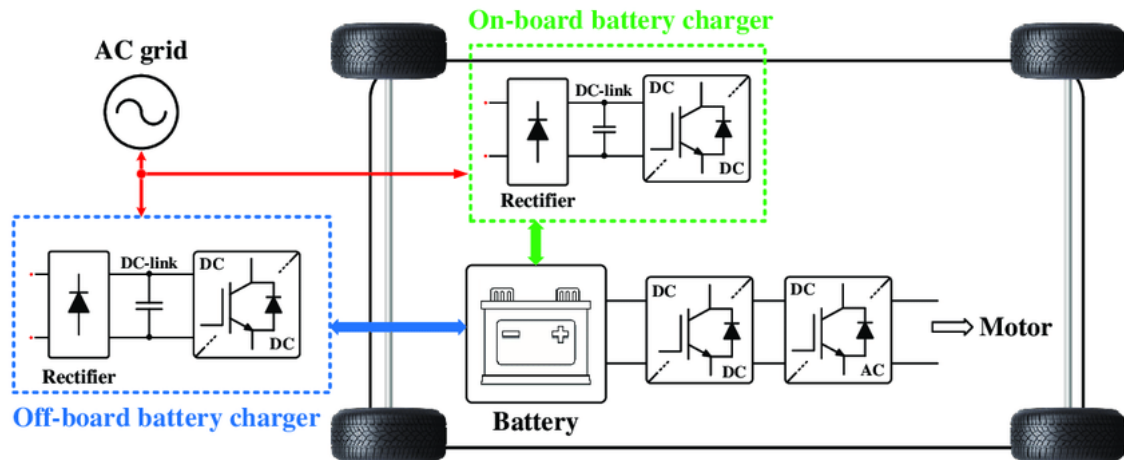


Figure 10.3: Electric vehicle (EV) charging system including off-board and on-board charger

Chapter 11

Comparison Between On-Board and Off-Board Chargers

Electric vehicle (EV) chargers are essential components for recharging the batteries of electric vehicles. Chargers can be categorized into two main types based on their fixed positions: on-board chargers and off-board chargers. Each type has its own set of advantages and disadvantages, impacting their suitability for different applications.

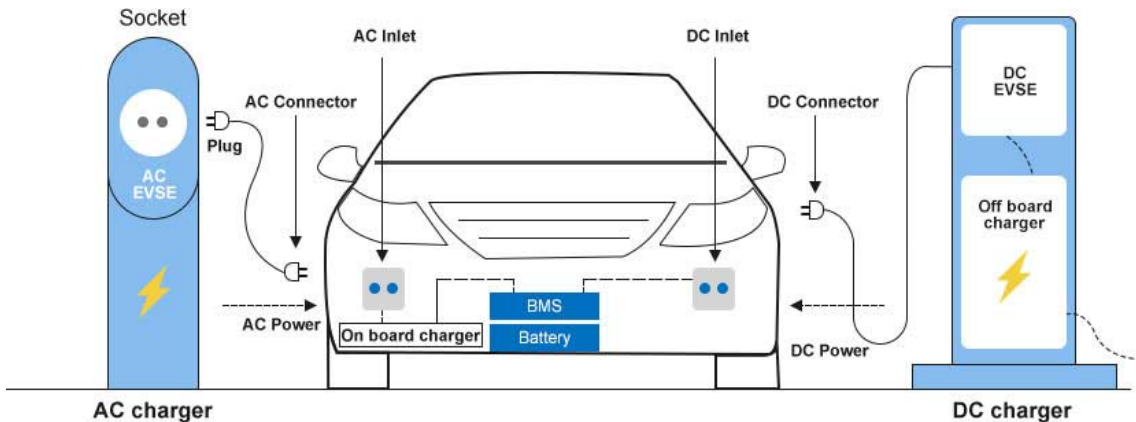


Figure 11.1: On-board charger versus off-board charger.

11.1 On-Board Chargers

On-board chargers are integrated into the vehicle itself. They are limited to level 1 and level 2 (slow charging) due to cost, weight, and space constraints. The main advantage of on-board chargers is their ability to charge the batteries wherever a suitable power source, such as a household outlet, is available, thereby increasing the acceptance of Plug-in Electric Vehicles (PEVs). On-board chargers are most often used at home, typically charging overnight with minimal impact on the supply grid [19].

Another approach to on-board charging involves integrating the battery charger into the electric drive system of the PEV. In this configuration, the motor windings serve as filter inductors and the motor inverter acts as a bidirectional AC/DC converter, reducing weight, volume, and cost while en-

abling faster charging (levels 2 and 3). However, this method introduces increased control complexity and additional hardware requirements [19].

11.2 Off-Board Chargers

Off-board chargers are located outside the vehicle and are not constrained by space or weight limitations, making them suitable for fast charging applications. They convert AC power from the grid into DC power, which is then delivered to the vehicle [19]. Although off-board chargers entail redundant power electronics, increasing the overall cost, they offer the advantage of higher power levels, enabling rapid charging. This feature, however, can potentially overload the distribution network due to the high power demand.

Off-board chargers provide several benefits, such as lighter vehicle weight, high power levels, faster charging capabilities, and improved battery management systems. However, the high construction costs and immobility of DC fast charging stations limit their widespread deployment [20].

11.3 Summarized Comparison

The main differences between on-board and off-board chargers are summarized below:

<i>Aspect</i>	<i>On – Board Charger</i>	<i>Off – Board Charger</i>
Fixed Positions	Fixed within the vehicle, limited by space and weight, small in size and power	Fixed outside the vehicle, not limited by space or weight, larger in volume and power
Power Supply Modes	Connects to an AC socket and converts AC to DC for the vehicle battery; suitable for slow charging	Converts AC power to DC for the vehicle battery; suitable for fast charging [21]
Advantages	<ul style="list-style-type: none"> - Convenient charging anywhere with AC power - Promotes battery longevity through slow charging 	<ul style="list-style-type: none"> - Not constrained by vehicle space - Fast charging and high power
Disadvantages	<ul style="list-style-type: none"> - Longer charging time - Limited power 	<ul style="list-style-type: none"> - Potential to shorten battery life with frequent fast charging - High construction cost and immobility

Table 11.1: Comparison between On-Board and Off-Board Chargers

11.4 Why Use Off-Board Chargers?

Off-board chargers are increasingly favored for several reasons:

- **Higher Power Levels:** Off-board chargers can deliver significantly higher power compared to on-board chargers, enabling faster charging times. This is crucial for reducing downtime and increasing the usability of EVs [19, 20].
- **No Space Constraints:** Being external to the vehicle, off-board chargers are not limited by the vehicle's space and weight constraints, allowing them to incorporate larger and more efficient components [21].
- **Advanced Battery Management:** Off-board chargers can incorporate sophisticated battery management systems that improve the efficiency and safety of the charging process. These systems can handle higher currents and voltages, providing better control over the charging parameters [20].
- **Infrastructure Scalability:** Off-board chargers are part of a larger infrastructure that can be scaled up to meet growing demand. They can be installed at strategic locations, such as highways, parking lots, and commercial areas, facilitating convenient access to fast charging [21].
- **Reduced Vehicle Weight:** Since the charging equipment is external, the vehicle itself can be lighter, improving its efficiency and performance. This is particularly important for optimizing the range and dynamics of electric vehicles.

Off-board chargers, with their high efficiency, power density, reliability, and safety, are widely recognized and used globally in various applications, from passenger cars to commercial vehicles and special-purpose vehicles [21].

Chapter 12

MATLAB Simulation

12.1 Integrating the AFE Rectifier with DAB Converter

It is very crucial to simulate the circuit before diving in hardware design to make sure that the circuit would work fine when it's fabricated. Therefore, for this chapter we will provide the steps to simulate an Integration between an AC/DC converter and a Dc/DC Converter.

Refer to figure 2.1 that shows the model circuit diagram of the AC/DC converter that was built on MATLAB Simulink for 1KW system which is almost the same implementation for the high-rating system in aspect of circuit diagram.

Refer to figure 8.9 that shows the model circuit diagram of the DC/DC converter that was built on MATLAB Simulink.

As we discussed all the details about both converters later in this book.

The implementation of a three-phase rectifier was done to produce 800V at the DC-link as an output while the input line-to-line voltage was 380V at 50Hz frequency

After the DC-link, a DC/DC converter was set with a rated input voltage of 800V and a reference output current which was 25A.

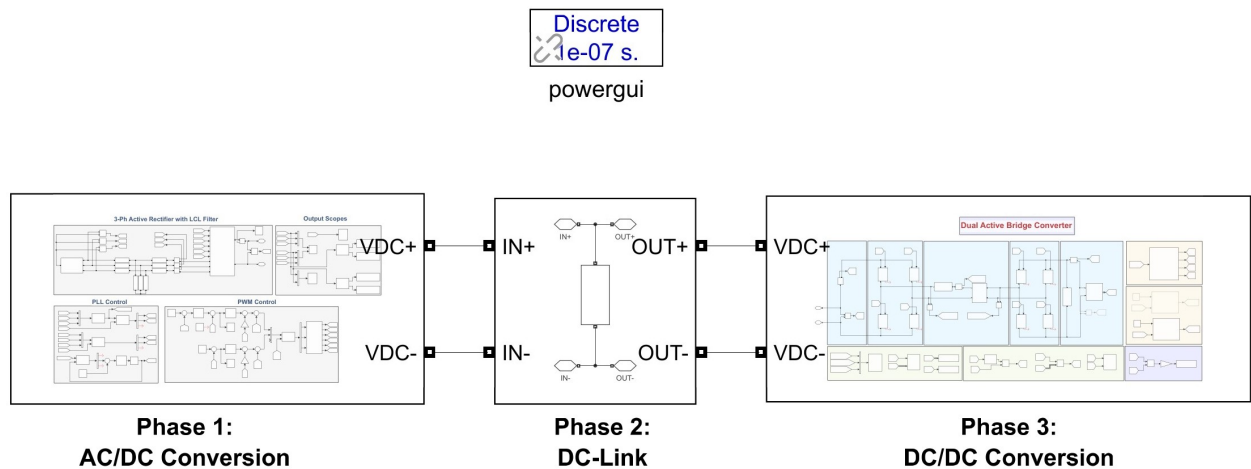


Figure 12.1: The integration model

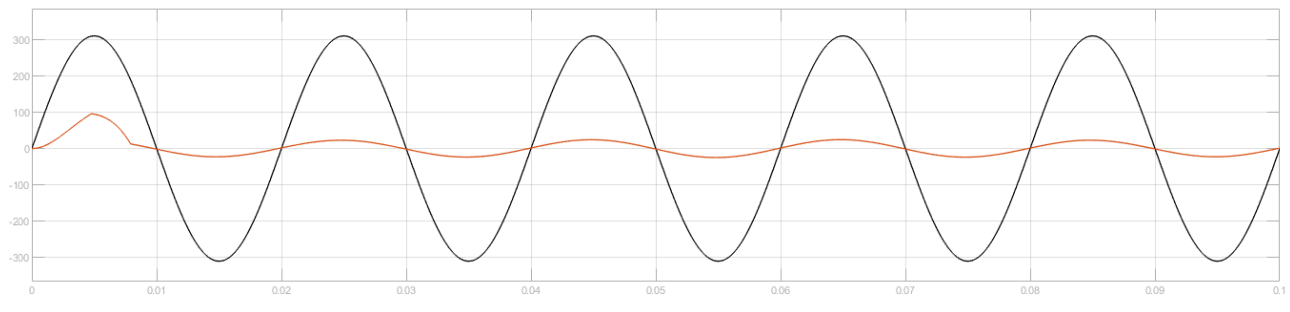


Figure 12.2: The phase input voltage and current

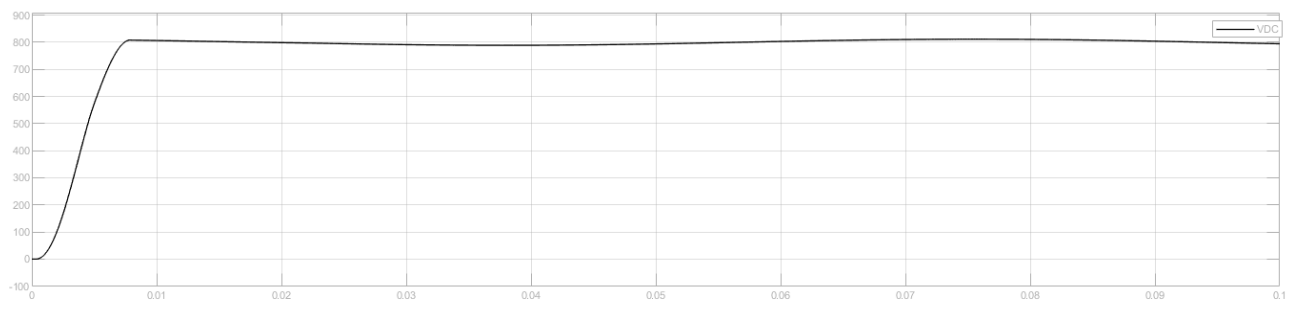


Figure 12.3: The DC output voltage from the rectifier side (DC-link voltage)

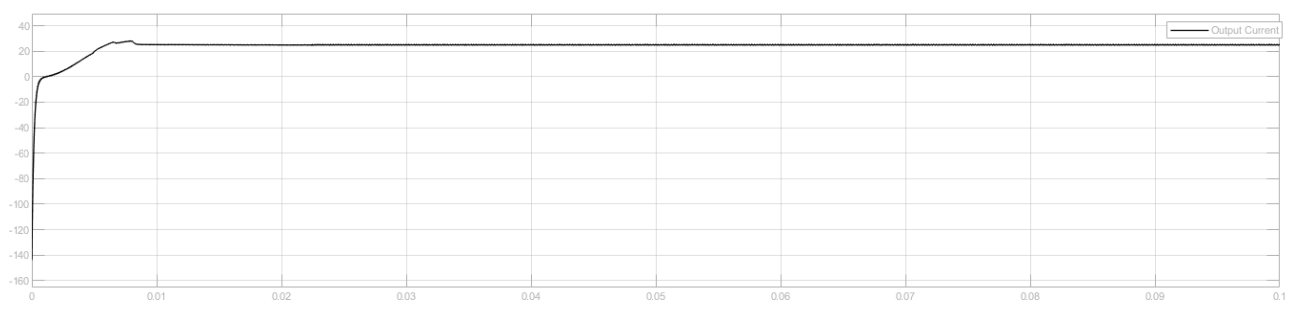


Figure 12.4: The DC output voltage from the DAB side (battery voltage)

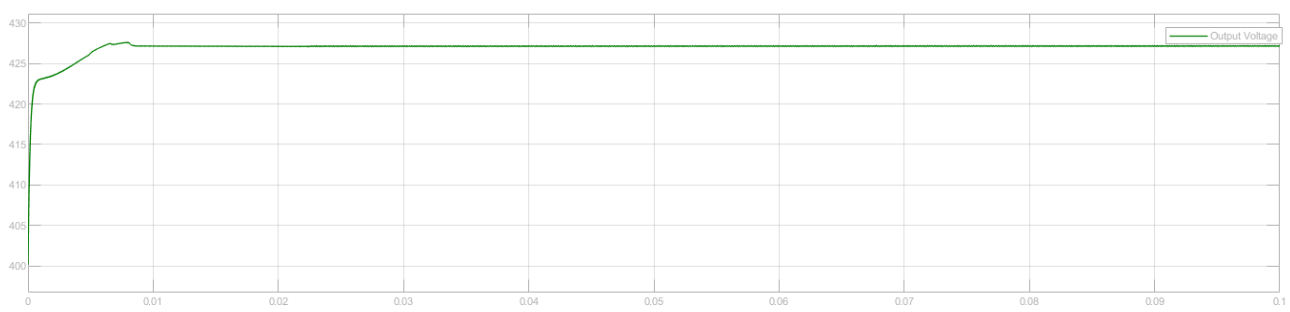


Figure 12.5: The output current flowing through the load (battery)

12.2 Integrating the AFE Rectifier with LLC Converter

The charger system contained of three phases, the 1st phase is the AC to DC rectification , 2nd phase the Dc-link and the final phase is the Dc to DC converter.

In this case the LLC converter is used for the final phase.

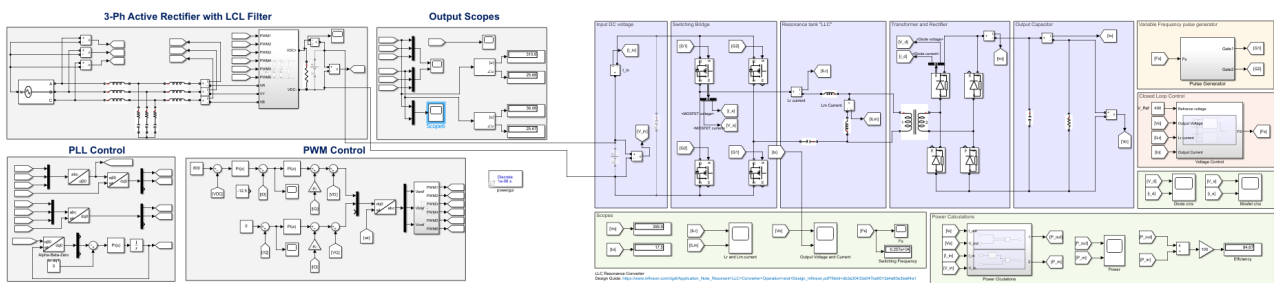


Figure 12.6: The overall system

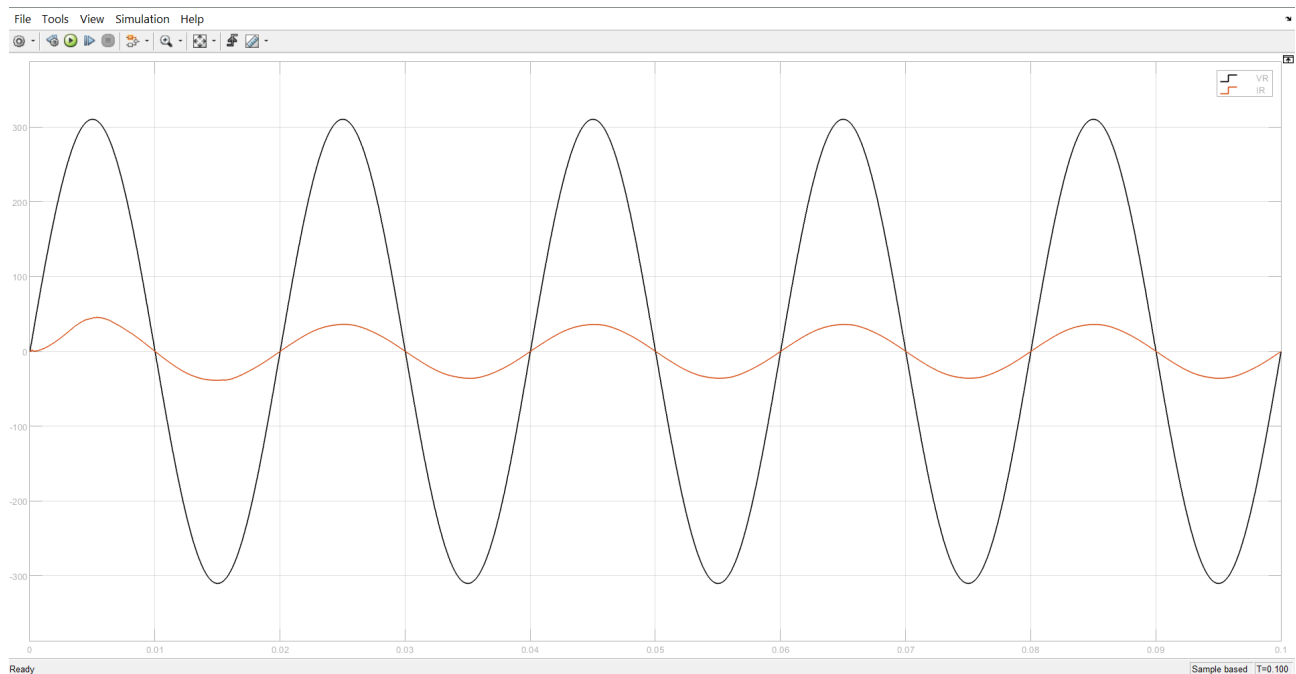


Figure 12.7: The power factor in AC to Dc phase

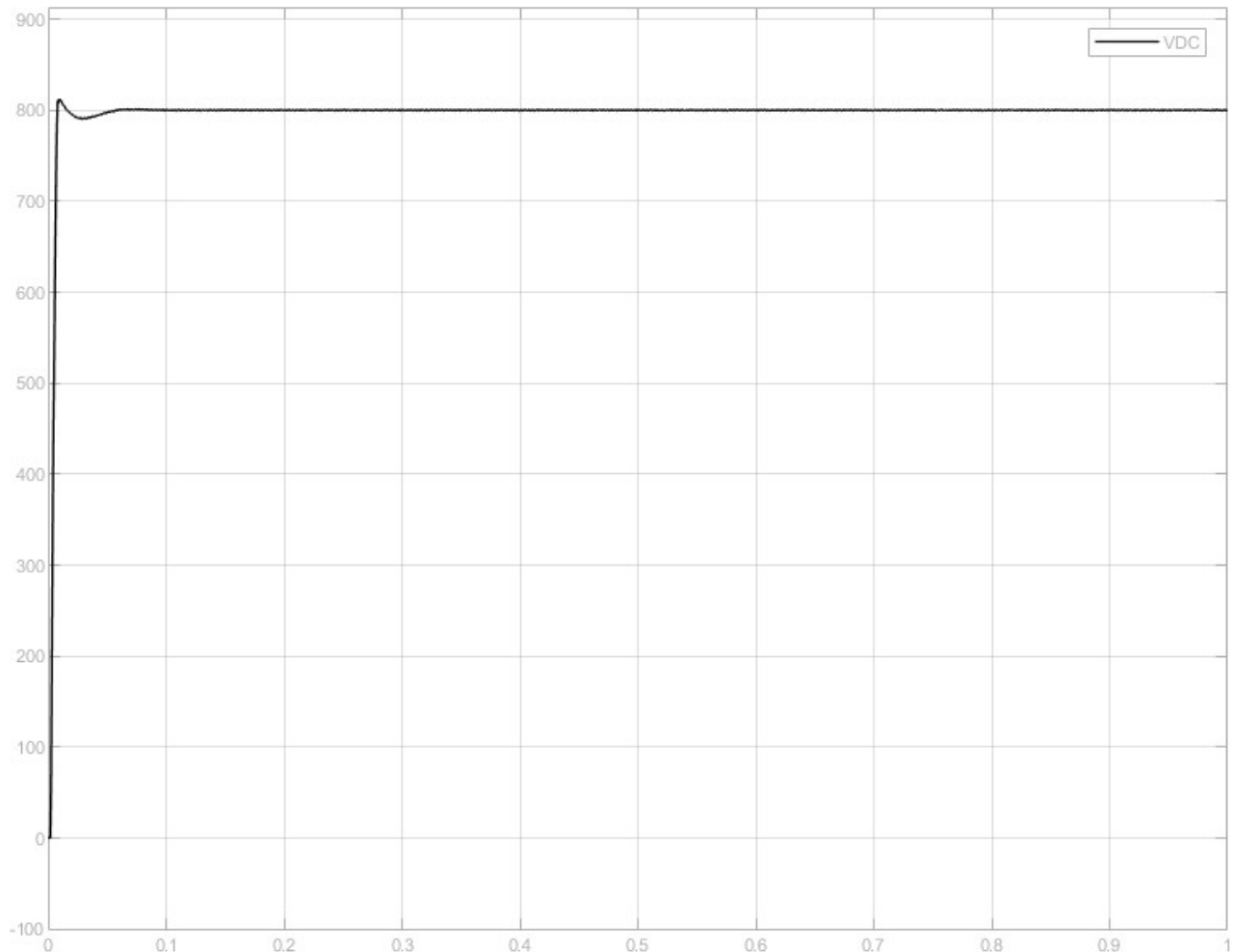


Figure 12.8: The output DC voltage of the rectifier part

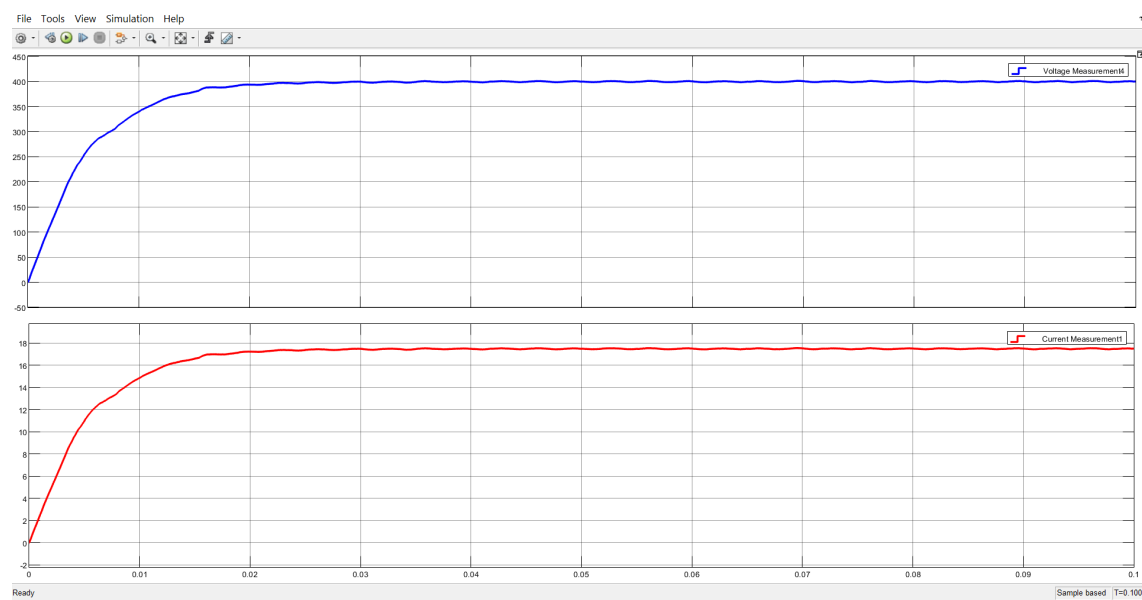


Figure 12.9: The output voltage and current in DC to DC

Bibliography

- [1] Steve Roberts. *AC/DC BOOK OF KNOWLEDGE*. RECOM Enginnering GmbH and Co.KG, 2018.
- [2] Saumitra Jagdale. Overview of ac/dc converters for fast-charging stations, 2023. [Online; posted 09-March-2023].
- [3] Harshada. Review of control techniques of three phase boost type pwm rectifiers. 2016.
- [4] Evren Isen and Ahmet Faruk Bakan. Development of 10 kw three-phase grid connected inverter. *Automatika*, 57(2):319–328, 2016.
- [5] Menna Ali and Muhammad Ibrahim. Analysis of different filter design methods for grid-connected inverter, 12 2023.
- [6] A. Reznik, M. Godoy Simões, Ahmed Al-Durra, and S. M. Muyeen. Lcl filter design and performance analysis for small wind turbine systems. In *2012 IEEE Power Electronics and Machines in Wind Applications*, pages 1–7, 2012.
- [7] Monolithic Power Systems. Introduction to dc-dc converters, 2023. Accessed: 2024-06-19.
- [8] Haifeng Fan. Understanding isolated dc/dc converter voltage regulation, 2014. [Online; posted 15 November, 2014].
- [9] Anushree Ramanath. Dc/dc converter applications, 2022. [Online; posted July 12, 2022].
- [10] Myoungho Kim, Martin Rosekeit, Seung-Ki Sul, and Rik W. A. A. De Doncker. A dual-phase-shift control strategy for dual-active-bridge dc-dc converter in wide voltage range. In *8th International Conference on Power Electronics - ECCE Asia*, pages 364–371, 2011.
- [11] Xueping Gao, Lijun Fu, Feng Ji, and You Wu. Virtual current based direct power control strategy of dual-active-bridge dc-dc converter. In *2019 IEEE International Conference on Mechatronics and Automation (ICMA)*, pages 1947–1952, 2019.
- [12] Dalina Krasniqi. Dual active bridge converter, 2021. [Online; posted 27 January, 2021].
- [13] Texas Instruments Incorporated. *Design Guide: TIDA-010054 Bidirectional, Dual Active Bridge Reference Design for Level 3 Electric Vehicle Charging Stations*, June, revised July 2022 2022. <https://www.ti.com/lit/pdf/TIDUE0>.
- [14] Shuai Shao, Linglin Chen, Zhenyu Shan, Fei Gao, Hui Chen, Deshang Sha, and Tomislav Dragičević. Modeling and advanced control of dual-active-bridge dc–dc converters: A review. *IEEE Transactions on Power Electronics*, 37(2):1524–1547, 2022.

- [15] Jun Liu, Licheng Sheng, Jianjiang Shi, Zhongchao Zhang, and Xiangning He. Design of high voltage, high power and high frequency transformer in lcc resonant converter. In *2009 Twenty-Fourth Annual IEEE Applied Power Electronics Conference and Exposition*, pages 1034–1038, 2009.
- [16] Bharat Singh Rajpurohit Siddhant Kumar, Adil Usman. Battery charging topology, infrastructure, and standards for electric vehicle applications: A comprehensive review, 2021. [Online; posted 31-October-2023].
- [17] Jin-Woo Jung Sadeq Ali Qasem Mohammed. A comprehensive state-of-the-art review of wired/wireless charging technologies for battery electric vehicles: Classification/common topologies/future research issues, 2021. [Online; posted 27 January, 2021].
- [18] Md Safayatullah, Mohamed Tamasas Elrais, Sumana Ghosh, and Reza Rezaii. A comprehensive review of power converter topologies and control methods for electric vehicle fast charging applications, 2022. [Online; posted 12 April, 2022].
- [19] María Quílez, Mohamed Abdel-Monem, Mohamed El Baghdadi, Yang Yang, Joeri Van Mierlo, and Omar Hegazy. Modelling, analysis and performance evaluation of power conversion unit in g2v/v2g application—a review. *Energies*, 11:1082, 04 2018.
- [20] Salman Habib, Muhammad Khan, Farukh Abbas, and Houjun Tang. Assessment of electric vehicles concerning impacts, charging infrastructure with unidirectional and bidirectional chargers, and power flow comparisons. *International Journal of Energy Research*, 42, 10 2017.
- [21] Onboard Charger. Difference between on-board charger and off-board charger, 2023. Accessed: 2024-06-19.